A Mechanical Strain Sensor for Polymeric Materials and Photophusical Investigations of Large Molecules

Spanggaard, Holger

Publication date:
2003

Document Version
Publisher's PDF, also known as Version of record

A MECHANICAL STRAIN SENSOR FOR POLYMERIC MATERIALS

AND

PHOTOPHYSICAL INVESTIGATIONS OF LARGE MOLECULES

Ph.D. thesis

Holger Spanggaard

February 2003

The Danish Polymer Centre
Department of Chemical Engineering
Technical University of Denmark

Thesis supervisors
Senior Scientist Mikkel Jørgensen, Polymer Department, Risø
Program leader Kristoffer Almdal, Polymer Department, Risø
Prof. Jørgen Kops, Department of Chemical Engineering, DTU

ISBN 87-90142-85-3.
Printed by Book Partner, Nørhaven Digital, Copenhagen, Denmark

Table of contents

Preface

The work described in this thesis has been carried out at the Danish Polymer Centre, Risø National Laboratory in the period from February 2000 to January 2003, under the supervision of Mikkel Jørgensen (Risø), Kristoffer Almdal (Risø) and Jørgen Kops (DTU).

About the report

This thesis is divided in two parts. Part one (chapters 1-4) deals with the design and synthesis of a fluorescent strain sensor. The basic concept is to place a sensor unit in the middle of elastomeric triblock copolymer (polystyrene-polyisoprene-polystyrene) and monitor the sensor unit's emission change as the material is stretched. Chapter one (Introduction to fluorescence) and chapter two (Fluorescent probes in macromolecular science) is meant as introductory chapters. In chapter three (A mechanical strain sensor for polymeric materials) the major part of my work is described. And finally is the experimental given in Chapter four.

Part two describes work carried out in collaboration with Frederik Krebs. Chapter 5 (An exceptional red shift of the emission maxima upon fluorine substitution) describes the florescent properties of a large donor-acceptor molecule. In chapter 6 (Energy transfer in polymers) the energy transfer from a conjugated polymer to two different chromophores is investigated.

Work carried out by me has contributed to four papers, copies can be found in the appendices.

Acknowledgements

I would like to express my sincere gratitude for the opportunity to work in the Polymer Department of Risø. It has been very rewarding to work in a new scientific field.

I would like to thank Mikkel Jørgensen for his supervision. Mikkel is a resourceful chemist and has taught me much about chemistry and science in general. Also, I have received many useful suggestions regarding this manuscript. I would also like to thank Kristoffer Almdal for useful discussions on polymer chemistry and polymer physics. Even though my contact with Jørgen Kops naturally has been limited, I would like to thank Jørgen for always showing interest in my work, and making sure that the paperwork was done in time.

In addition I would like to thank the following: Frederik Krebs for fruitful collaboration, Walther Batsberg for teaching me about SEC and for his generous sharing of his hands-on experience with polymer materials. Lotte Nielsen for analysing a number of samples using SEC. Peter Sommer Larsen for theoretical discussions, Jan Alstrup, Kell

Mortensen, Niels Bent Larsen, Torben Kjær, Theis Sølling and many others that have helped me in one way or the other.

I have been lucky to be surrounded by a number of pleasant colleagues through the past three years. Especially I would like to thank Hasse, Sune, Carina and Frederik for being good friends.

Finally, I would like to thank Joan for her continuing support.

Abstract

The degree of deformation (strain) observed when a given force (stress) is applied to a polymeric material, and the relationship between deformation and force are a fundamental property when the mechanical state of a polymeric material is described. A number of methods exist to investigate this relationship on a macroscopic level (rheology measurements etc.). However, the molecular processes that parallels macroscopic deformation is not well understood. A tool that allows measurement of the molecular changes when the material is strained or stressed may produce new insight into the structure-property relationship of polymeric materials, and lay ground for new advanced polymer based materials. In addition, the current theory of rubber elasticity and molecular deformation might be experimentally probed.

To investigate the molecular responds to deformation, a fluorescent sensor unit was placed in the middle of a polymer backbone, as depicted below. It was envisaged that straining the polymer chains would produce affect the fluorescent properties of the single site sensor unit.

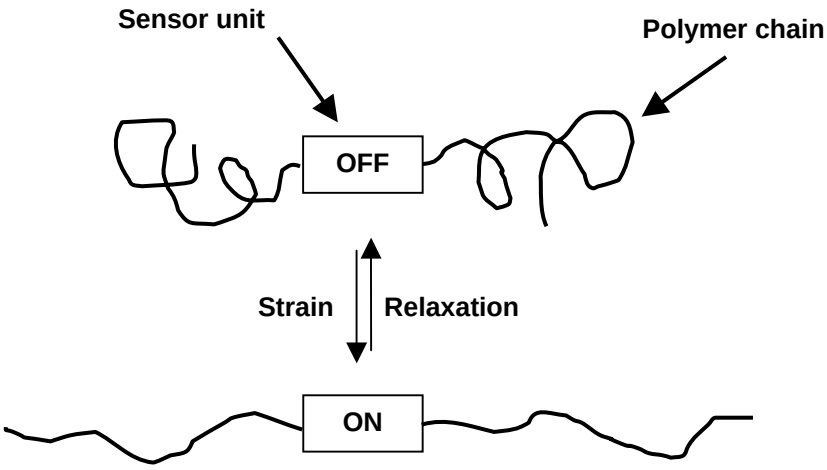

Basic concept

Abstract

Four fluorescent strain probes with one or two carbazole units placed in the middle of an elastomeric tri-block of polystyrene-polyisoprene-polystyrene (SIS) have been prepared (see below) and their fluorescence behaviour investigated under strain.

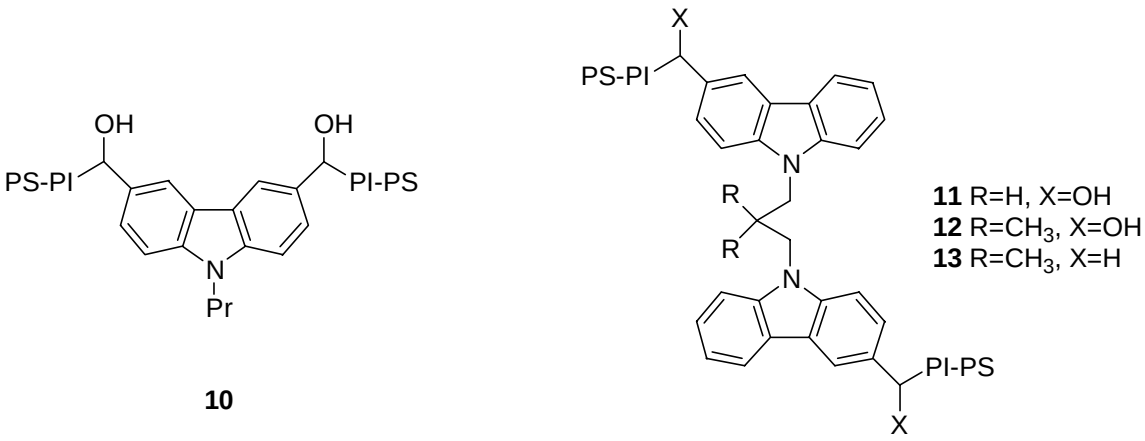

Fluorescent probes investigated

The idea with the probes **11-13** was that the carbazole-carbazole interaction could be changed with strain (see below). In the conformation shown left the carbazole units interact, and upon excitation and excimer might form. To right the carbazole moieties are isolated and excimer formation is not likely. Emission form the carbazole excimer can be distinguished from the fluorescence from the isolated carbazole. Thus the conformation change shown below should be detectable using fluorescence spectroscopy.

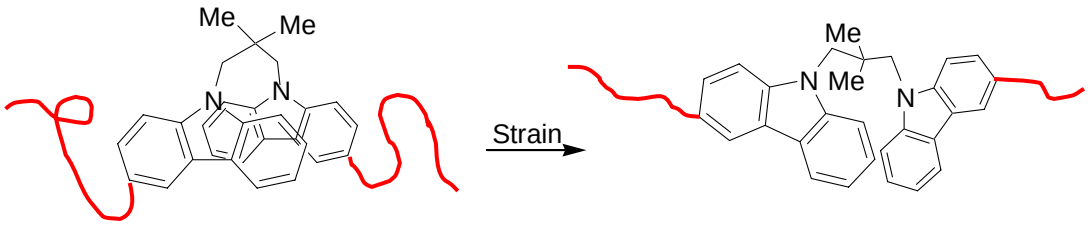

The carbazole-carbazole interaction changes when the polymer chain (red) is strained

The synthesised probes were dissolved in commercial SIS type rubbers in low levels of 0.1 weight-%. Films cast from this blend were subjected to tensile elongation while the fluorescence spectra were obtained. Below are the fluorescence spectra of probe **12** shown at varying strain levels.

Thus the fluorescence of the probe changes considerably with macroscopic strain. Shown below is a plot of the relative intensity of the low wavelength peak (I_{354}/I_{370}) as function of tensile strain for the four probes.

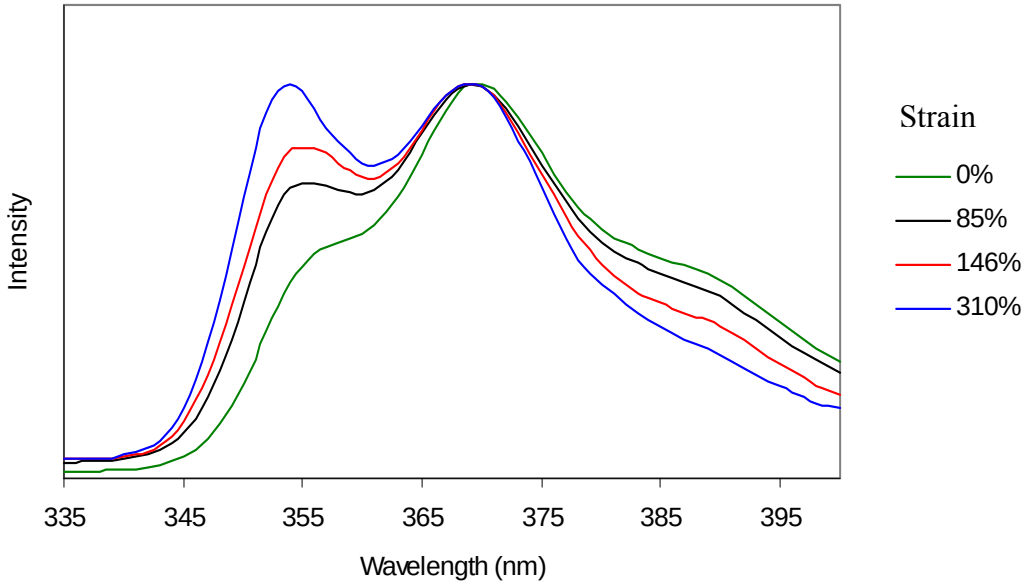

Fluorescence from probe* 12 *changes with strain

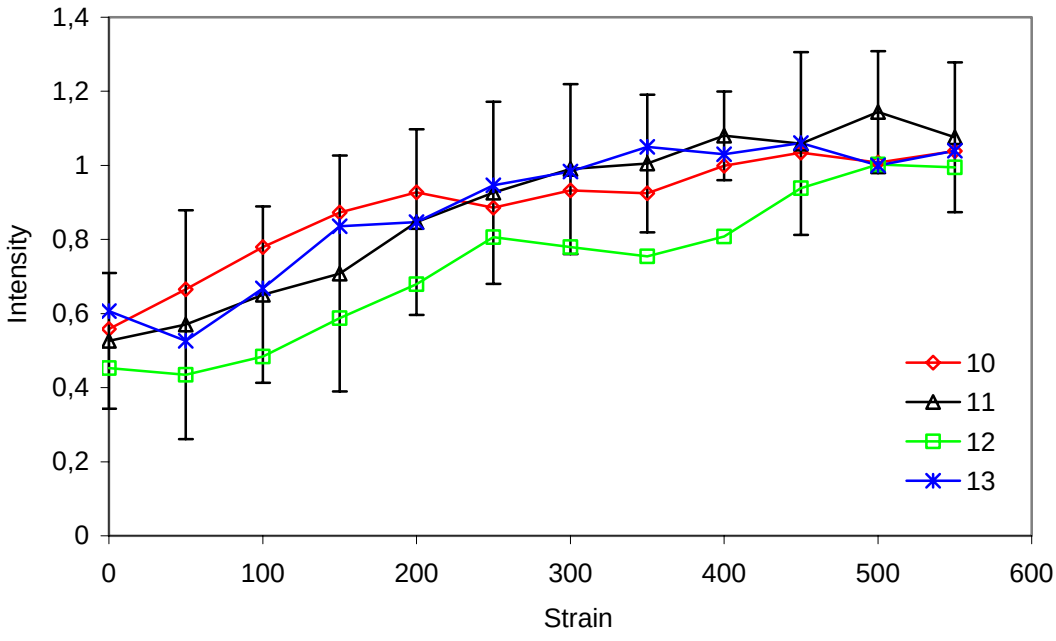

Relative intensity of the low wavelength peak as function of tensile strain

Abstract

A rather large change from ca. 0.7 to 1.1 in the relative intensity at two wavelengths (I_{354}/I_{370}) was observed on elongations up to 400%. The spectroscopic change is strongest for small strain levels around 0-200% and levelled out above 300-400%. All four strain probes gave similar results on uniaxial elongation, even probe **10** with only one carbazole unit. Thus, there seems to be no significant effect of the close proximity of the two carbazole units in probes **11-13**. This rules out any major contribution from excimer to monomer type shifts in the fluorescence of the probes. Since probe **10** show the same emission change as probes **11-13** it was concluded that changes in the emission vibronic bands are the major effect involved in the emission change measured.

Abstract in Danish – Resumé på dansk

Graden af deformation (forlængelse) som observeres når et polymer materiale påvirkes af en given kraft (stress), og sammenhængen mellem deformation og kraft er en fundamental egenskab når de mekaniske egenskaber af et polymermateriale beskrives. Der eksisterer en række af metoder til bestemmelse af sammenhængen mellem deformation og kraft på det makroskopiske niveau (rheologi målinger osv.). Imidlertid er de molekylære processer som følges af makroskopisk deformation ikke vel forstået. Det forventes at en teknik som tillader måling af disse parametre på en molekylær skala, vil danne grundlag for ny viden om struktur-egenskab sammenhænge for polymermaterialer. Endvidere vil en sådan eksperimental teknik muligvis kunne bruges til at eftervise og videreudvikle teori om gummi elasticitet og molekylær deformation.

For at undersøge den molekylære ændring som makroskopisk deformation resulterer i, blev en fluorescerende sensor enhed placeret i midten af en polymer kæde, som vist neden for. Det var forventet at forlængelse ville have en effekt på sensor enhedens fluorescens egenskaber.

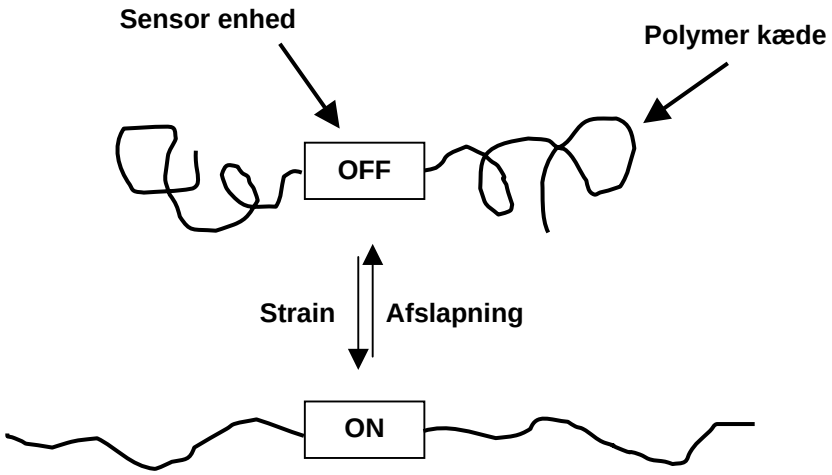

Det grundlæggende koncept

Fire fluorescerende strain prober med én eller to carbazol enheder placeret i midten af en elastomer triblok af polystyren-polyisopren-polystyren (SIS) er blevet syntetiseret (se neden for) og deres fluorescens egenskaber er blevet undersøgt under strain.

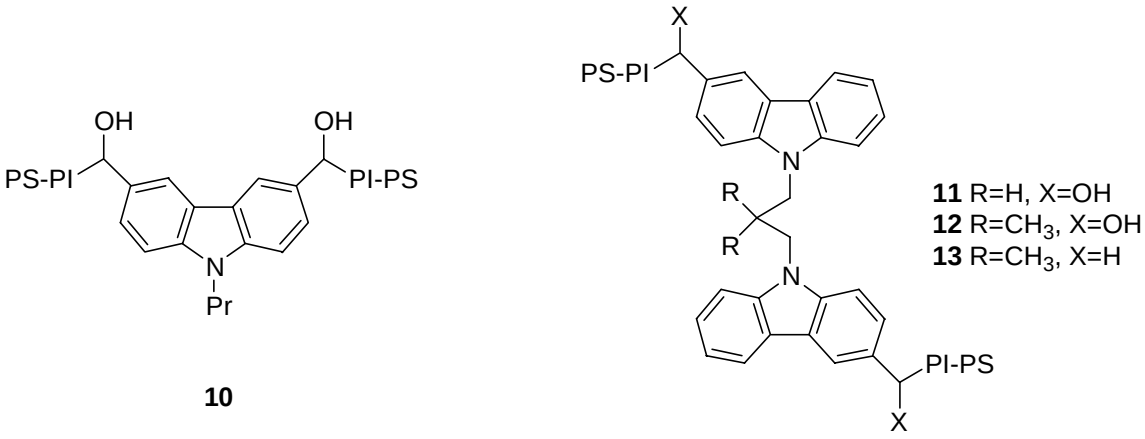

Fluorescerende prober undersøgt

Ideen med proberne **11**-**13** var at carbazol-carbazol vekselvirkningen kunne ændres med strain (se neden for). I konformationen vist til venstre vekselvirker carbazol enhederne og når systems exciteres kan en excimer dannes. Til højre er carbazol enhederne isoleret og excimer dannelse er ikke sandsynlig. Emission fra en carbazol excimer kan skelnes fra emissionen fra en isoleret carbazol enhed. Altså burde en konformations ændring som vist nedenfor kunne følges vha. fluorescens spektroskopi.

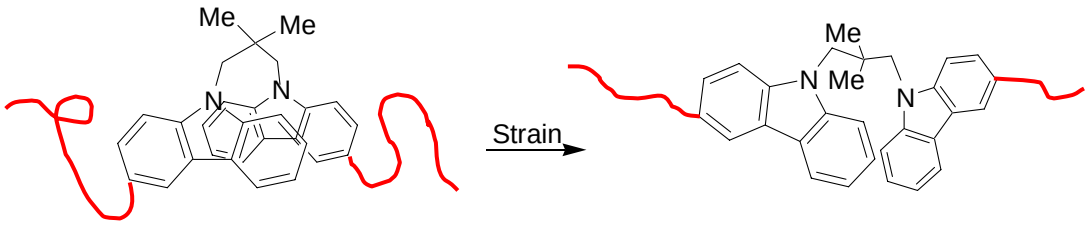

Carbazol-carbazol vekselvirkningen ændres når polymer kæderne (røde) strained.

De syntetiserede prober blev opløst i en kommerciel SIS gummi i lav koncentration (0,1 vægt-%). Film lavet af denne blanding blev strakt og deres fluorescens spektrer optaget. Neden for er fluorescens spekteret af probe **12** vist ved forskellige strain niveauer.

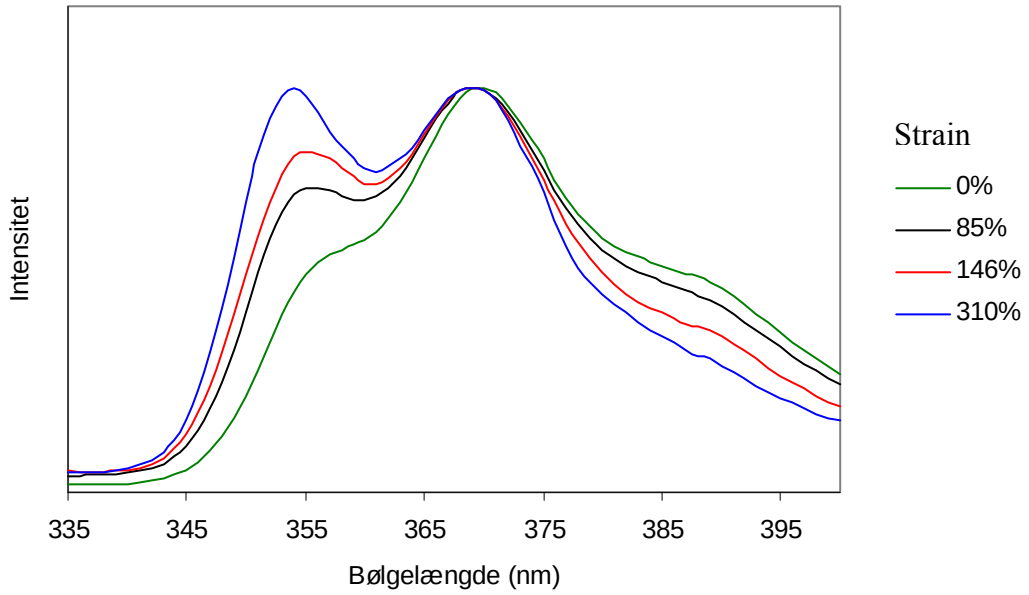

Fluorescens emissionen fra probe 12 ændres med strain

Fluorescens emissionen ændres altså dramatisk med makroskopisk strain. Neden for er et plot vist af den relative intensitet af det første vibrations bånd (omkring 354nm i ovenstående figur) som funktion af strain for de fire prober.

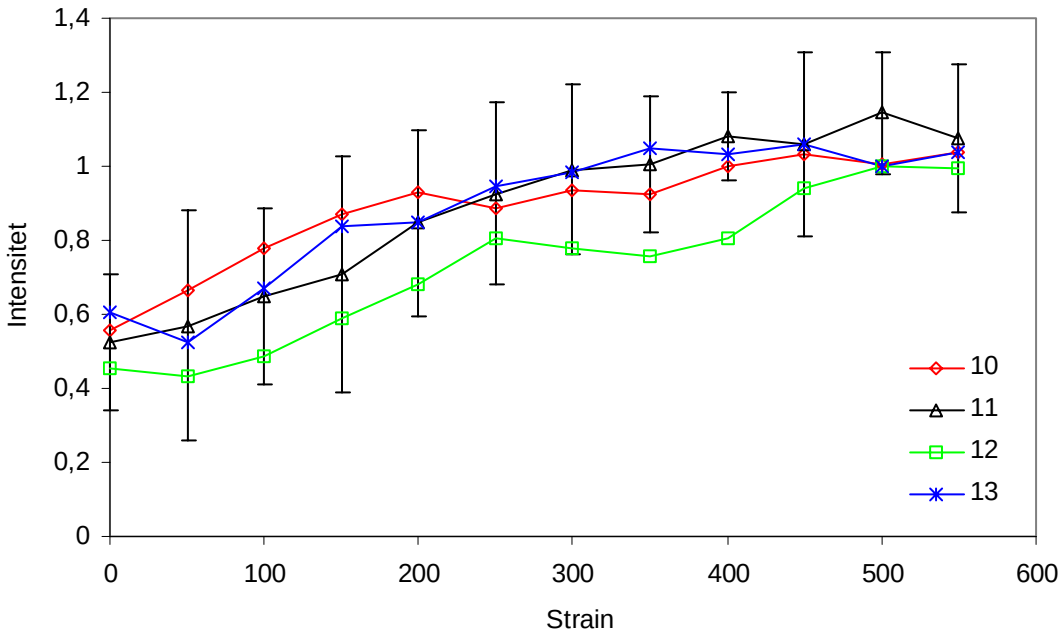

Den relative intensitet af det første vibrations bånd som funktion af strain

En forholdsvis stor ændring af den relative intensitet (fra 0,7 til 1,1) af toppen ved 354nm blev målt ved stræk op til 400%. Den spektroskopiske ændring var størst ved små strain niveauer (0-200%) og aftog derefter omkring 300-400%. Alle fire prober gav lignende resultater ved stræk, selv probe **10** med kun en enkelt carbazol enhed. Der ser således ikke ud til at være nogen signifikant effekt af den umiddelbare nærhed af to carbazol enheder i proberne **11**-**13**. Dette udelukker væsentlige bidrag fra en excimer-til-monomer mekanisme i probernes fluorescens. Siden probe **10** med kun en enkelt carbazol enhed viser den samme emissions ændring som proberne **11**-**13** var konklusionen at emissions ændringen primært skyldes en intensitets ændring af vibrations båndene.

List of abbreviations

BuLi	Butyl lithium
Cbz	Carbazole
DMAB	dimethylamino benzoates
DMABN	Dimethylamino benzonitrile
DTAB	Dodecyltrimethylammonium bromide
DMF	Dimethylformamide -
NBS	*N*-bromo-succinimide
Pd	Poly dispersity (Mw/Mn)
PMMA	Poly(methyl methacrylate)
PMA	poly(methacrylic acid)
PNMMA	CoPoly(1-naphthylmethyl methacrylate/methyl methacrylate)
PS	Polystyrene
PI	Polyisoprene
PVCz	Poly(*N*-vinylcarbazole)
Py	Pyrene
RT	Room temperature
SEC	Size exclusion chromatography
SIS	*Block*-copoly(styrene/isoprene/styrene)
t-BuOK	Potassium tert-butoxide
THF	Tetrahydrofurane
TICT	Twisted intramolecular charge transfer
TRES	Time resolved emission spectroscopy
TsCl	Tosylchloride
Φ	Fluorescence quantum yield

C H A P T E R 1

INTRODUCTION TO FLUORESCENCE

This chapter is included because fluorescence is the single subject that is common for the following chapters. Also, having no prior experience with fluorescence a great deal of my time has been devoted to the subject.

1.1 Introduction

In this chapter I will give an introduction to the theory and instrumentation of fluorescence. I have tried to keep this chapter as short as possible and only include the most fundamental aspects of fluorescence. In depth coverage of the subject can be found elsewhere.[1-4]

The emission of light from any substance is called luminescence. Some of the first scientific reports of luminescence appeared in the middle of the 18th century. In 1845 Sir J.F.W. Herschel reports on an experiment he did twenty years earlier, but was unable to repeat because of the lack of "a specimen of the wood". Herschel observed that an otherwise colourless solution of quinine (Figure 1-1, quinine absorbs in the UV region) in water emitted a blue colour under certain circumstances.[5] Herschel concludes that a specie in the solution, "exert its peculiar power on the incident light" and disperses the blue light. The experiment can be repeated simply by observing a glass of tonic water exposed to sunlight. Often a blue glow is visible at the surface.

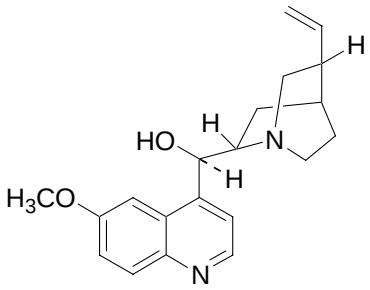

Figure 1-1. Quinine.

Sir G.G. Stokes studied the same compound and found that the emitted light has a longer wavelength than the light absorbed, the so-called Stokes' shift. Stokes' paper appeared in 1852[6] and I cannot resist the temptation to show the experimental set-up Stokes used to discover this fundamental property of fluorescence (see Figure 1-2).

In the experiment outlined, the blue glass transmits light below 400nm that is absorbed by quinine. The light emitted from quinine has a longer wavelength (450nm) and is allowed to pass through the glass of wine and reach the observer. If however the filters

(blue glass and glass of wine) switched place the UV radiation could not reach the quinine solution, and the emission could not penetrate the wineglass.

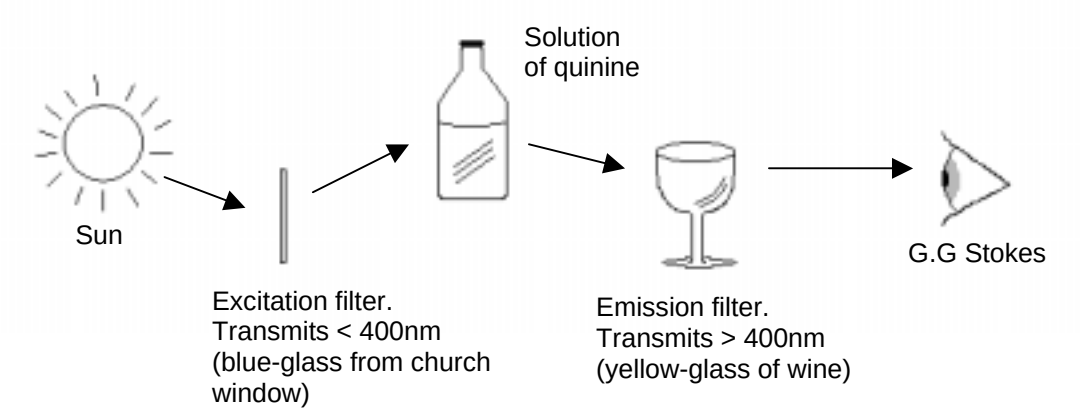

Figure 1-2. Experimental set-up used by G.G. Stokes. The drawing is reproduced from ref. 1.

A. Jabłoński and others developed a modern theoretical understanding of Stokes observation some 70 years later. In the 1920s and 1930s Jabłoński investigated polarized light and fluorescence and was able to show that the transition moments in absorption and emission are two different things. Thus the foundation for the concept of anisotropy was laid. For that and other accomplishments Jabłoński has been referred to as the father of fluorescence, and his work has had a major impact on the theoretical understanding of photophysics.

1.2 Basic theory of fluorescence

The photophysical processes that occur from absorption to emission are often shown in a so-called Jabłoński diagram. Of course all possible energy routes cannot be encompassed in single figure, and different forms of the diagram can be found in different contexts. The diagram below is a simple version, where intersystem crossing (from singlet to triplet states) leading to phosphorescence and delayed fluorescence as well as intermolecular processes (e.g. quenching, energy transfer, solvent interaction etc.) are omitted.

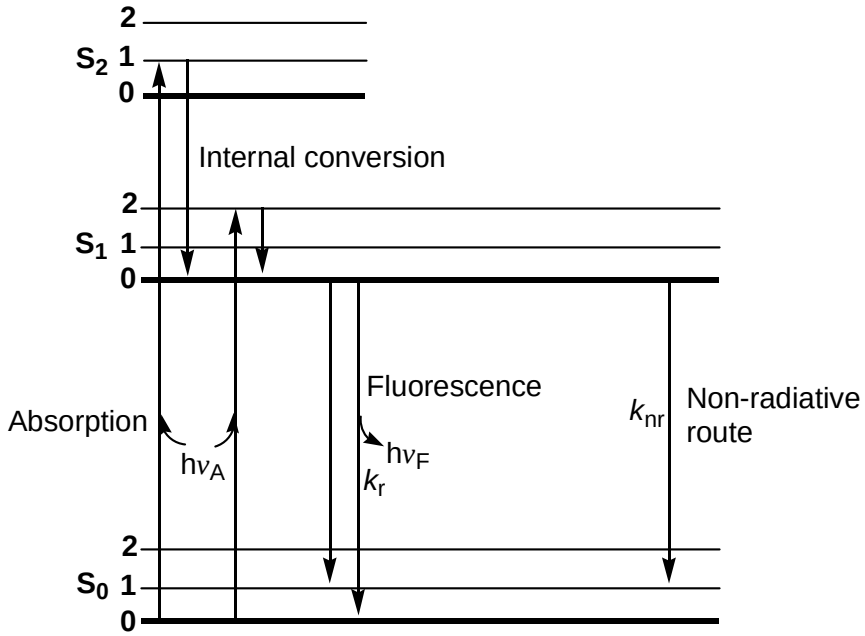

Figure 1-3. A simple Jabłoński diagram. Three electronic levels are depicted along with three vibrational energy levels. $h\nu_A$ and $h\nu_F$ denotes absorption and fluorescence respectively. k_r is the rate constant for fluorescence and k_{nr} is the rate for the competing non-radiative route.

In the diagram the electronic singlet states S_0, S_1 and S_2 along with three vibrational energy levels are shown. In the ground state the molecule will be in lowest vibrational level of S_0. At room temperature the higher vibratonal energy levels is in general not populated (less than 1% according to Boltzmann statistics). The magnitude of the absorbed energy ($h\nu_A$ in the figure) decides which vibrational level of S_1 (or S_2) becomes populated. This process is very fast and happens within 10^{-15}s. In the next 10^{-12}s the molecule relaxes to the lowest vibrational level of S_1, a process called internal conversion. Since emission typically occurs after 10^{-9}s the molecule is fully relaxed at the time of emission, hence, as a rule, emission occurs from the lowest vibrational level of S_1 (Kasha's rule) and the fluorescence spectrum is generally independent of the excitation wavelength. After emission ($h\nu_F$ in the figure) the molecule returns to the ground state, possibly after vibrational relaxation. This completes the simplest case of fluorescence: excitation, internal conversion, emission and relaxation. The energy lost to the surroundings, due to vibrational relaxation and internal conversion is the reason why a Stokes' shift is observed (This is also illustrated in Figure 1-4 right).

Since the energy spacing between the vibrational levels in S_0 or S_1 is of the same size, there often exist mirror image symmetry between the emission spectrum and the $S_0 \rightarrow S_1$ absorption spectrum (not the $S_0 \rightarrow S_2$ absorption), needless to say there are plenty of exceptions to the rule.[2] The mirror relationship between absorption and fluorescence is illustrated in Figure 1-4 left. Which transitions that will predominate in a given case can be rationalized using the Franck-Condon principle (Figure 1-4, right). The principle states that since electronic transition is extremely fast the position of the nuclei is fixed, that is that the transitions are vertical, as illustrated by the arrows. In the example

shown, both the absorption and emission is most likely to be a 0-2 transition resulting in more intense 0-2 peaks in the absorption and emission spectrum.

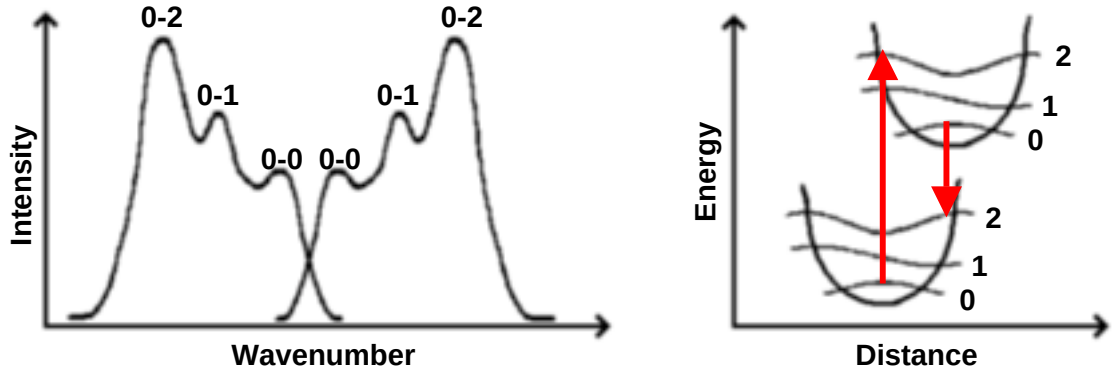

Figure 1-4. Left: The mirror image rule: the absorption spectrum right is a mirror image of the emission spectrum left. Right: Franck-Condon principle: transitions are vertical. The 0-2 transition is the most probable. The figure is adopted from ref. 1.

While the relative peak intensity is governed by the Franck-Condon principle, the total fluorescence intensity I is related to the quantum yield (Φ), defined as the ratio of photons emitted to photons absorbed. I is given by the expression

$$I = I_0 K \Phi \varepsilon c l$$

where I_0 is the lamp intensity, K is a machine constant, εcl is the well known expression for absorption (ε: extinction coefficient, c: concentration, l: length of light path.). The expression is valid for dilute solutions (optical density < 0.05). Returning to the Jabłoński diagram, two routes from S_1 to the ground state is shown. Besides fluorescence a molecule can typically choose between a number of non-radiative routes. Φ can be expressed as the rate of photons emitted divided by the total rate of depopulation of the excited state:

$$\Phi = \frac{k_r}{k_r + k_{nr}}$$

If the non-radiative relaxation is fast compared to fluorescence ($k_{nr} > k_r$), Φ will be small, that is the compound will fluoresce very little or not at all. Often different non-radiative events are limited in the solid phase, and long-lived luminescence (e.g. phosphorescence) is often studied in frozen solution or other solid phases. Quenchers make non-radiative relaxation routes more favourable and often there is a simple relation between Φ and the quencher concentration. The best-known quencher is probably O_2, which quench almost all fluorophores, other quenchers only quench a limited range of fluorophores. If a molecule is subject to intramolecular quenching, Φ may yield information about the structure.[7]

When an emission spectrum is obtained, data are typically collected for more than 0.1 sec. at each wavelength increment (typically 1nm), but since fluorescence lifetimes typically is measured in nanoseconds, it follows that the obtained spectrum is a time-average of a many events. The time averaging loses much information, and time-resolved experiments are often the more interesting when a system is investigated. The fluorescent lifetime of the excited state, τ, is the average time a molecule stays in the excited state before returning to ground state. Thus τ can be expressed as the inverse of the total depopulation rate:

$$\tau = \frac{1}{k_r + k_{nr}}$$

Typically fluorescence lifetime values are in the 5-15ns range. The above expression is related to the expression for Φ, in that way that they have a common denominator. Actually an approximation of τ can be obtained by measuring Φ in aired and degassed solutions.[8]

In the absence of non-radiative relaxation (k_{nr}= 0), the lifetime becomes the inverse of k_r and is often called the natural lifetime, denoted τ_N. For many compounds the natural lifetime can be calculated from the measured lifetime τ and the measured quantum yield Φ:

$$\tau_N = \frac{\tau}{\phi}$$

It is important to notice that the fluorescent lifetime is what is experimentally obtained, and the natural lifetime can be calculated.

The fluorescence lifetime, τ, is determined by observing the decay in fluorescence intensity (decay profile) of a fluorophore after excitation. Immediately after a molecule is excited the fluorescence intensity will be at a maximum and then decrease exponentially:

$$I(t) = I_o e^{-t/\tau}$$

Thus after a period of τ the intensity has dropped to 37% of I_0, that is 63% of the molecules return to the ground state before τ. In many cases the above expression needs to be modified into more complex expressions. First of all it is assumed that the instrument yields an infinite (or very) short light pulse at time zero. In cases where τ is small I_0 must be replaced by a function, that describes the lamp profile of the instrument. Also, more than one lifetime parameter is often needed to describe the decay profile, that is I(t) must be expressed as a sum of exponentials.

Finally the concept of anisotropy should be mentioned. Anisotropy is based on selectively exciting molecules with their absorption transition moments aligned parallel to the electric vector of polarized light. By looking at the polarization of the emission

the orientation of the fluorophore can be measured. The anisotropy of the system is defined as:

$$r = \frac{I_{\parallel} - I_{\perp}}{I_{\parallel} + 2I_{\perp}} = \frac{3 < \cos^2 \theta > -1}{2}$$

The oval in Figure 1-5 symbolized the absorption transition moment. Vertical polarized excitation light enters along the x-axis and $I_{\perp}$ and $I_{\parallel}$ are measured along the y-axis, setting the emission polarizer perpendicular and parallel to the excitation polarizor respectively. θ is the angle of the emission to the z-axis[9] (see Figure 1-5), the squared brackets indicates that it is the average value. If all absorption transition moments are aligned along the z-axis then $I_{\perp}$ = 0 and θ = 0, leading to r = 1, the maximum anisotropy.

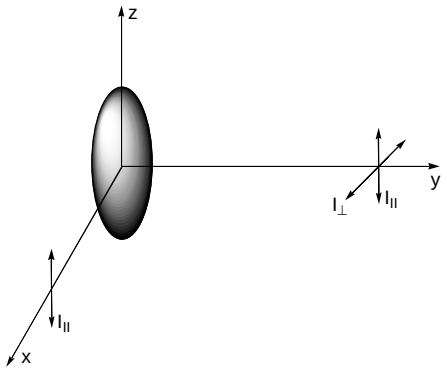

Figure 1-5. The absorption dipole is aligned along the z-axis. The excitation light is vertical aligned and follows the x-axis. Emission is measured along the y-axis.

By combining anisotropy with time-resolved measurements it is possible to measure the mobility of a fluorophore. Immediately after excitation all excited molecules will be oriented along a common axis. In the solid phase the system will retain its anisotropy until emission. However, if the fluorophores are free to move, the anisotropy of the system will decrease before emission. Numerous biological systems have been investigated using this technique, e.g. the viscosity in membranes has been measured using DPH[10] (see Figure 1-6) and other rod shaped molecules.

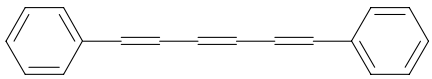

Figure 1-6. DPH (1,6-diphenyl hexatriene).

1.3 Instrumentation

The fluorescence spectrophotometer in the Danish Polymer Centre, a FLS920 from Edinburgh Instruments, is shown below (Figure 1-7), along with a principal sketch. It consists of a light source, an excitation and emission monochromator (1800 grooves/mm), polarizors (Glan-Thompson prisms), sample chamber and a detector (photomultiplier tupe). For steady state measurements the light source consist of a 450W xenon arc lamp, and for time resolved measurements it is equipped with nanosecond flash lamp. Most simple spectrometers have a similar geometry, but often extra detectors and/or light sources are fitted resulting in a T- or X-geometry.

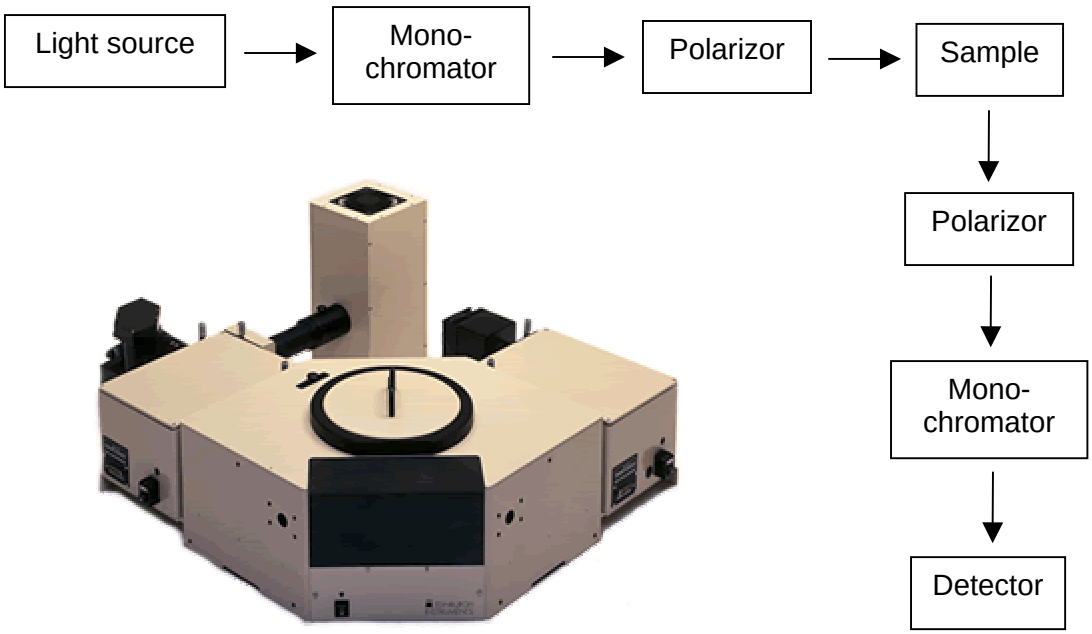

Figure 1-7. The FLS920 fluorescence spectrometer and a principal sketch.

Below three modes of excitation is shown (see Figure 1-8). To the left a dilute solution in a standard 1 x 1cm cuvette is shown, this is the way most measurements are done. In very concentrated solutions all the light gets absorbed right at the edge of the cuvette (*inner filter effect*) and the measured intensity drops very fast across the cuvette. In this case front-face illumination can be used, as shown in the middle. This method can also be used to measure on surfaces of solid samples. If the solid sample is transparent back-face illumination becomes possible. Itagaki recommends the back-face over the front-face arrangement in these cases, because in front-face illumination there is a risk that the reflected light from the surface and back surface interfere with each other to give regular peaks.[11] Moreover large amounts of light may be reflected directly into the emission monochromator possibly resulting in large amount of stray light.

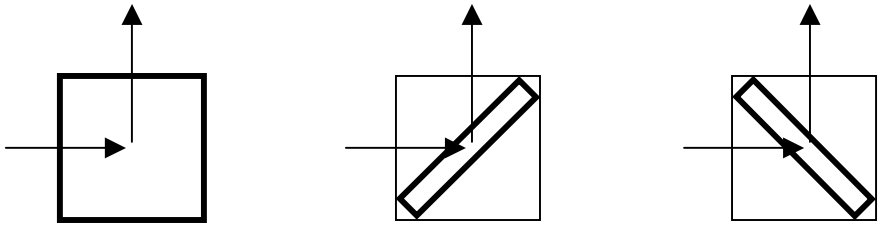

Figure 1-8. Different modes of excitation are illustrated: dilute solution (left), concentrated solution or solid sample (middle) and transparent solid sample (right). The horizontal arrow illustrates excitation light and the vertical arrow fluorescence.

References and notes

1. For an excellent book on the subject see *Principles of Fluorescence Spectroscopy*, Sec. Ed, J.R. Lakowicz, Kluwer Academic / Plenum Publishers, New York: 1999.
2. *Handbook of Fluorescence Spectra of Aromatic Molecules*, Sec. Ed., Isadore B. Berlman, Academic Press, New York and London: 1971.
3. For a good introduction for the undergraduate student see *Fluorescence and Phosphorescence*, Rendell. D, John Wiley & Sons: 1987.
4. For an excellent monograph see: *Topics in Fluorescence Spectroscopy* Vol. 1-6, Ed.: J.R. Lakowicz, Kluwer Academic / Plenum Publishers, New York: 1991-2000.
5. Herschel, Sir J. F. W. Phil. Trans. Roy. Soc. (London) 1982, 135, 143.
6. Stokes, G.G. Phil. Trans. R. Soc. (London) 1852, 142, 463.
7. 1) Eftink, M.R.; Jia, Y.-W.; Graves, D.E.; Wiczk, W.; Gryczynski, I.; Lakowicz, J.R. Photochem. Photobiol. 1989, 49, 725. 2) Green, S.A.; Simpson; D.J.; Zhou G.; Ho, P.S.; Blough, N.V. J. Am. Chem. Soc 1990, 112, 7337.
8. Umberger, J.Q.; LaMer, V.K. J. Am. Chem. Soc. 1945, 67, 1099.
9. The math leading to the expression for r can be found in ref. 1
10. Shinitzky, M.; Barenholz, Y. Biochim. Biophys. Acta. 1978, 515, 367.
11. Itagaki, H. in *Experimental Methods in Polymer Science, ed.: Tanaka, T; Chapter 3, Fluorescence Spectroscopy*.

CHAPTER 2

FLUORESCENT PROBES IN MACROMOLECULAR SCIENCE

In this chapter a few examples of fluorescent probes in polymer science are given. These examples have served as inspiration in the design of strain sensor (described in chapter three), and may be considered as background knowledge.

2.1 Introduction

The idea of using the high sensitivity of fluorescence in tracers and probes is not new. One of the earliest uses of fluorescent dyes dates back to 1877. In the Alps there is large limestone region with water-filled caves. At the time it was believed that there might be a subterranean connection between the Rhine and Danube Rivers in that particular region. To verify the hypothesis 10 kg of fluorescein where thrown into the Danube River and sixty(!) hours later the characteristic color of fluorescein was observed in a small river, with no visible connection to Danube. The small river is emptying into Lake Constance and from that into the Rhine. Thus the high sensitivity of fluorescence made it possible to establish the connection between the Danube and Rhine Rivers.

There are a number of reasons why fluorescence probes is a versatile and effective tool in the study of macromolecules. Fluorescence spectroscopy are a very sensitive technique (e.g. orders of magnitudes more sensitive that uv-vis), which makes it possible to keep the probe concentration very low, whereby the bulk properties of the investigated material is not altered by the probe itself. Furthermore, a number of different types of measurement can be done using fluorescence, such as steady-state emission, time resolved measurement in the picosecond range, fluorescence microscopy and confocal microscopy can produce images in two and three dimensions, anisotropy measurements can be used to investigate orientation, ordered domains etc. Thus there is a wealth of techniques available, each capable of providing unique information. In this chapter I have listed some representative cases chosen from the huge body of investigated systems.[1-3]

2.2 Pyrene

Pyrene is one of the most used fluorophores for a number of reasons: Pyrene has a long fluorescence lifetime (ca. 400 ns in argon purged tetradecane[4]) that forms a good basis for time resolved experiments, a relatively high quantum yield (0.32 in cyclohexane[5]), high tendency for excimer formation (explained below), well resolved from the monomer emission, hence easily detectable. Finally pyrene emission shows a number of peaks that are sensitive to solvent polarity.

Kalyanasundaram *et al.*[6] have made a very thorough study on influence of solvent polarity on the emission from pyrene. It was found that the intensity of the 0-0 transition increased at the expense of the other bands, most notably the 3rd vibronic band, in polar solvents. The ratio of vibronic band 1st and 3rd (I_1 / I_3) can thus be used to probe the polarity of the environment of pyrene. Chu *et al.*[7] studied the chain conformation of poly(methacrylic acid) (PMA) in aqueous solution. Pyrene was added to a solution of PMA and the pH was varied. At low pH values (<4) the polymer coils up. When the pH is increased the polymer tends to open up, to minimize the anionic repulsion between adjacent carboxylate. This could be followed by the I_1 / I_3 ratio: at low pH pyrene seek the less polar polymer environment and I_1 / I_3 = 1.0, but at higher pH pyrene is ejected into the water phase and I_1 / I_3 = 1.7. The effects of different surfactants were also investigated. By adding the cationic surfactant dodecyltrimethylammonium bromide (DTAB) to the solution a much smaller I_1 / I_3 ratio change was observed: only going from 0.9 to 0.7. Thus DTAB effectively prevents the chain opening at high pH (>8) values. On the other hand tetrabutylammonium iodide has almost no effect. Thus the long alkyl chain in DTAB is of paramount importance. Recently Tiera *et al.*[8] have conducted a similar study on the interaction between acrylic acid-ethyl methacrylate copolymers and sodium dodecylsolfate in water.

2.3 Probes based on excimer formation

Excimer fluorescence is one of the most studied probe principles. An excimer, as defined by Birks, is a dimer which is associated in an electronicly excited state, but is dissociative in its ground state.[9,10] When the excimer looses its excitation the association is no longer favourable and the species will dissociate. If the two species associating are different it is called an *exciplex*. A number of species form excimers, most notably "simple" aromatic molecules such as benzene, naphthalene, anthracene, pyrene etc. But also the noble gases form dimers in the excited state that may be defined as excimers. Excimer formation for an aromatic molecule and the corresponding fluorescence is illustrated below (see Figure 2-1).

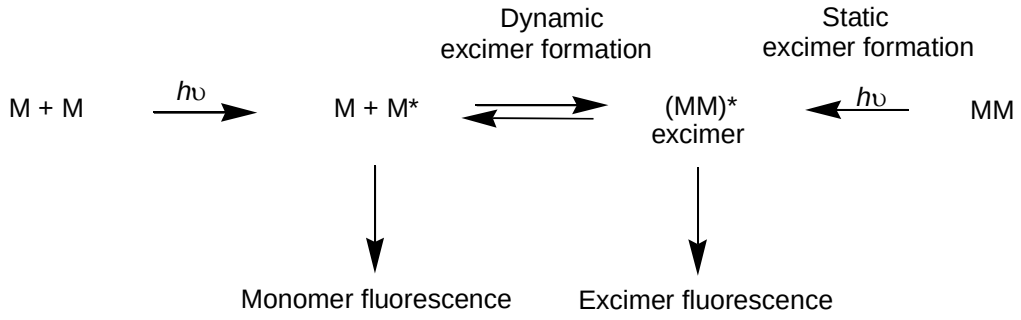

Figure 2-1. Dynamic and static excimer formation.

The time window for excimer formation is determined by the monomer lifetime, which may be reduced by quenchers etc. Whether the given time is enough to reach another monomer is dependent on concentration, viscosity etc. Static excimer formation refers to the situation where the molecules are held in a position conducive of excimer formation prior to excitation,[11] e.g. in crystals and other rigid systems.[12] The excimer fluorescence is redshifted with respect to the monomer fluorescence. Thus situations where the two monomers are in close vicinity, typically 3-4Å, can be spectroscopically distinguished from situations where they are isolated.

By attaching pyrene at each end of different polystyrenes (M_n = 3900, 6600 and 9200) Winnik *et al.*[13] was able to investigate the cyclization dynamics in toluene (see Figure 2-2). End-to-end distance is a fundamental property of polymers and is related to the preferred conformation of polymers. Whether intramolecular excimer formation forms depends on the diffusion rate of pyrene and the end-to-end distance at the time of excitation. As expected, intramolecular excimer formation increases with decreasing chain length, because the average end-to-end distance decreases. Also increasing temperature led to increasing excimer formation. This is a kinetic effect related to the reduced chain stiffness with increasing temperature.

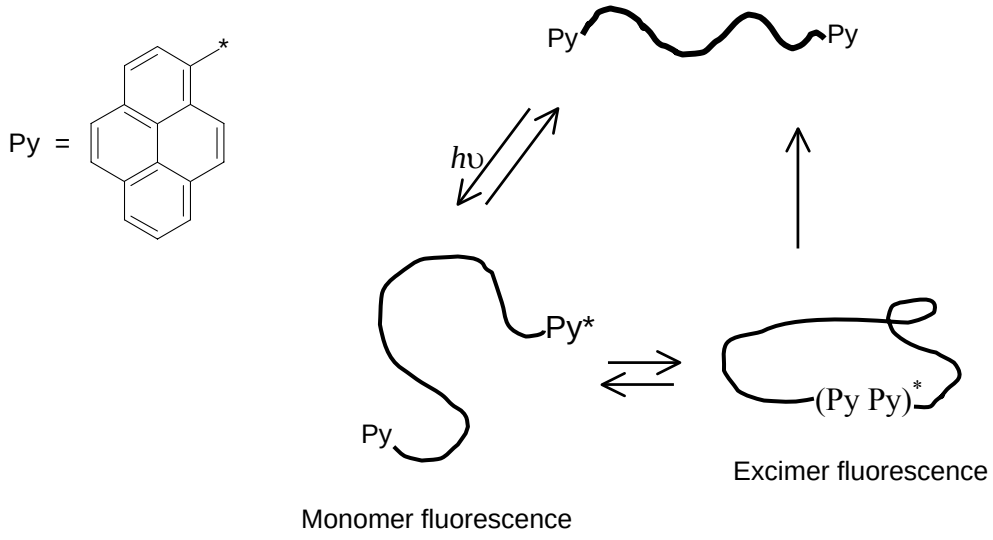

Figure 2-2. Dynamic excimer formation in a pyrene-polystyrene-pyrene system.

Zachariasse *et al.* [14-16] have conducted similar studies of much smaller systems (see Figure 2-3). In the ester system the excimer formation peaks at n=5 (corresponding to a total of 9 atoms between the pyrene units) and then slowly decreases.

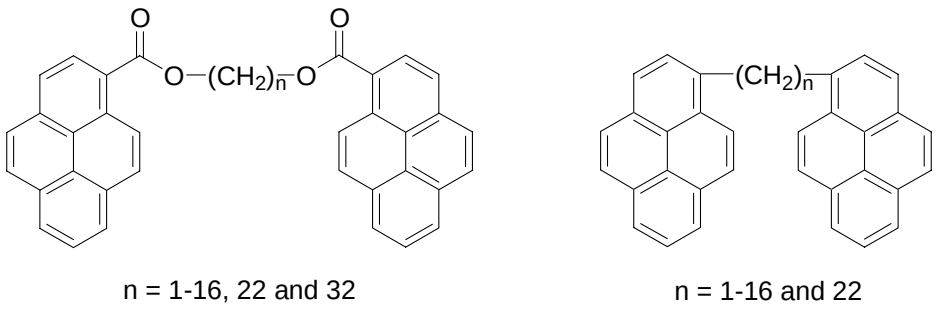

Figure 2-3. Pyrene dimers with two kinds of linkers.

In contrast to this, the excimer formation peaks at n=3 in the alkyl system, and then decreases sharply and approaches zero for n=6-10. At n=14 a new maximum is reached, and afterwards the excimer formation decreases slowly. The peak at n=3 has been referred to as the n=3 rule,[17] observed for a range of similar systems with different aromatic units. The very low excimer formation observed for medium sized alkyl chain length is compatible with the low yield often observed for ring-closure reactions of medium sized rings.

The same concept of connecting pyrenes at the end of chains can thus be used on both very large polymer systems but also on smaller macromolecules. In both cases valuable information has been obtained.

2.4 Excimer forming polymers

Poly vinyl-aromatics have aromatic groups on alternate carbon atoms, e.g. polystyrene. This 1,3 arrangement is optimal for excimer formation as described above. However, unlike in the case where the fluorophores are connected by a simple alkyl chain, different types of excimer may form depending on whether the aromatics are in a *meso* (isotactic) of *rac* (syndiotactic) arrangement with one another, i.e. the tacticity of the polymer. Poly(*N*-vinylcarbazole) (PVCz) and other carbazole containing polymers are some of the most studied excimer forming polymers.[18-25] Also, excessive studies have focused on model compounds, 2,4-dicarbazolyl pentanes and similar, of PVCz and other poly aromatics to investigate the dynamics of excimer formation of different isomers.[26-31]

Carbazole can form two excimer species: full overlap (emission is centred at 420nm) and partial overlab (emission is centred at 370nm). Vandendriessche *et al.* [27] have made a thorough study on the dynamic structure of *meso*- and *rac*- 2,4-di-*N*-carbazole pentane as well as 1,3-*N*-carbazole propane, using ^{1}H NMR and fluorescence data. The two *rac* and *meso*-isomer are interesting as models for isotactic and syndiotactic arrangement in polymers. In Figure 2-4 the two isomers of 2,4-di(*N*-carbazolyl) pentane are shown.

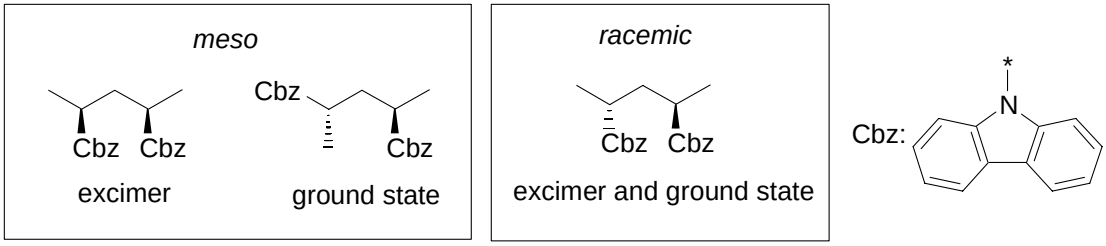

Figure 2-4. Excimer and ground state conformations of 2,4-bis(*N*-carbazolyl) pentane

In the ground state of the racmic isomer 89% has the conformation indicated on Figure 2-4, where one of the rings in each carbazole overlap (the remaining 11% adapts a conformation where the aromatic units do not interact). This conformation is conducive off partial excimer formation, and partial excimer can thus form upon excitation without any bond rotation or other structural change. The *meso* form may form a full overlap excimer with a structure similar to the one shown. But in the ground state the two carbazole units are rotated away from each other, so bond rotation is a prerequisite for intramolecular excimer formation.

Ikawa *et al.*[32] has made a study on the effect of strain on excimer formation in PVCz. To minimize intermolecular excimer formation the PVCz was dissolved in polystyrene (PS) in 0.1 wt-% (Figure 2-5). A film was cast from solution and then uniaxially stretched. When the film was stretched (0-1%) an increase in partial overlap excimer emission was observed. On the other hand no increase in full overlap excimer emission was observed. No time delay between monomer emission and partial excimer emission was observed using time resolved measurements. Thus the conformation giving rise to the partial excimer emission already exists prior to excitation. This is expected, since the ground state and partial excimer conformation is identical in the model compound, *rac*-2,4-di(*N*-carbazolyl) pentane. On the other hand, strain did not produce more of the full overlap excimer emission. The model compound, *meso*-2,4-di(*N*-carbazolyl) pentane indicates that bond rotation is necessary for full overlap excimer formation. Since the PS-PVCz film is a glass there is not much motional freedom of the individual chains. Moreover the rotation must be completed within the lifetime of the monomer emission. From these observation Ikawa concludes that strain increases the partial overlap of the syndiotactic dyads.

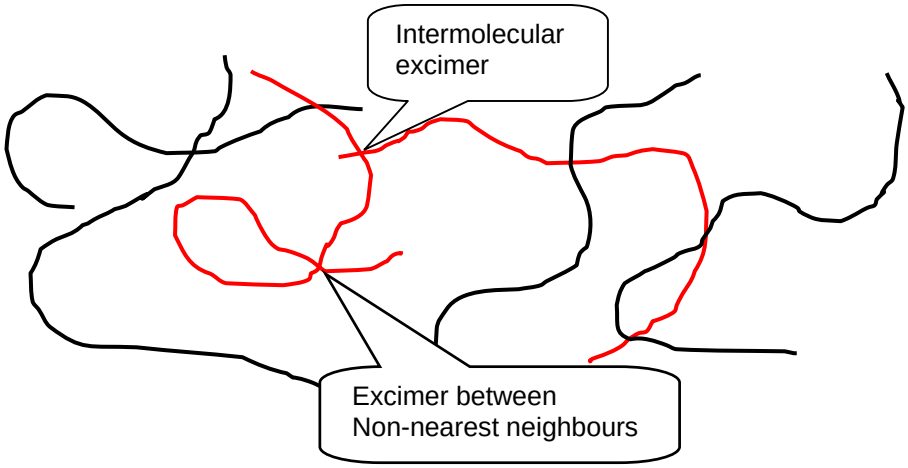

Figure 2-5. PVCz (red) dissolved in polystyrene (black). Beside excimer formation between nearest neighbours along the backbone of PVCz, excimer between non-nearest neighbours and intramolecular excimer formation may occur as indicated.

Recently Yang *et al.*[33] have conducted a similar study on copolymers of methyl methacrylate (MMA) and 1-naphthylmethyl methacrylate (NMMA) dispersed in poly(methyl methacrylate) (PMMA). Firstly, Yang found that a certain amount of fluorophore was demanded in order to observe excimer fluorescence. Of three copolymers with 0.59 mol-%, 22 mol-% and 57 mol-% naphthalene monomer only the later gave excimer fluorescence. To minimize intermolecular excimer formation less than 1 wt-% of the of the 57% naphthalene copolymer was mixed with PMMA. This sample showed an increase in excimer fluorescence when stretched (0-80%) at elevated temperature (80°C). Thus there seems to be good agreement with the PVCz experiment described above. However, interestingly enough when the homopolymer of PNMMA was dispersed in PMMA no change in the monomer-excimer ratio was observed upon elongation. From this Yang argues that the observed excimer fluorescence is not

primarily from nearest neighbours, but from non-nearest neighbours (see Figure 2-6). Yang suggests that the increased excimer formation stems from the denser packing induced by stretching the sample, which facilitates the close proximity of the aromatic units.

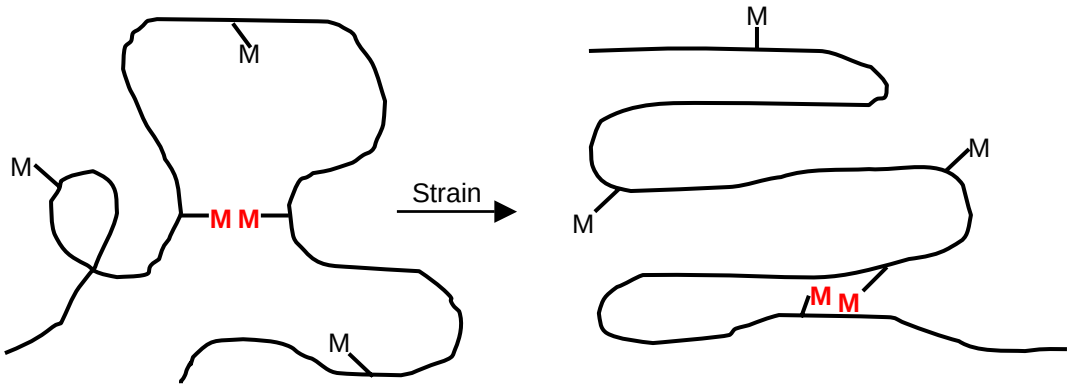

Figure 2-6. Proposed mechanism for strain induced excimer formation in naphthalene labelled PMMA. Isolated monomers (M = naphtyl) and monomer in excimer forming sites (red) are shown.

2.5 Twisted intramolecular charge transfer (TICT)[34,35]

Twisted intramolecular charge transfer (TICT) and excimer both belongs to a class of proceses called adiabatic photochemical reactions. The twisted intramolecular charge transfer (TICT) model was put forward to explain the "dual" florescence spectrum of DMABN[36] (di-methyl-amino-benzonitrile) and similar donor-acceptor molecules (see Figure 2-7).

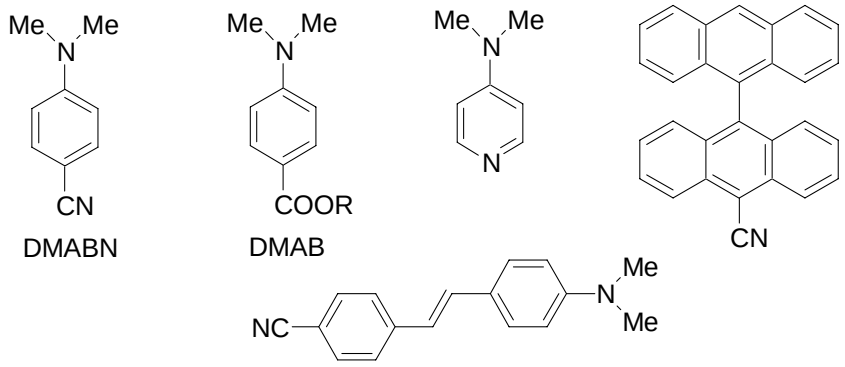

Figure 2-7. Donor-acceptor molecules forming TICT states upon excitation.

In these systems two fluorescence bands appear. For DMABN a "normal" band around 350nm and an "anomalous" band around 450nm occurs. In the ground state DMABN will prefer a planar arrangement that facilitates conjugation between the donor (the free electron pair on *N*) and acceptor unit. However upon excitation the donor unit transfers an electron to the acceptor system, and the methylamino group is free to rotate to minimize the steric repulsion between the methyl groups and π-system[37] (see Figure 2-8).

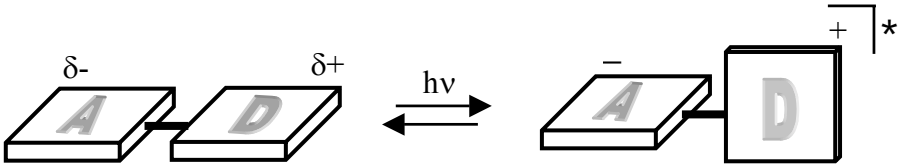

Figure 2-8. The TICT mechanism. The planar donor-acceptor system adapts a twisted structure upon excitation.

The "normal" B band stems from the planar structure and the "anomalous" A band from the TICT state. Immediately after excitation the molecule will be in the planar state, and then twist into the TICT state. This mother-daughter relation between the two states can be confirmed using time resolved fluorescence spectroscopy. Due to the charge separation, the TICT state is favoured in more polar media (solvatochromism) and can be used to monitor the polarity in the immediate surroundings.[38]

A certain amount of free space is needed in order for the molecule to twist into the TICT state. This has been exploited by Guo and Tazuke to measure the free volume in varying distances from the backbone in a number of poly(alkyl methacrylate)s using dimethylamino benzoates (DMAB) as probe(see Figure 2-9).[39,40] In solution the TICT state forms readily and the A band is 4-5 times more intense than the B band. Not surprisingly, the relative intensity of the A bands drops below 0.3 in the solid state. Guo and Tazuke observed that the relative TICT intensity increased gradually around T_g as expected.

Guo and Tazuke observed that the relative TICT emission increased with spacer length and plateaued as *y* approaches 12. At the same time the TICT emission decreased with increasing side chain length *x*. These findings are interpreted as the free volume around the polymer backbone decreases with increasing side chain length, which intuitively seems reasonable, and increases with increasing distance from the backbone.

Jager *et al.*[41] have used 4-(dimethylamino)-4'-nitrostilbene, another donor-acceptor molecule capable of TICT formation, to study the viscosity increase during photopolymerisation of dimethacrylates. As expected the increasing viscosity, that follows polymerisation, hamper the TICT formation and the intensity of the corresponding A band decreases. Lutfy has made a similar study on the polymerisation of polystyrene using *p*-(*N*,*N*-dialkylamino) benzylidene malononitriles.[42]

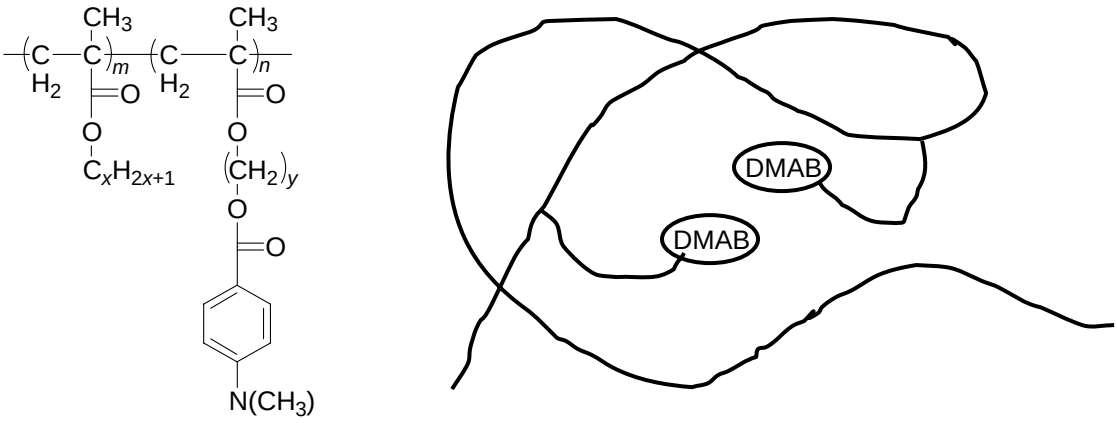

Figure 2-9. Left: the polymers synthesised. Right a schematic representation.

2.6 Anisotropy

As described in chapter one, polarized light can be used to measure orientation. The sample is excited with polarized light, and the relative intensity of horizontal and vertical polarized emission is measured. Monnerie and co-workes have studied the orientation of *cis*-1,4-polyisoprene networks using a number of anthracene derivatives (Figure 2-10, right).[43] The obtained results were correlated with anthracene incorporated into the polymer backbone (Figure 2-10, left).

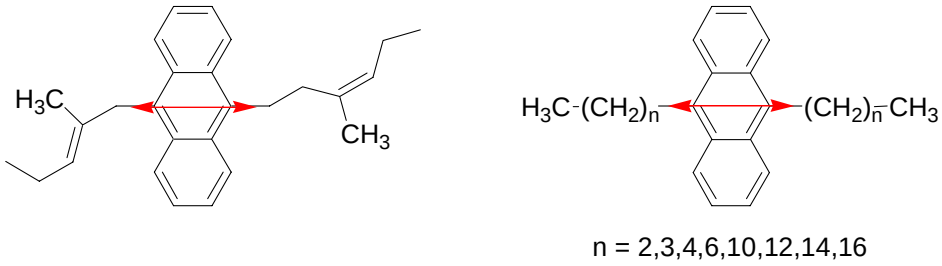

Figure 2-10. Left: Anthracene labelled polyisoprene. Right: Anthracene probes of different lengths. The red arrows symbolized orientation of the absorption moment.

Monnerie found that as *n* increases the measured anisotropy using the alkyl substituted anthracenes approaches the value obtained using anthracene in the polymer backbone. In general the best correlation was found for small strain values (0-300 %). For $n = 16$ the measure anisotropy is 0.6 of the maximum attainable at high strain levels. The maximum attainable is measured on the system depicted left. Extrapolating the data indicates that a perfect correlation should be reached as *n* approached 26 for high strain

values > 300%. Other similar systems has been investigated using the same principles.[44,45]

Bur *et al.*[46,47] have measured orientation when shear stress was applied to two samples of polybutadiene with varying amount of cetane (1-hexadecane). Again anthracene was incorporated into the polymer backbone. As the amount of cetane is increased the measured anisotropy decrease. This may be explained by the increasing entanglement molecular weight as more cetane is added. With a lower degree of entanglement the motional freedom of the anthracene labelled polymer is increased and not so sensitive to the direction of flow.

Other examples of the use of fluorescence anisotropy in polymerscience include the determination of the degree of order in important fibers such as poly(*p*-phenyleneterephtalamide)[48] (the commercial fiber kevelar 49) and poly(ethylene terephthalate) tapes.[49] Time resolved anisotropy measurement has also been carried out in the study of the dynamics of polymer segments in solid and solution.[50]

References and notes

1. For a comprehensive review of fluorescent probes in polymer systems see: Itagaki, H. in *Experimental Methods in Polymer Science*, ed.: Tanaka, T. Chapter 3, Fluorescence Spectroscopy, Academic Press: **2000**.
2. For a comprehensive review of fluorescent probes in solid polymers see: Itagaki, H; Horie, K.; Mita, I. *Prog. Polym. Sci.*, **1990**, *15*, 361.
3. Bokobza, L. *Prog. Polym. Sci.*, **1990**, *15*, 337.
4. Dyke, D.A.V.; Pryor, B.A.; Smith, P.G.; Topp, M.R. *J. Chem. Ed.* **1998**, *75*, 615.
5. *Handbook of Fluorescence Spectra of Aromatic Molecules*, Sec. Ed., Isadore B. Berlman, Academic Press, New York and London: **1971**.
6. Kalyanasundaram, K.; Thomas, J.K. *J. Am. Chem. Soc.* **1977**, *99*, 2039.
7. Chu, D-y.; Thomas, J.K. *J. Am. Chem. Soc.* **1986**, *108*, 6270.
8. Tiera, V.A.O.; Tiera, M.J.; Neumann, M.G. *J. Disper. Sci. Tech.* **2001**, *22(2&3)*, 177.
9. Birks, J.B. *Rep. Prog. Phys.* **1975**, *38*, 903.
10. For a book on excimers and the photophysics of organic molecules in general see *Organic Molecular Photophysics,* vol. 1-2, ed.: Birks, J.B. John Wiley & Sons: **1973**.
11. For en excellent review on pyrene and excimer formation see Winnik, F.M. *Chem. Rev.* **1993**, *93*, 587.
12. Staab, H.A.; Riegler, N.; Diedrich, F.; Krieger, C.; Schweitzer, D. *Chem. Ber.* **1984**, *117*, 246.
13. Redpath, A.E.C.; Winnik, M.A. *J. Am. Chem. Soc.* **1982**, *104*, 5604.
14. Zachariasse, K.A.; Maçanita, A.L.; Kühnle, W. *J. Phys. Chem. B* **1999**, *103*, 9356.

15. Zachariasse, K.A.; Kühnle, W. *J. Phys. Chem. B* **1976**, *101*, 276.
16. Zachariasse, K.A.; Duveneck, G.; Kühnle, W.; Leinhos, U.; Reynders, P. in *Photochemical Processes in Organized Molecular Systems, ed.: Honda, K. p 83,*
17. Klöpffer, W. in *Organic Molecular Photophysics,* vol. 1, chap. 7., ed.: Birks, J.B. John Wiley & Sons: **1973**.
18. Johnson, G.E.; Good, T.A. *Macromolecules* **1982**, *15*, 409.
19. Gallego, J.; Pérez-Foullerat, D.; Mendicuti, F.; Mattice, W.L. *J. Polym. Sci., Part B.* **2001**, *39*, 1272.
20. Shinzaburo, I.; Takami, K.; Yamamoto, M. *Makromol. Chem. Rapid Comm.* **989**, *10*, 79.
21. Skilton, P.F.; Ghiggino, K.P. *Polym. Photochem.* **1984**, *5*, 179.
22. Itoh, Y.; Nakada, M.; Satoh, H.; Hachimori, A.; Webber, S.E. *Macromolecules* **1993**, *26*, 1941.
23. Du, F.-S.; Li, Z.-C.; Hong, W.; Gao, Q.; Li, F.-M. *J. Polym. Sci., Part A.* **2000**, *38*, 679.
24. Grazulevicius, J.V.; Soutar, I.; Swanson, L. *Macromolecules* **1998**, *31*, 4820.
25. Sakai, H.; Itaya, A.; Masuhara, H.; Sasaki, K.; Kawata, S. *Polymer* **1996**, *37*, 31.
26. Schryver, F.C. De; Vandendriessche, J.; Toppet, S.; Demeyer, K.; Boens, N. *Macromolecules* **1982**, *15*, 406.
27. Vandendriessche, J.; Palmans, P.; Toppet, S.; Boens, N.; Schryver, F.C. De; Masuhara, H. *J. Am. Chem. Soc.* **1984**, *106*, 8057.
28 Evers, F.; Kobs, K.; Memmig, R.; Terrelli, D.R. *J. Am. Chem. Soc* **1983**, *105*, 5988.
29. Zachariasse, K.A.; Duveneck, G.; Kühnle, W.; Reynders, P.; Striker, G. *Chem. Phys. Lett.* **1987**, *133*, 390.
30. Zachariasse, K.A.; Duveneck, G.; Kühnle, W. *Chem. Phys. Lett.* **1985**, *113*, 337.
31. Reynders, P.; Dreeskamp, H.; Kühnle, W.; Zachariasse, K.A. *J. Phys. Chem.* **1987**, *91*, 3982.
32. Ikawa, T.; Shiga, T.; Okada, A. *J. Appl. Polym. Sci.* **1997**, *66*, 1569.
33. Yang, L.; Li, H.; Wang, G.; He, B. *J. Appl. Polym. Sci.* **2001**, *82*, 2347.
34. For an excellent review see Rettig, W. *Angew. Chem. Int. Ed. Engl.* **1986**, *25*, 971.
35. For an excellent review see Rettig, W. in *Top. Curr, Chem.*, **1994**, *169*, 254.
36. Rotkiewicz, K.; Grellmann, K.H.; Grabowski, Z.R.; *Chem. Phys. Lett.* **1973**, *19*, 315.
37. Besides twisting other mechanisms may be involved, see for example Rettig, W.; Zietz, B. *Chem. Phys. Lett.* **2000**, *317*, 187.
38. For an example see Nag, A.; Bhattacharyya, K. *Chem. Phys. Lett.* **1990**, *169*, 12.
39. Guo, R.K.; Tazuke, S. *Macromolecules*, **1989**, *22*, 3286.
40. Guo, R.K.; Tazuke, S. *Macromolecules*, **1990**, *23*, 719.
41. Jager, W.F.; Volkers, A.A., Neckers, D.D. *Macromolecules*, **1995**, *28*, 8153.
42. Lutfy, R.O. *Pure & Appl. Chem.***1986**, *58*, 1239.
43. Queslel, J.P.; Jarry, J.P.; Monnerie,L. *Polymer*, **1986**, *27*, 1228.
44. Queslel, J.-P., Erman, B; Monnerie, L. *Polymer*, **1988**, *29*, 1818.
45. Jarry, J.P.; Monnerie, L. *J. Polym. Sci.: Polym. Phys. Ed.* **1980**, *18*, 1879.
46. Bur, A.J.; Lowry, R.E.; Thomas, C.L.; Roth, S.C.; Wang, F.W. *ANTEC* **1992**, 2088.

47. Bur, A.J.; Lowry, R.E.; Thomas, C.L.; Roth, S.C.; Wang, F.W. *ANTEC* **1991**, 842.
48. Chapoy, L.L.; Spaseska, D.; Rasmussen, K. *Macromolecules* **1979**, *12*, 681.
49. Nobbs, J.H.; Bover, D.I.; Ward, I.M.; Patterson, D. *Polymer* **1974**, *15*, 287.
50. Soutar, I.; Jones, Craig.; Lucas, M.D.; Swanson, L. *J. Photochem. Photobiol. A: Chemistry* **1996,** *102*, 87.

CHAPTER 3

A MECHANICAL STRAIN SENSOR FOR POLYMERIC MATERIALS

This chapter describes most of the work I have performed during my three years of Ph.D.-study at Risø. The short version is given in the paper *Mechanical strain sensing in a SIS type elastomer with single site strain probes based on carbazole* in appendix 1. This is the long version.

3.1 Introduction

The degree of deformation (strain) observed when a given force (stress) is applied to a polymeric material, and the relationship between deformation and force are a fundamental property of polymeric materials. A number of methods exist to investigate this relationship on a macroscopic level (rheology measurements etc.). However, the molecular processes that parallels macroscopic deformation is not well understood. A tool that allows measurement of the molecular changes when the material is strained or stressed may produce new insight into the structure-property relationship of polymeric materials, and lay ground for new advanced polymer based materials. In addition, the current theory of rubber elasticity and molecular deformation might be experimentally probed. The goal of this Ph.D.-project was to develop a fluorescent sensor that could be used to investigate the molecular changes that follows macroscopic strain.

Considering a material being uniaxialy stretched, the tensile strain, ε, is defined as change in length, *l*, of the sample:

$$\varepsilon = \frac{\Delta l}{l}$$

The stress used to produce the tensile strain, σ, is the force applied, *F*, divided by the cross-sectional area, *A*:

$$\sigma = \frac{F}{A}$$

in units newtons per square meter (SI). Tensile strain and tensile stress is related through the tensile modulus, *E*;

$$E = \frac{\sigma}{\varepsilon}$$

The modulus is the resistance to strain. Since tensile strain is dimensionless, tensile modulus gets the same units as tensile stress. Below is the tensile stress plotted as function of tensile strain for a typical elastomer.

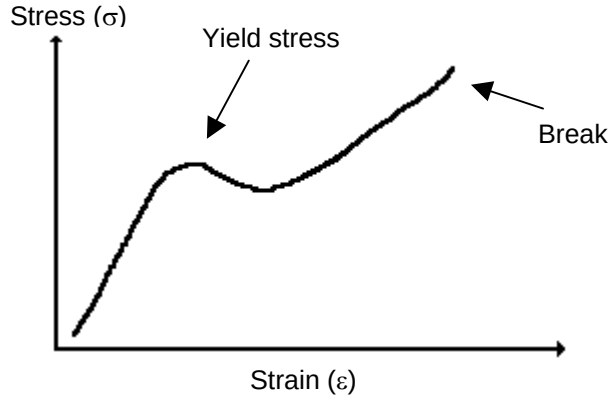

Figure 3-1. Tensile stress-strain behaviour of a typical elastomer.

As the material is progressively strained, higher levels of stress is necessary, as expected. At a certain level of stress the material deforms or yields. At this point enough stress has been applied to untangle the polymer chains, and they start to flow past each other. As a consequence, deformation above the yield point is irreversible. It is important to notice that in general, increasing stress leads to increasing strain, except around the yield point.

According to the theory of rubber elasticity, elongation of an elastomer causes the polymer chains to be oriented (Figure 3-2, top). This diminishes the pool of available conformations, and causes a decrease in entropy accompanying the stretching (Figure 3-2, bottom).

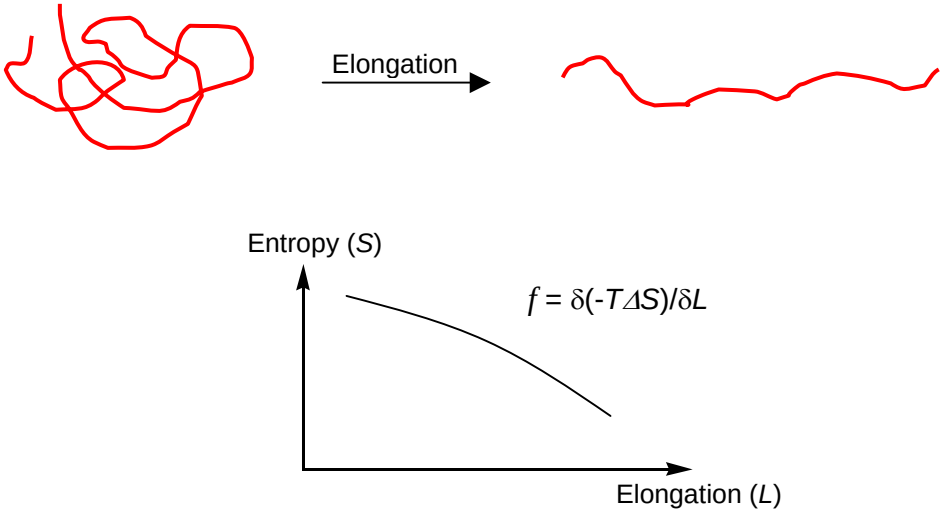

Figure 3-2. Entropy-driven elasticity of rubber materials. The figure has been adopted from ref. 1.

This entropy change is the primary driving force in rubber elasticity, although entropy is not the sole contribution involved. The force *f* acting on a rubber network that produces a certain elongation (strain), δL, can be expressed as a sum of two terms:[1]

$$f = \left(\frac{\delta E}{\delta L}\right)_{p,T} - T\left(\frac{\delta S}{\delta L}\right)_{p,T}$$

The first term is related to change in the internal free energy (δE) of the polymer chain with elongation. The second term is related to the entropy change (δS) with elongation. The fact that a polymer chain has a large amount of isoenergetic conformations to choose from is the reason why the internal energy only increases relatively little. This is especially so at low strain values. For example in the case of natural rubber the first term in equation 1 contributes less than 20% to *f* at low strain levels.[2] However at higher strain levels large segments may be forced into high-energy conformations upon stretching, and the internal energy may contribute more to *f*.

We speculated that by placing a strain sensitive sensor unit in the polymer backbone it might be possible to measure the molecular strain. Also, if the sensor unit is forced into a high-energy conformation it might be possible to investigate the changes in internal energy of the polymer chain. On a molecular scale, stress is primarily transferred through the polymer backbone (think of the superior strength of fibres due to the orientation of the polymer chains), hence it is anticipated that the sensing unit should be part of the backbone to elucidate on mechanical stress most successfully (as opposed to the TICT molecules attached on side chains, in the free volume study described in chapter two). Yang *et al.*[3] and Ikawa *et al.*[4] have used fluorescent polymers to monitor strain (also described in chapter two). Thus the sensing unit is indeed part of the

polymer backbone, however two fundamental problems remains. The measurements are due to the sensor polymer, since it is the sensor that fluoresce, and not the bulk polymer. To which degree the obtained result mirrors the changes in the bulk material depends on the similarity between the bulk polymer and the sensor polymer, i.e. flexibility of the polymer backbone, T_g, miscibility, chain length etc. Thus PVCz may be a good sensor in polystyrene, but poor in the aliphatic polyethylene due to low miscibility or other deficiencies. This also makes it very difficult to compare data obtained in different systems. The other fundamental problem is that it is not clear what causes the change in fluorescence emission: Ikawa *et al.* concludes that interaction between nearest neighbours is responsible of excimer formation in PVCz, while Yang concludes that interactions between non-nearest neighbours play a key role in excimer formation in the naphtyl labelled methacrylates. Further, different parts of the polymer might have different fluorescence properties. Indeed Johnson *et al.* found that the emission properties of PVCz is molecular weight dependent.[5] But also the different parts of the polymer might have different response to strain, e.g. towards the ends where low levels of entanglement makes the chain inclined to slip when strained. Finally, intermolecular interactions cannot be completely rule out, even though the sensor polymer is in low concentration. When two polymers of different chemical composition are mixed they tend to coil up or even phase separate. This favours intermolecular interactions as well as non-neighbour interactions. Thus a mix of interactions will be present, which complicates the interpretation of the observed fluorescence.

From these considerations we concluded that in the optimal probe, emission should originate from one well-defined position in the polymer, and that the probe should be identical, or nearly identical, to the bulk material. In Figure 3-3 a schematic concept of a single site sensor outlined.

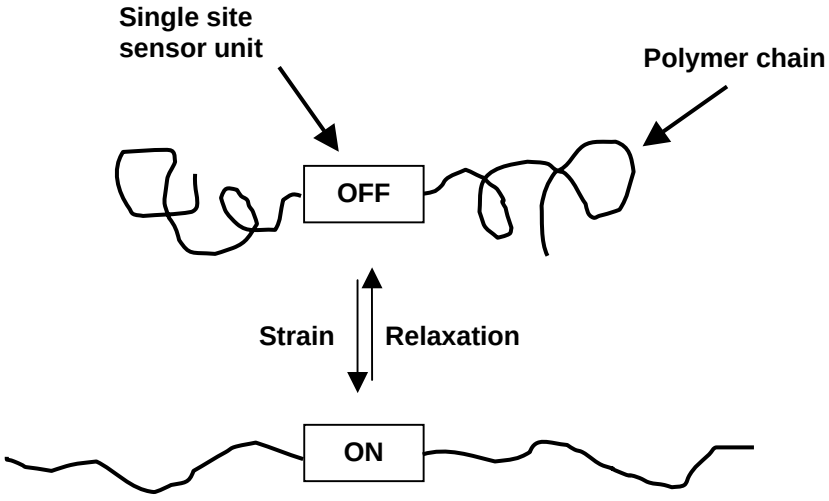

Figure 3- 3. The The sensor unit changes emission upon strain from ‘off’ to ‘on’.

The fluorescent sensor unit is placed in the middle of the probe. When strained the sensor unit will change its fluorescence emission in a well-defined way: from 'off' to 'on'. From a spectroscopic viewpoint the 'on' and 'off' fluorescence should be well resolved, this is especially important when small changes are measured. In the PVCz case investigated of Ikawa *et al.* the 'on' and 'off' corresponds to excimer fluorescence and monomer fluorescence respectively.

Single site strain sensors will be more synthetically demanding than simple polymer sensors, constructed from a fluorescencent monomer like PVCz, since they are built from separate different units that have to be assembled in discrete steps. However, several advantages of this design are envisaged. The polymeric end groups may (at least in theory) be comprised by any type of polymeric (or oligomeric) residue and one can therefore choose groups that are miscible with commercially interesting bulk polymers. Since the signal observed originates from a single site in each probe molecule a simpler response function can (in principle) be obtained. In addition, one can imagine the sensor unit can be placed in different parts of a polymer (or block-co-polymer) and relate properties to different parts (or blocks) of the bulk polymer.

3.2 Design of the sensor unit

A sensor unit based on monomer-excimer fluorescence as the 'on'-'off' signal could consist of two aromatic moieties, like the fluorophores carbazole or pyrene (see chapter two). The aromatic groups should be connected via a small bridge. In the simplest case two conformations exist: one with a face-to-face contact between the two aromatic units and another where these are splayed (Figure 3-4). When the units are splayed the fluorescence spectrum of the isolated carbazole or pyrene units is observed. When the units are in a face-to-face arrangement, the excimer type fluorescence is seen. With the correct choice of bridge (length and steric rigidity) the relaxed ground state excimer fluorescence will be observed. But when the material is strained this will be translated to the molecular level splaying the two fluorophores resulting in the usual fluorescence observed for the isolated fluorophores.

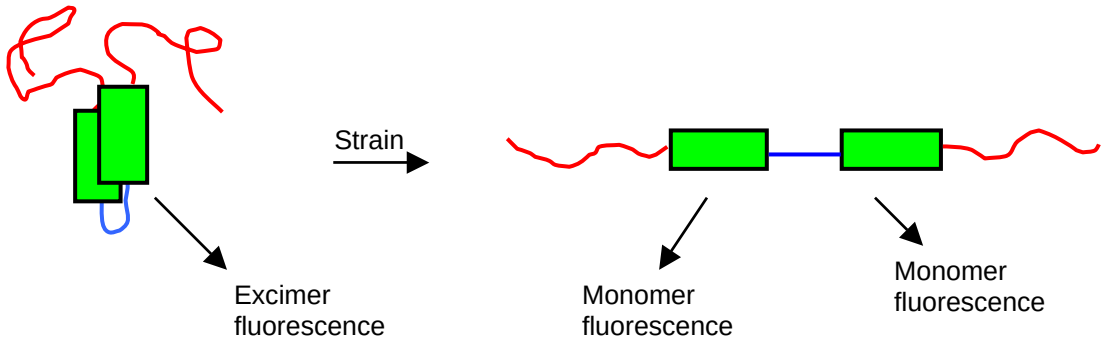

Figure 3-4. Schematic representation of a sensor unit with two aromatic moieties. The two fluorophores (green) are connected by a short bridge (blue) and two larger polymeric ends (red). In the ideal case the relaxed molecule will be in the conformation shown to the left with the chromophores in a conformation that allows excimer formation. When strain is applied, the chromophores are splayed and only monomer fluorescence is seen.

In the transition depicted in Figure 3-4 the sensor unit is strained. The molecular strain can be derived from the elongation of the sensor unit. It is more difficult to measure the change in internal free energy (δE). However, if it is known which conformation the sensor unit adopts before and after strain, along with the relative energy of these conformations, it might be possible to relate the energy difference of the two conformations to the internal energy of the polymer chain.

Two examples of the excimer sensor have been considered during this project differing mainly in the choice of fluorophores (Figure 3-5). The first case is based on pyrene units where the attachment points for the two polymer chains was chosen to be at two bridge atoms instead of other sites on the pyrene units. This arrangement allows for an easier synthetic target. The other sensor unit is based on carbazole moieties as the chromophores. The bridge unit was chosen to be three atoms long and connected at each end to the nitrogen atoms in the two carbazoles. The attachment points for the polymer ends was chosen to be the 3- and 3’ positions in the carbazole units.

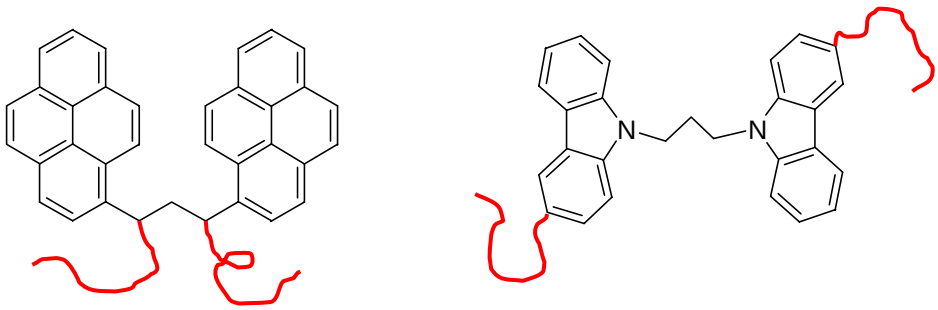

Figure 3-5. Synthetic targets of the excimer type sensors with either pyrene (left) or carbazole (right) units. The polymer chains are shown in red.

The synthetic strategy for assembling the single site sensors outlined in Figure 3-5 is to build them from the inside out. A first step would be to link the two fluorophoric units to the bridge component, which could then be purified easily as a small molecular weight compound. Lastly, the outer polymeric chains should be attached using a very efficient coupling reaction in order to minimize any unreacted or partly reacted sensor material that would confuse the interpretation of the emission spectra. Monnerie and co-workers have developed an attractive methology for the successful attachment of two polyisoprene groups to anthracene.[6] Polyisoprenyl anions were prepared by living anionic polymerisation and these anions where then quenched with the electrophilic 9,10-di(bromomethyl)-anthracene. Thus a single anthracene unit was incorporated in the middle of polyisoprene. The prepared polyisoprene was finally cross-linked resulting in a rubber. Rubber is a favourable material in this context because it allows strain levels up to 1000%. Thus a very large working range is available, compared to the brittle PS glass used by Ikawa that only allows less than 1% strain. However with the curing procedures normally used to prepare a rubber, there is little or no control over the exact cross-linking positions. Thus an amount of uncertainty is introduced when the material is cross-linked. One can imagine that a sensor unit between two closely spaced cross-linking positions might experience different strains than in a situation where there cross-linking positions are far from each other.

To keep the system as well defined as possible we decided to synthesize PS-PI-PS triblock copolymers (SIS) with the sensor unit in the middle of the PI block. These materials are elastomers and can be stretched by a factor of more than ten. The microstructure of the SIS elastomers is well known.[7] If the styrene component is less than 30 wt-% the two blocks separates to form PS domains (the Mw of PS must be >6000 to phase seperate) of spherical symmetry surrounded by a matrix of interconnecting PI chains (see Figure 3-6). If larger amounts of PS are present, the PS domains may adopt a lamellae or rod like structures. When this material is stretched at room temperature, the PS domains ($T_g \approx 100°C$) behaves as rigid bodies that serve as physical crosslinking points. Thus most or all of the strain develops in the PI blocks (the PS domains deforms only a little).

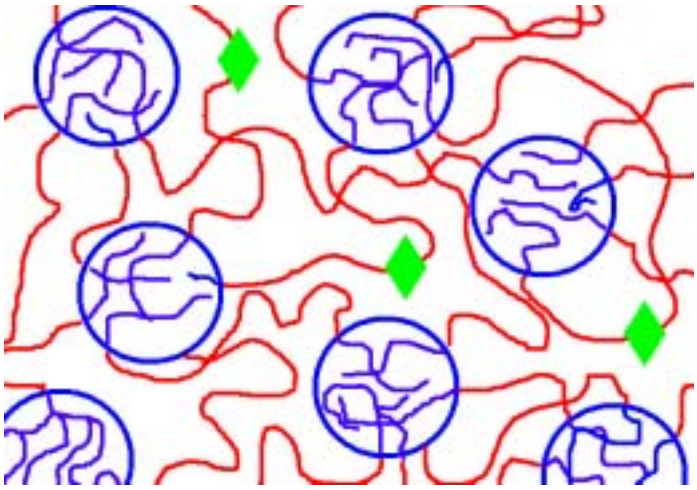

Figure 3-6. The microstructure of the prepared SIS triblocks. The blue spheres are the PS domains, the PI domain is red and the green diamonds symbolizes the sensor units.

3.3 First attempt towards a single site sensor

Our initial idea was to use pyrene as the aromatic moiety in the sensor unit. Pyrene can give strong excimer fluorescence, well resolved from the monomer fluorescence, which is ideal in a sensor context. This makes it easy to distinguish between the relaxed and strained situation. Zachariasse[8-10] and co-workers have made extensive studies of 2,4-bis(2-pyrenyl) pentane, and the conformational distribution in solution. They found that the ground state conformation of *meso*-2,4-di(2-pyrenyl) pentane consisted of 94% *trans-gauge* (TG, see Figure 3-7). In this conformation the pyrene units cannot interact and excimer formation will not readily take place.

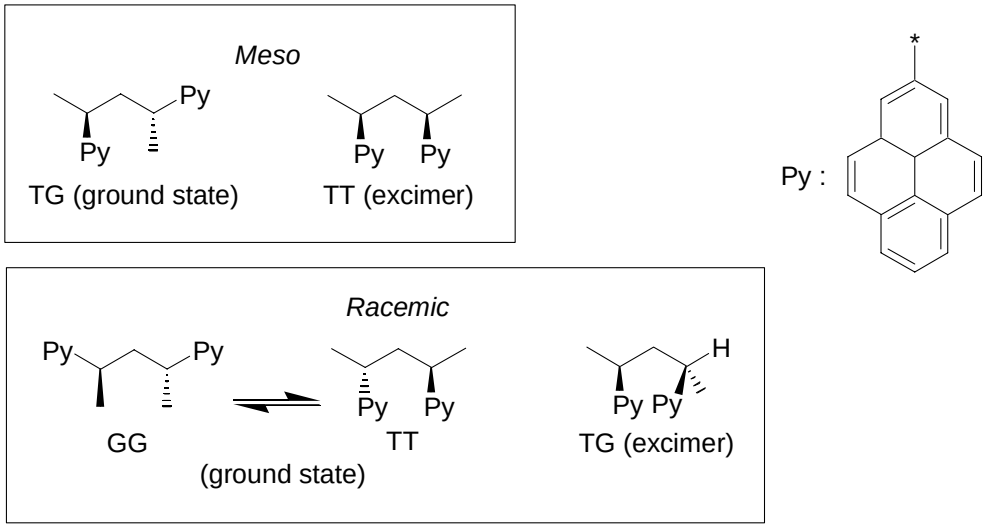

Figure 3-7. Ground state conformations of *Meso*- and *rac*-2,4-di(2-pyreneyl) pentane. The excimer conformation of the *meso* isomer corresponds to the TT conformation, while the excimer conformation of the *racemic* isomer corresponds to the TG conformation.

If polymer chains replace the methyl groups, one can imagine that with increasing levels of strain, the excimer forming TT conformation will be increasingly favoured, since in this conformation the polymer chains are splayed the most (notice that this is the reversed of the situation depicted on Figure 3-4). The *meso* isomer thus seems to be ideal as the central part of a sensor unit.

The *racemic* isomer is less favourable. In the ground state, equilibrium between the TT and GG conformation exist, neither of which is conducive to excimer formation. In the TT conformation the methyl groups are most splayed and is thus expected to be the more favoured conformation with increasing strain. Hence strain is not expected to change the monomer/excimer fluorescence ratio. However, it cannot be ruled out that strain will change the emission, but as opposed to the *meso* isomer, the mechanism is not clear. Note that the ground state conformation of the two isomers is similar to the ground state conformation of corresponding carbazole compound (Figure 2-4).

Looking at the structure of *meso*-2,4-(2-pyrenyl) pentane two potential problems comes to mind. How is the meso isomer to be synthesised or isolated from the racemic isomer. and how is the polymer going to be attached. Reynders *et al.* separated the meso and racemic derivatives of 2,4-(2-pyrenyl) pentane using HPLC,[10] so it might be possible to use this technique also on a more elaborate sensor molecule.

In the synthesised sensor molecule, two functional groups capable of terminating the living polymers must be present. Chlorosilanes has often been used to terminate or couple anionic living polymers. However these groups are very reactive, and are difficult to handle, e.g. moisture has to be rigorously excluded etc. Primary halogens are less labile but still effective electrophiles and more preferable.

A possible route to the central bis-pyrene structure with a C-3 bridge and primary alkyl halogen groups for the latter attachment of polymer groups is shown in Scheme 3-1. Note that pyrene groups substituted in the 1-position are used. Ideally 2-substituted pyrene would be preferred to avoid an added complication of different rotamers that might confuse the interpretation of the emission spectra as noted by Winnik.[11] It is however, far easier to use 1-substituted pyrene from a synthetic view point.[12] In order to test the feasibility of the synthetic scheme this isomer was used.

Treating pyrene with *N*-bromo-succinimide (NBS) afforded 2-bromo-pyrene according to the literature procedure.[13] Bromine-to-lithium exchange with butyl lithium in THF followed by reaction with undecen-1-al gave the unsaturated alcohol **3**. Reaction with *p*-Tosyl chlorid using standard conditions gave the corresponding Tosylated compound **4** that was utilized as an electrophile with the anion of 1,3-dithiane to give compound **5**. Unfortunately all attempts to substitute **5** with one more equivalent of **4** to give the bis-pyrene compound **6** failed. The probable reason is the increased steric hindrance at the nucleophilic center of **5**. A number of other synthetic routes were attempted, but all failed at the final assembly. In general steric hindrance as well as the low nucleophilicity of lithium pyrene was major obstacles. It should also be noted that reasonable overall yields of **8** is necessary for optical purification and the final coupling reaction.

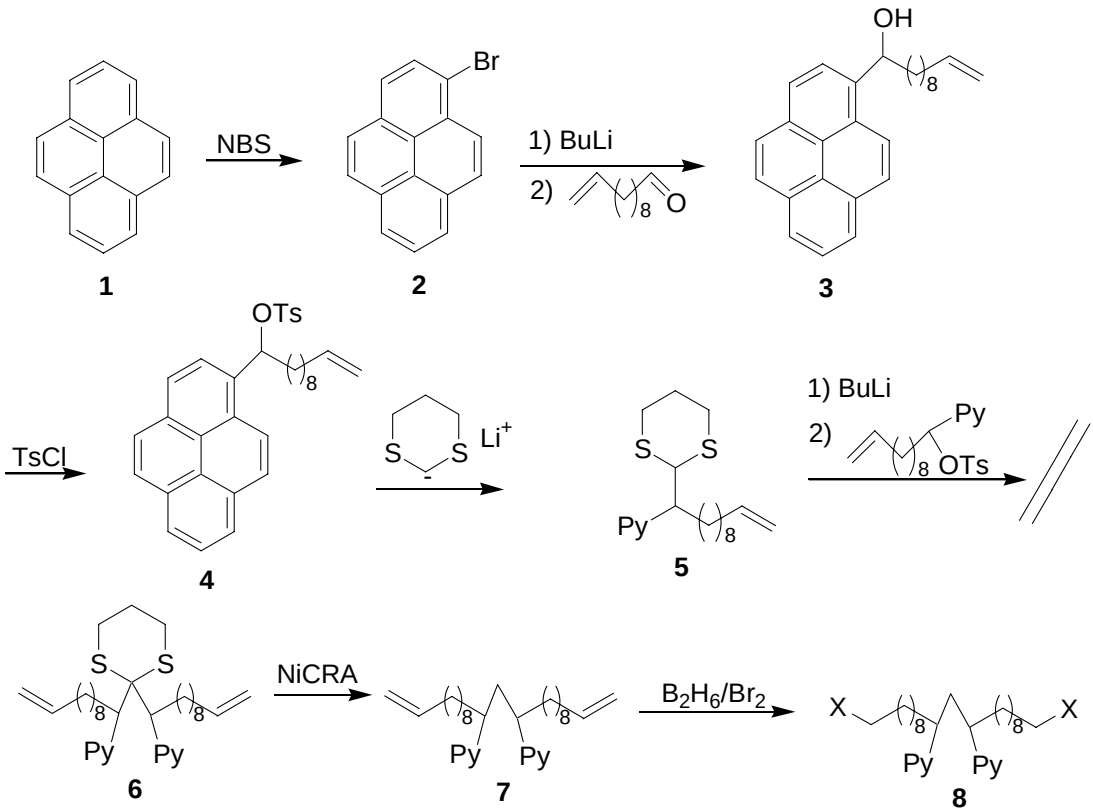

Scheme 3-1. Proposed synthetic route to a bis-pyrene. (NiCRA is a reducing nickel complex).

3.4 A single site sensor based on carbazole

3.4.1 Introduction

Having abandoned pyrene we considered carbazole as the fluorophore. Comparing the two fluorophores, carbazole is more attractive than pyrene to the synthetic chemist for two reasons: cabazole has an inbuilt *N*-functionality that can easily be functionalised and carbazole posses lower symmetry, which makes regioselective synthesis more accessible. However the fluorescent properties of carbazole are not equally attractive. The main difference is that the monomer emission is not well resolved from the partial overlap excimer emission. Also, carbazole has a shorter fluorescence lifetime than pyrene, with a corresponding smaller time window for time resolved measurements. However the prime focus was to synthesis a sensor system that actually worked, and the non-ideal optical properties was considered to be a minor problem.

Shown below are the spectra of the absorbance, monomer and partial excimer emission of carbazole. Notice that the partial excimer emission overlaps with the monomer emission. The full overlap excimer is centred around 420nm. It should be noted that even in 1M solution of carbazole the major signal is the monomer fluorescence, and emission of the two excimers has been acquired on 2,4-bis(*N*-carbazole) pentane that favours intramolecular carba zole-carbazole interactions. This is in contrast to pyrene where intermolecular excimer formation is evident in 10^{-3}M solution.[14] This shows the relative weak tendency of carbazole to form excimers compared to pyrene.

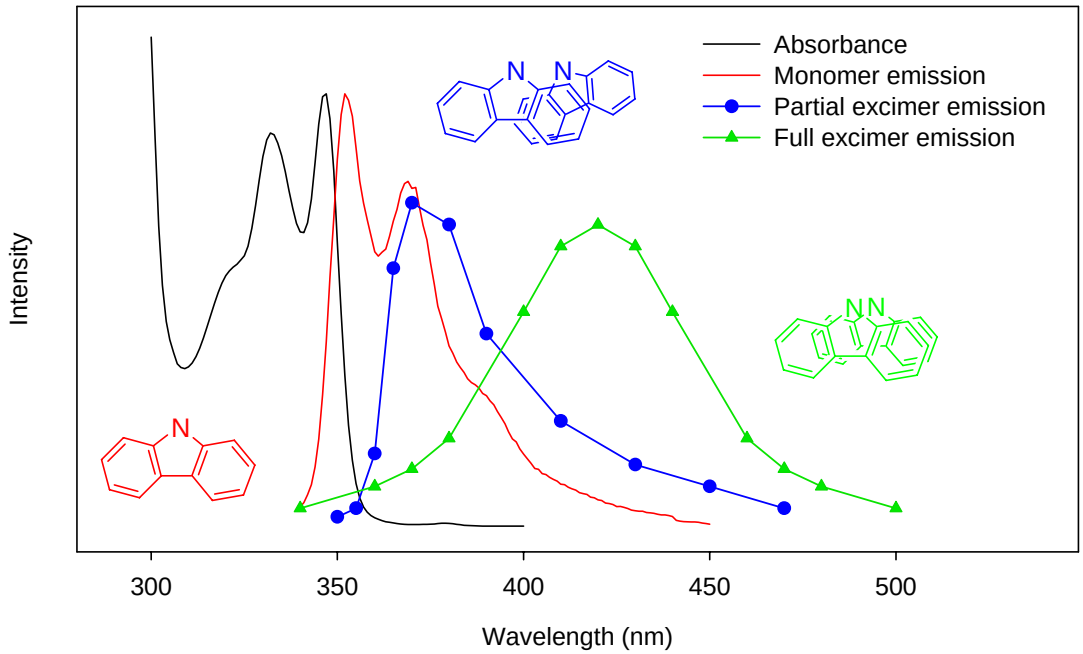

Figure 3-8. Absorption spectrum of *N*-propyl carbazole and emission spectra from isolated carbazole (red), partial overlap excimer (blue) and full overlap (green) is shown. Absorbance and emission of *N*-propyl carbazole was obtained in chloroform (10^{-5}M). Excitation wavelength was 330nm. Notice the mirror symmetry between absorbance and monomer emission. The spectra of partial and full overlap excimer emission has been adopted from ref. 15.

In Figure 3-9 the two isomers of 2,4-di(*N*-carbazolyl) pentane is shown (also described in chapter two). *Meso*-2,4-bis(*N*-carbazolyl) pentane has the same conformational distribution and optical properties as *meso*-2,4-bis(1-pyrenyl) pentane, discussed above.[15] Again strain is expected to favour a transition from the ground state conformation to the excimer conformation.

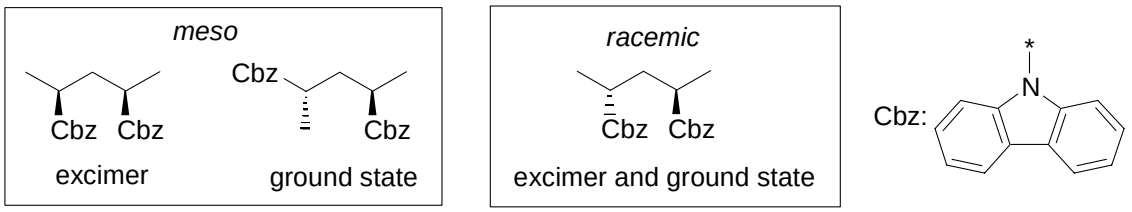

Figure 3-9. The conformation of *meso*- and *rac*-2,4-bis(*N*-carbazolyl) pentane. The figure is also shown en chapter two.

Meso-2,4-bis(*N*-carbazolyl) pentane was our original target molecule, however Evers *et al.* found that the preparation of 2,4-bis(*N*-carbazolyl) pentane through substitution of 2,4-ditosyl pentane was very difficult.[16] Indeed the more nucleophilic 1,2,3,4,10,11 hexahydrocarbazole was needed in order to complete the reaction. The compound could then be aromatizied in a later reaction step. Thus a synthetic route, similar to the one tried with pyrene, based on carbazole might very well prove to be equally fruitless. However, we did try with the corresponding iodo and bromo compounds (Scheme 3-2), and varying bases and solvents, but all attempts failed. Only one carbazole unit could be attached using this strategy.

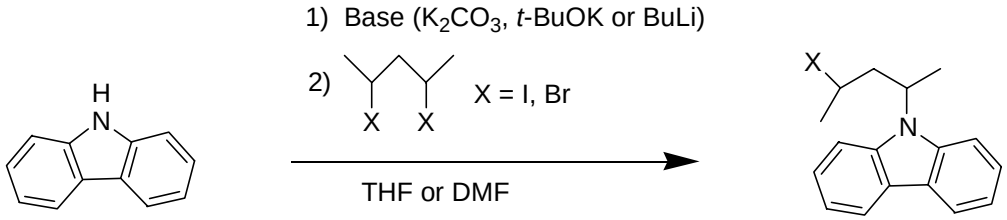

Scheme 3-2. Proposed synthetic route to a bis-pyrene.

3.4.2 A new linker

Having abandoned pentane as bridge between the two carbazole units, we looked for other carbazole linkers that would potentially favour excimer interactions. Preferably, carbazole should be attached at a primary carbon atom that facilitates nucleophilic substitution. We speculated that 1,3-di(9-carbazolyl)-2,2-dimethyl propane might posses a ground state conformation where the two aromatic groups where placed in an

excimer conducive face-to-face arrangement, due to the steric repulsion between the methyl groups and the aromatic units. This would be similar to *rac*-2,4-di(*N*-carbazolyl) pentane that has a ground state conformation similar to the partial excimer conformation. The polymer chains must be attached in a way that changes the ground state conformation upon strain. Accepting that the ground state conformation is conducive of excimer formation, strain must splay the aromatic units. Since carbazole is easily monobrominated at the 3-position, it seemed reasonable to attach the polymers at this position. In 1,3-di(*N*-carbazolyl)-2,2-dimethyl propane with two polymer chains attached is depicted. The ground state conformation (left) was anticipated to be capable of excimer formation (full or partial overlap). But with increasing strain, conformations with the carbazole units splayed should be increasingly favoured.

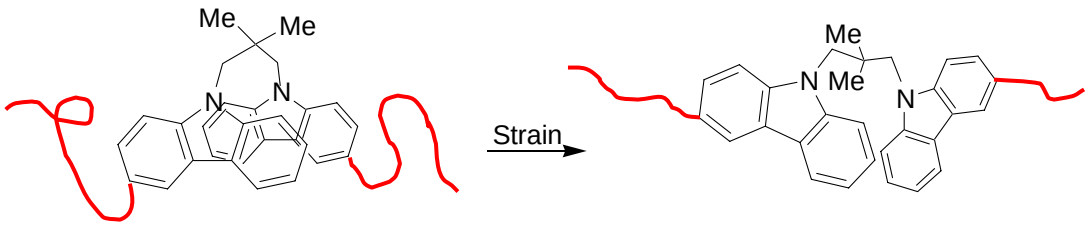

Figure 3-10. 1,3-di(*N*-carbazolyl)-2,2-dimethyl propane with two polymer chains (red) attached. With strain the conformation to the right was expected to be favoured.

The synthetic strategy consisted of monobrominating carbazole, linking the carbazoles using an appropriate bridge and finally transforming the bromo compound into a derivative with electrophiles capable of reacting anionic polymers. In the present work we have prepared and investigated four different single-site probes based on this concept. Two diblock polystyrene-polyisoprene (PS-PI) units were linked to either one carbazole group through the 3 and 6 positions (probe **10**) or to the 3 and 3' positions of a carbazole dimer (probes **11**, **12** and **13**). In the latter cases propyl groups were used to bridge the carbazole units via the nitrogen atoms. (See Figure 3-11).

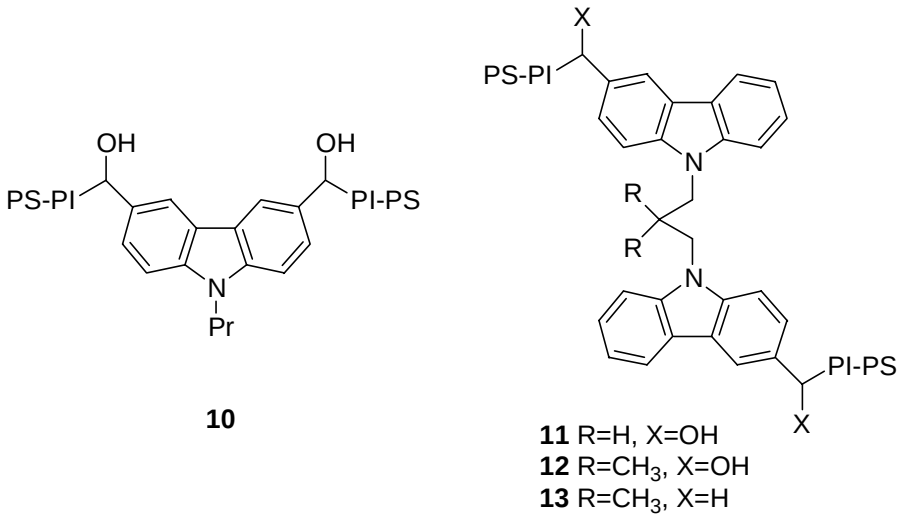

Figure 3-11. Single site probes prepared in this study, with one or two carbazole units linked to PS-PI elastomer groups.

3.4.3 Synthesis

The preparation of the three bis-carbazole sensors is outlined below (Scheme 3-3). 2,2-Dimethyl-1,3-propanediol was reacted with *p*-tolenesulfonyl chloride to prepare the corresponding reactive tosyl esters using literature procedures.[17] The ditosylate and 1,3-dibromopropane were used to alkylate 3-bromo-carbazole[13] to prepare the carbazole dimer **15** and **16** bridged by a propyl unit, either unsubstituted or with two methyl groups in the 2-position of the bridge. Primary alkyl halogenides are electrophiles capable of reacting with polyisoprenyl lithium. Earlier attempts include reacting the bis-carbazole **16** with alkyl dihalogenides such as 1,3-dibromo propane to produce bis-carbazoles with two alkyl chains terminated with primary halogens. However, the synthesis was in general of low yield, possibly due to elimination. Also, the products was typically oilish and the workup difficult. However, the formyl group is easily introduced by bromine-to-lithium exchange followed by reaction with dimethyl formamide yielding the aldehyde substituted bis-carbazoles **17** and **18**. The aldehyde groups of **18** were reduced with sodium borohydride to the benzylic alcohols that were transformed into the corresponding chloromethyl derivative **19**

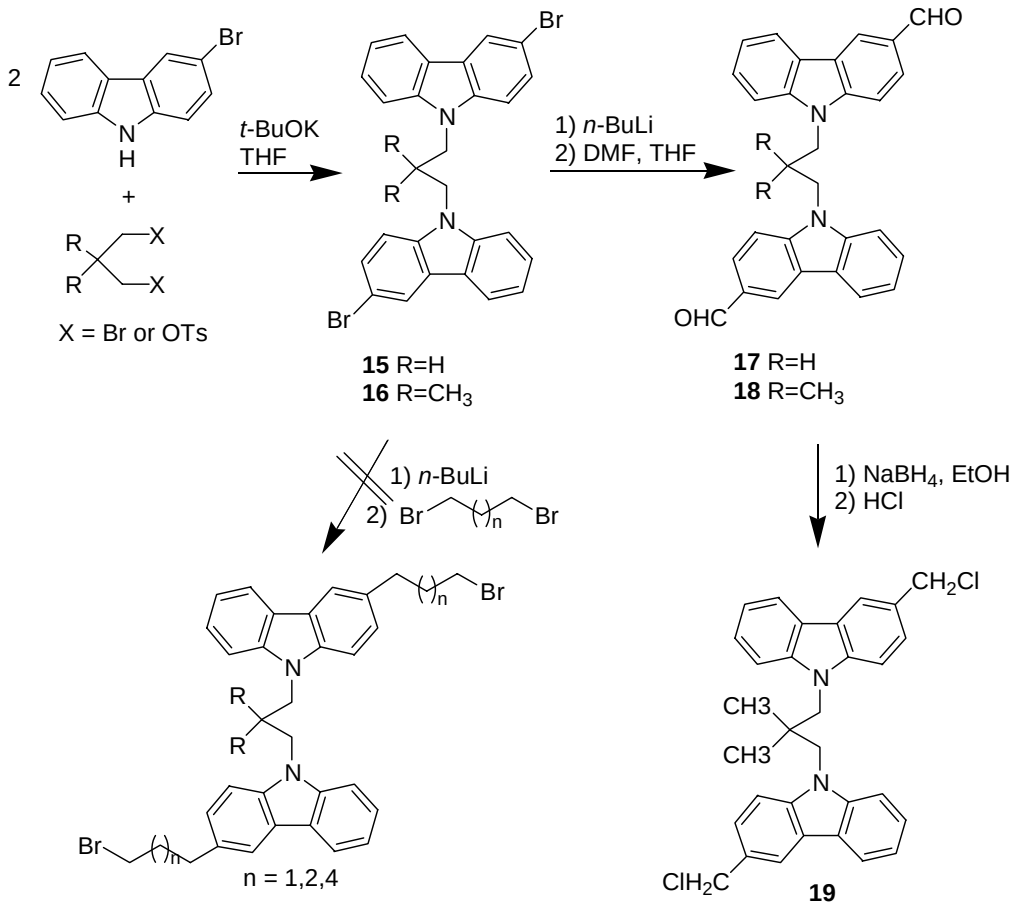

Scheme 3-3. Synthesis of three sensor molecules with varying spacer and electrophiles.

Synthesis of the polystyrene-polyisoprene (PS-PI) block-copolymer units and their attachment to the sensor unit is outlined in Scheme 3-4. Anionic living polymerization of styrene followed by polymerization of isoprene in non-polar solvent (methyl cyclohexane) give a PS-PI-Li diblock (19 weight % styrene and 81 weight % isoprene and total a weight of 75 kg/mol, Pd. = 1.1). The compounds **17**, **18** or **19** were then added to the reaction mixture in less than equivalent amount in order to ensure complete conversion to the desired probe **11-13**. It was found advantageous to add tetrahydrofurane at this step as a co-solvent to augment the relatively weak nucleophilicity of the lithiated polymer, as also noted by Hirao *et al.*[18] Purification by repeated precipitation from chloroform-methanol gave compounds **11-13** mixed with some unreacted PS-PI diblock. Coupling of two PS-PI blocks to compounds **11-13** approximately doubles the molar mass, which was conveniently followed by SEC (Figure 3-12).

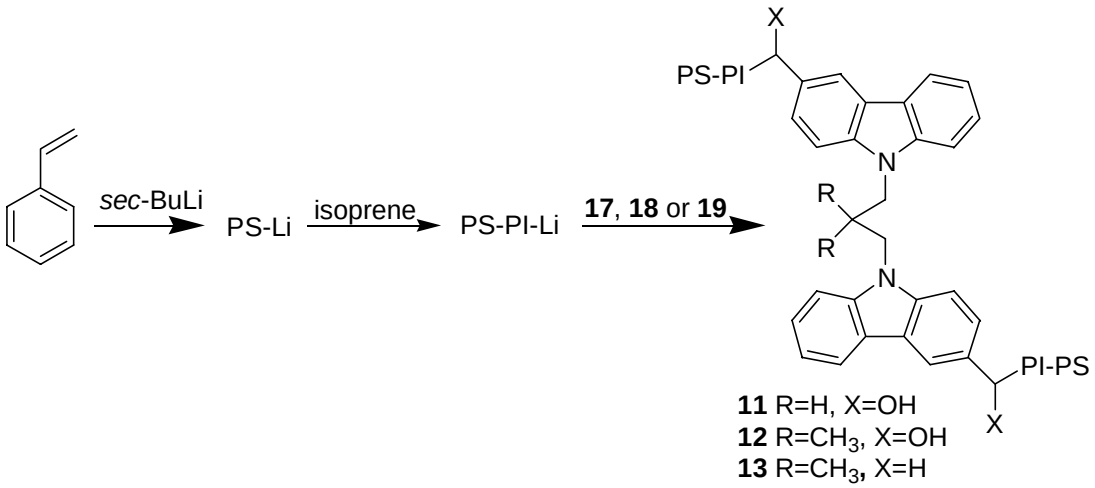

Scheme 3-4. Anionic polymerisation followed by coupling with the appropriate bis-carbazole.

Synthesis of probe **10** was carried out as shown in Scheme 3-5. *N*-Propyl-3,6-dibromo-carbazole[19] was converted into the corresponding dialdehyde **24** by bromine-to-lithium exchange with *t*-butyl-lithium in dry tetrahydrofuran followed by reaction with dimethyl formamide. **24** were then incorporated into SIS triblocks following similar procedures as described above.

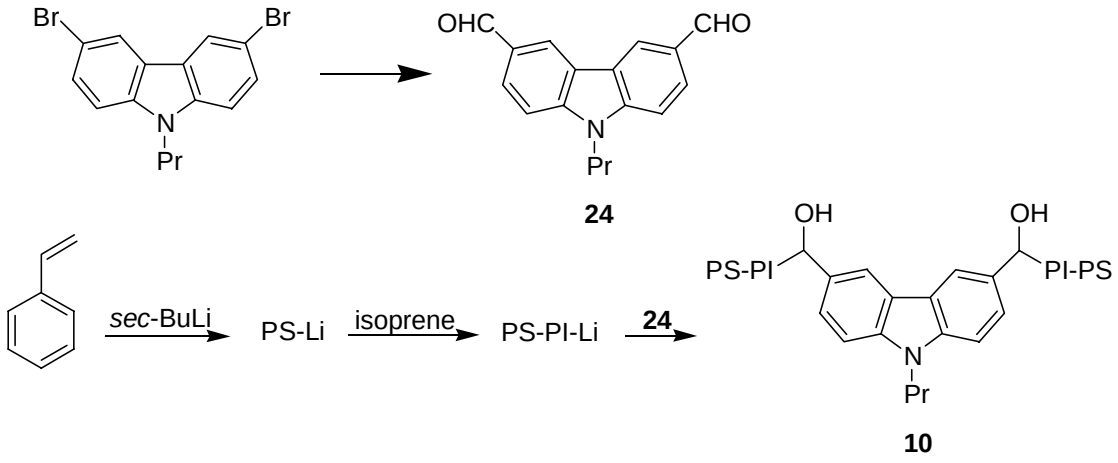

Scheme 3-5. Synthesis of probe **10**.

Below is typical SEC data for the prepared probes (Figure 3-12). Before coupling only a single peak is observed (the shoulder is the result of small amounts of coupling due to presence of oxygen when the sample is taken out of the reaction vessel), but after the addition of the sensor molecule a new peak with the double molecular weight is appeared. A UV-detector was used, and the showed intensities are proportional to concentration. The molecular weight was calculated using PS as reference. The

molecular weight of the PS domains was determined using SEC, before isoprene was polymerised. The hydrodynamic volume ratio of PI/PS is ca. 1.5 for high Mw PI. From this the probe was found to have a molar mass of 150 kg/mol with a polydispersity (Mw/Mn) of 1.2.

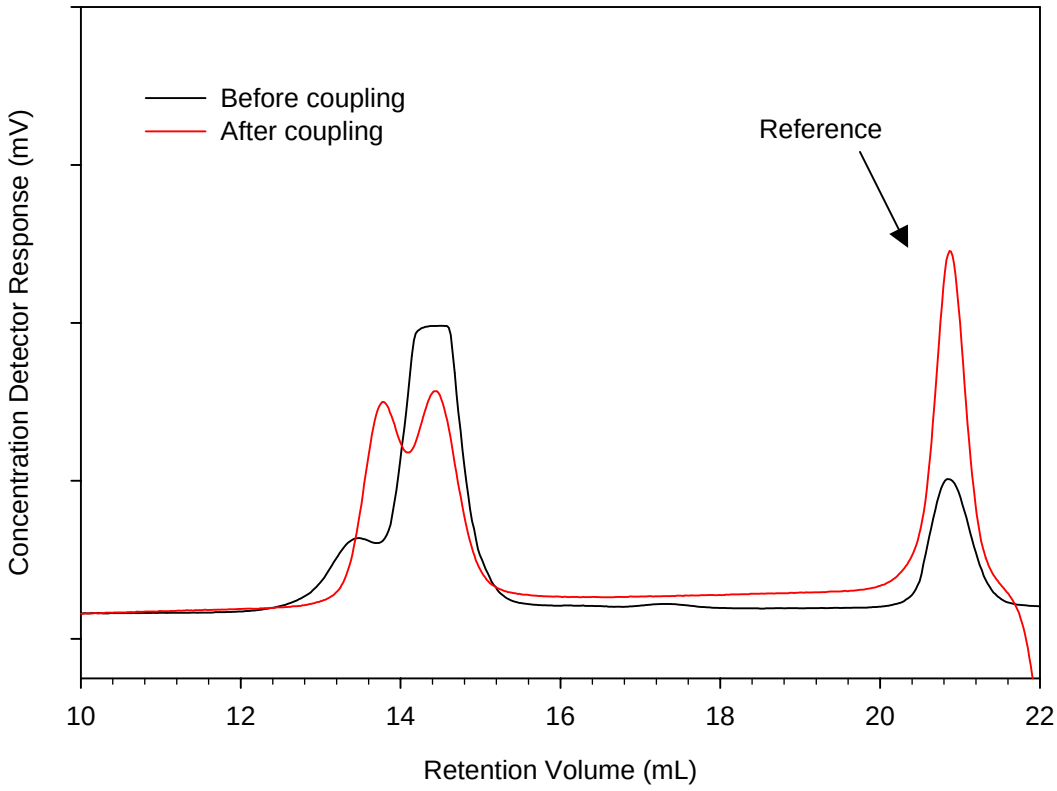

Figure 3-12. SEC data the prepared probe **10**. Irganox 1330 was used as reference.

An ^{1}H NMR spectrum of probe **10** is shown in Figure 3-13. From the integrals it can be inferred that there is approximately 17.4 (87/5) styrene units to 110.5 (100+21/2) isoprene units. This corresponds to a PS content of 19 wt-% (17.4*104g/mole / [17.4*104g/mole + 110.5*68.1g/mole]), and a PI content of 81 wt-%. From the spectrum it is not possible to distinguish the *cis*-1,4 from the *trans*-1,4 isomer. The content of 3,4-isomer in the PI is less than 10% (small amounts of the 1,2 isomer is only formed in polar solvents such as THF and diethyl ether).

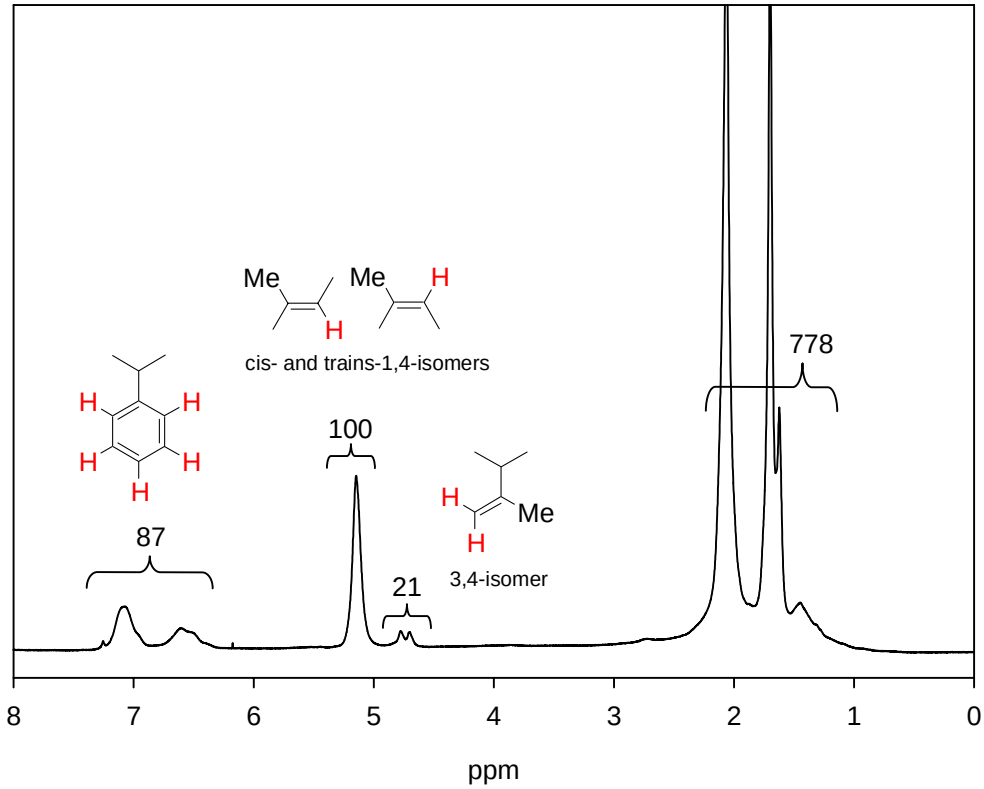

Figure 3-13. ^{1}HNMR spectrum of a prepared probe.

During anionic polymerisation water and oxygen must rigorously excluded. Anionic polymers are strong bases that will abstract proton from water and terminate. Also oxygen will terminate the polymerisation by oxidation. Special glass equipment and purification procedures of monomers and solvents must be applied.[20] Below a photo of the experimental set-up is shown (Figure 3-14)

Figure 3-14. Photo of experimental set-up here. The orange colour is due to polystyrenyl lithium in methyl-cyclohexane.

3.4.4 *Fluorescence of the carbazole probes and some reference compounds in solution and in polymer films*

Solution spectra of the strain probes **10-13** in chloroform are shown in Figure 3-15. There is a noticeable difference between the mono-carbazole compound **10** and the bis-carbazole probes **11-13.** Compound **10** is red shifted by ca. 10 nm relative to *N*-propyl-carbazole due to the 3,6-substitution and the relative intensities of the 360 and 375 nm bands are equal. The red shift observed upon 3,6-substitution was confirmed by comparing *N*-propyl-carbazole with 3-mehtyl-*N*-propyl-carbazole and 3,6-dimehtyl-*N*-propyl-carbazole, where a progressively red shift was observed with increasing levels of substitution. Compounds **12** and **13** have super imposable emission spectra with shoulders in the 390 to 400 nm range while probe **11** has a more intense 350 nm band.

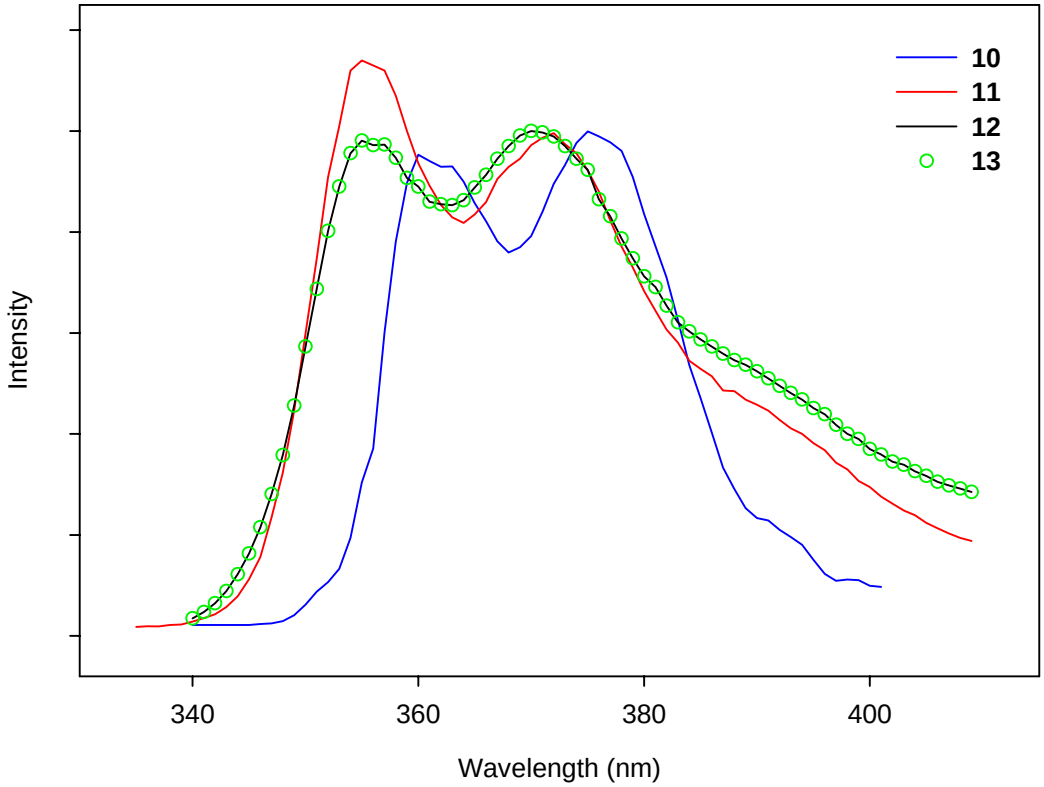

Figure 3-15. The bis-carbazole systems **11**, **12** and **13** have similar spectra while that of **10** are red-shifted around 6 nm. This is an effect of the two substituents on carbazole in **10** compared to one substituent on each carbazole in **11**, **12** and **13**. Notice that **12** and **13** are superimposed.

The effect of viscosity on the spectrum of *N*-propyl-carbazole, 3,6-dimethyl-*N*-propyl-carbazole and the probe molecule **10** with two pendant PS-PI groups in the 3- and 6-positions was studied by comparing the emission spectra in chloroform and in low molecular weight polyisoprene (MW=20k) (See Figure 3-16). In the case of *N*-propyl-carbazole only a small blue shift of 2-3 nm was observed going from chloroform solution to poly-isoprene. When methyl groups is attached to the 3- and 6-positions of carbazole a large red shift is observed, but the relative intensities of the two bands is approximate the same. However, if the methyl groups are replaced by the much larger (and heavier) polymerchains (**10**) the relative intensity of the low-wavelength peak is markedly decreased in chloroform. The low-wavelength peak is even further reduced in the 'solid' rubber state. Thus it can be inferred that the pendant polymer chains on probe **10** has marked influence on the emission properties in the solid film.

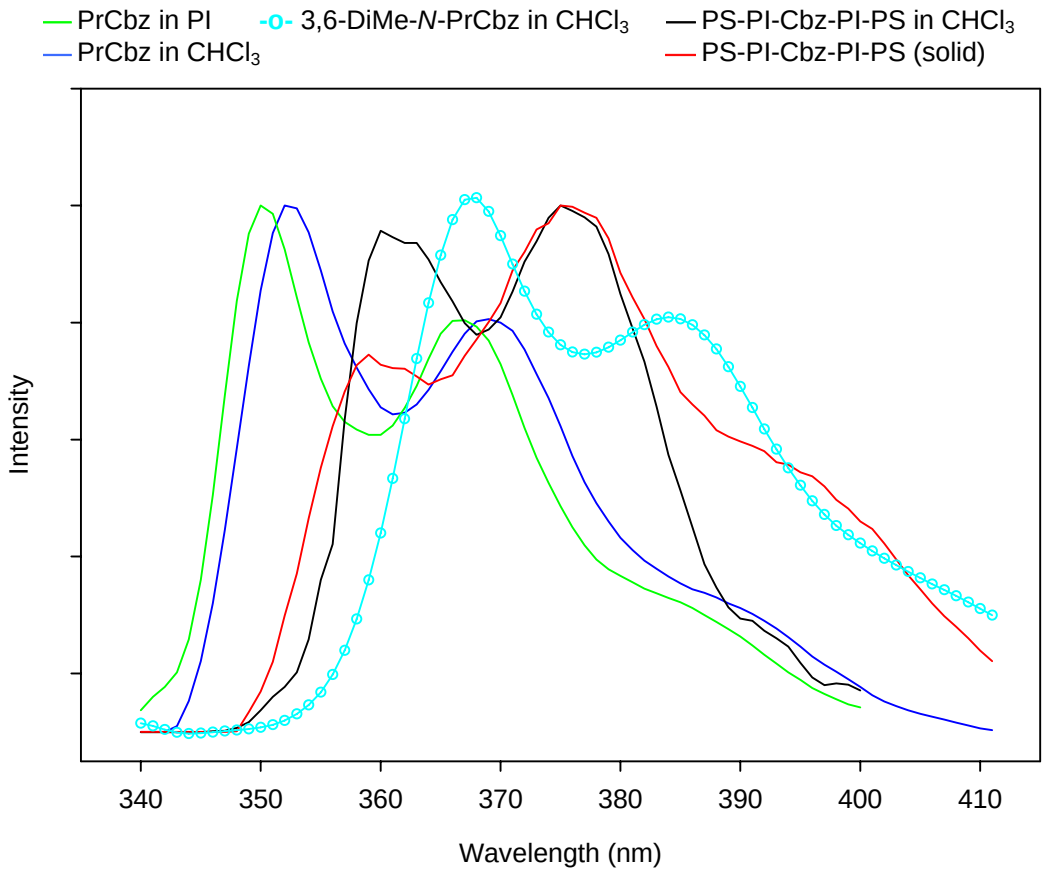

Figure 3-16. Normalized emission spectra of *N*-propyl carbazole (green and blue) and probe **10** (black and red) in chloroform and in PI surroundings. 3,6-Dimethyl-*N*-propyl-carbazole (cyan with circles) in $CHCl_3$ .Excitation wavelength is 310nm.

3.5 Strain experiments

This section describes the crucial strain experiments that demonstrate that the carbazole probes synthesized do in fact respond to straining an elastomer film containing them by a marked change of the fluorescence. Before relating the results of the fluorescence measurements it is necessary to give a description of the straining apparatus or jig that was designed specifically for these experiments. A small section on the preparation of the elastomer films has also been included.

3.5.1 Design of a straining jig

To strain the prepared film in a controlled manner a straining jig is needed (Figure 3-17). The jig was designed to fit the FLS920 spectromer at Risø. The material is made of

aniodized aluminium, which has a black dull surface. This was chosen to reduce possible light reflectance from the surface. The height of the jig was designed so that the excitation light would reach the middle of the sample fitted in the jig. In addition the arms holding the film are moved an equal distance in opposite directions during strain experiments, ensuring that the measurements are done on the same area of the film. The jig can be fixed in a permanent position in the spectrometer using screws.

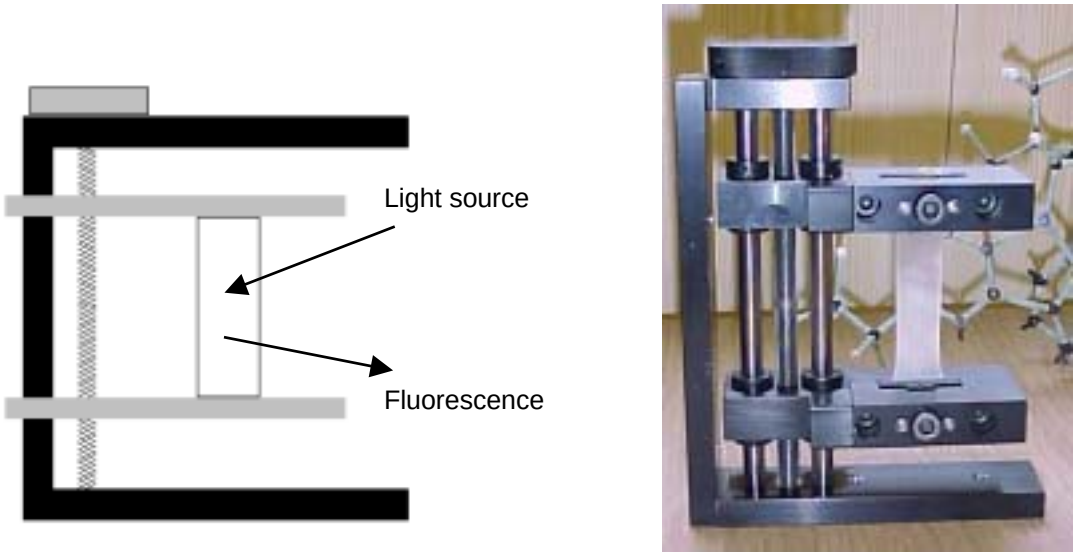

Figure 3-17. Custom designed jig for uniaxial elongation of prepared films. Sketch and photography.

3.5.2 Film preparation

About 30g of commercial PS-PI-PS were dissolved in chloroform and 0.03g of the synthesized probe was added. The solution was then poured into a petri dish and the solvent allowed to evaporate (Figure 3-18). The concentration of the probe compounds dispersed in the elastomer was ca. 10^{-5} M. Film strips with dimensions length=3 cm, width = 1 cm and thickness 1 mm was fastened to the clamps of the straining jig as shown in Figure 3-14. The straining jig was then placed in the spectrometer bay for back face illumination as described previously (chapter one).

Below (Figure 3-19) is the absorbance of a 0.8 mm thin film of commercial SIS rubber shown. The film absorbs strongly below 270 nm, but above 320nm the film is almost perfectly transparent. Excitation at 270nm produced the red peak shown, that can be ascribed to the PS domains.[21] Excitation at higher wavelengths did not produce any fluorescence. Carbazole absorbs above 320nm (Figure 3-8) and can thus be excited without exciting the PS domains.

Figure 3-18. The prepared film in a petri dish.

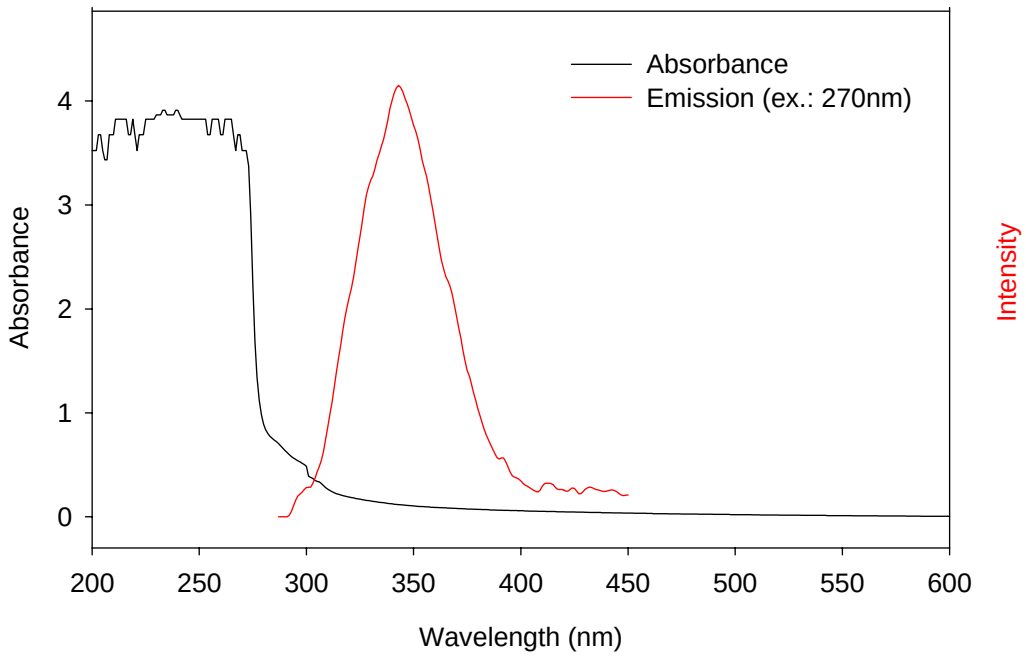

Figure 3-19. Absorbance and fluorescence of a commercial SIS film (0.8mm thick). The emission is caused by the PS domains.

The SIS elastomer was investigated using a standard stress relaxation apparatus. The measurements confirmed that the material did not relax to any significant extent within

hours at strain levels up to 800% (Figure 3-20). We may thus be confident that the material behaves as expected and know the emission change is not the consequence of a structural change, e.g. disruption of the PS domains etc., taking place in the material.

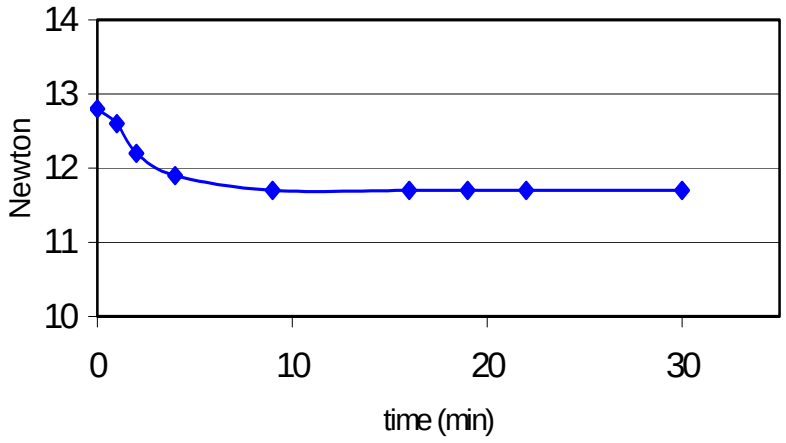

Figure 3-20. Stress relaxation experiment on commercial rubber at 800% elongation.

It is well known that triblock coplymers forms inhomogeneities upon strain. These inhomogeneities are caused by uneven linking of the PS-domains. The strain induced inhomogeneities can be observed by small-angle neutron scattering.[22] The milky appearance indicates that the light is effectively scattered (Figure 3-21).

Figure 3-21. When strained the film changes from clear (outside of the clamps) to opaque (between the clamps) after a few minutes.

3.5.3 Fluorescence under strain

In Figure 3-22 normalized spectra of probe **12** dissolved in a commercial SIS elastomer is shown as the film is stretched. The relative intensity around 352nm increases as the film is strained, while the intensity around 388nm decreases. The 310% strain curve is very similar to the monomer fluorescence (see Figure 3-8) while the 0% strain curve

indicates the presence of the partial overlap excimer fluorescence. Notice that the 0% strain curve is not perfectly identical with the spectrum of the solid probe shown in Figure 3-16. This is due to variation in the data obtained. The spectra could be interpreted as if the carbazole moieties interact in the relaxed state (as opposed to the solution spectra). And a conformation change, as depicted in Figure 3-10, is taking place. However, later we discovered that the emission change is dominated by the intensities of the different vibronic bands (this is described on p48). Thus the change is related to monomer fluorescence and not the excimer to monomer ratio. Aside from the intensity change it seems that the low wavelength peak at 354nm is blue shifted a 3-4 nanometres on strain, while the peak around 367nm remains constant.

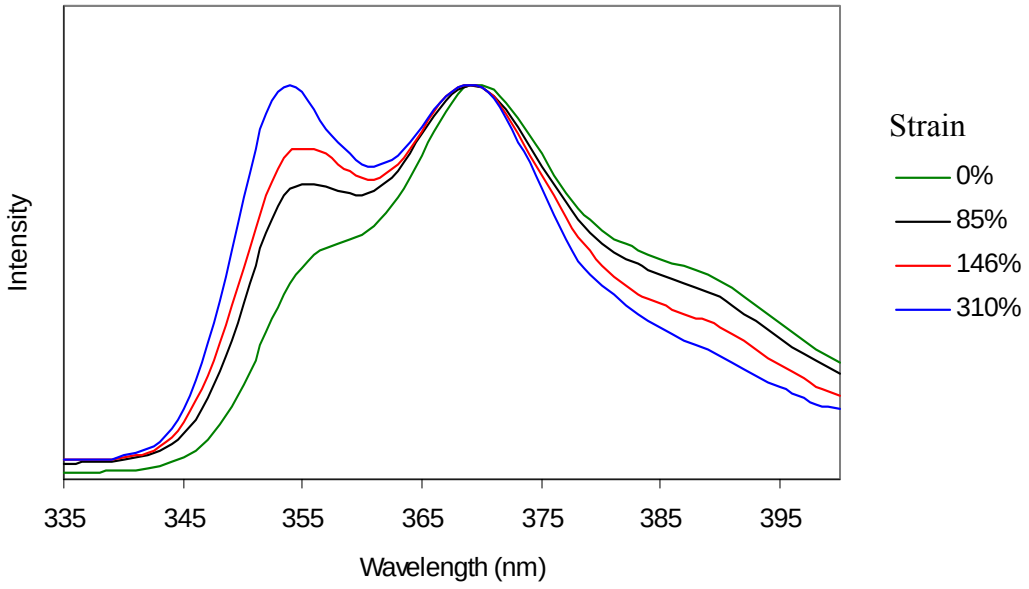

Figure 3-22. Representative normalized spectra at varying strain of **12** dissolved in a commercial SIS elastomer.

We did not observe any spectral changes within 20hrs. This is in line with the rheological investigations performed.

Below (Figure 3-23) is shown the relative fluorescence intensity at 354nm and 388nm plotted as a function of strain, for two samples. The straining jig was held in a fixed position while the samples were strained. The intensity around 388nm does not change as much as the intensity around 354nm as also can be seen in Figure 3-22. The largest response to strain is observed at low strain levels, and as the strain level approaches 300-400% the curves reach a plateau. The relative intensity around 354nm shows a clear trend: the intensity increases from 0.6 to 1.0 (a 67% increase). At the same time the intensity around 388nm is decreasing from around 0.6 to 0.5 (a 17% decrease). The intensity change is of course dependent on which wavelength one chooses to monitor, which to some extent is arbitrary. If for instance 345nm was plotted as function of strain, instead of 354nm, a much larger relative intensity change could be observed.

However, this would be partly due to the blue shift at higher strain levels more than actually intensity change of the low-wavelength peak. Moreover, at lower wavelengths the reduced intensity-to-noise ratio leads to larger variation in the data.

There are large variations in the data. Some of the series shown in Figure 3-23 seems to fall on two separate curves (se e.g. series 1, red triangles). At present we have no explanation, but it may be related to the inhomogeneities that develop with strain. An attempt to overcome this problem was to illuminate a large area of the sample (4-5 mm^2) to average out non-uniformities. This was however, only partly successful. In the end an average of ten measurements at each strain level was performed. The results for probes **10**-**13** are shown in Figure 3-24. In all cases a clear trend is observed. The relative intensity at 354nm increases with increasing strain.

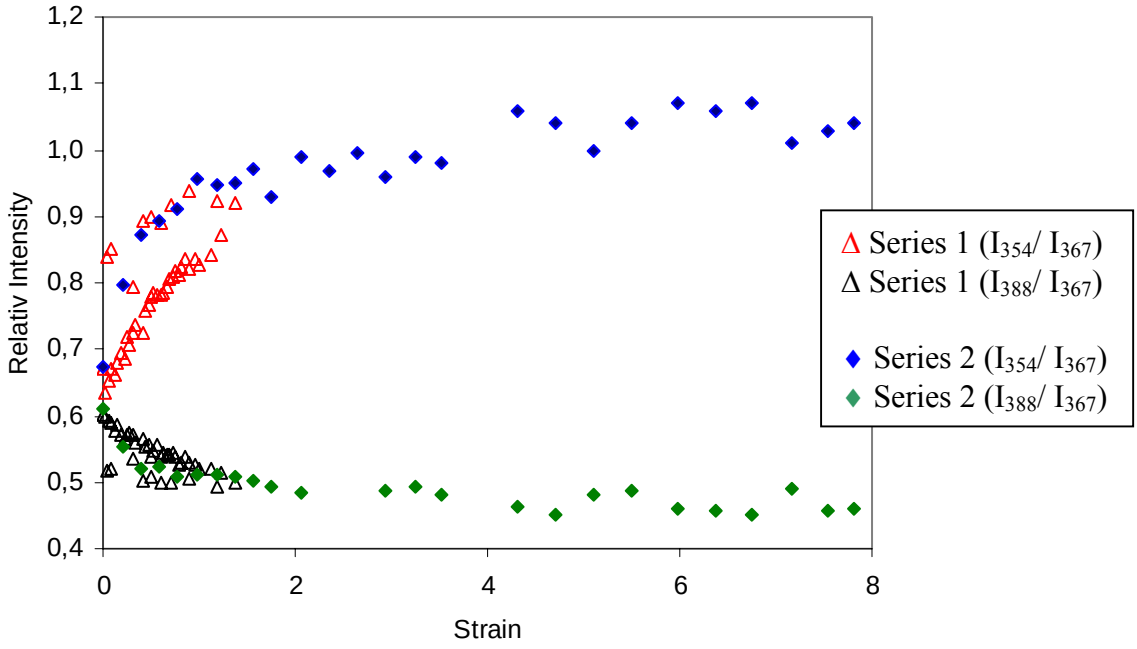

Figure 3-23. Relative intensity at 354nm and 388nm as function of strain for two samples.

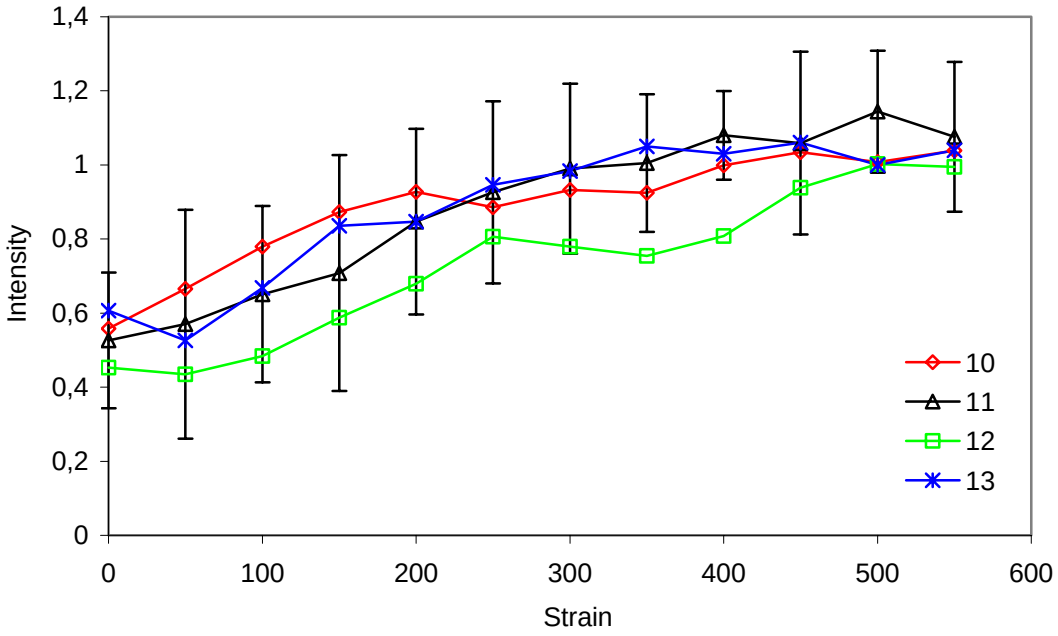

Figure 3-24. Relative intensity of the low-wavelength peak as function of strain.

All four strain probes gave similar results on uniaxial elongation. It is somewhat surprising that probe **10** with only one carbazole unit gave the same results as the biscarbazole probes **11**, **12** and **13**. This rules out any major contribution from excimer to monomer type shifts in the fluorescence of the latter probes. Thus an excimer-to-monomer change is not present to any significant amount in the probes **11-13**. Large changes in the relative intensities of the monomer emission bands are on the other hand related to the strain. A possible explanation could involve a progressive orientation of the carbazole units as the film was stretched. However, no orientation could be measured using polarized light.[23] The samples are sufficiently opaque that the polarization is lost due to multiple scattering. One can argue that since polarized light is depolarised in the sample, possible orientation of the fluorophore should not have any effect on the emission. Another explanation is that the relative intensity of the vibronic bands is altered with strain. In chapter two, a similar change for pyrene was described. In this case the emission change was solvent dependent. The spacing between the 0-0 and 0-1 transition corresponds to a vibration of 1111cm^{-1}. This is in the region that normally is associated with aromatic C-H in-plane bending. Gaussian (v98, Revision A.7) was used to calculate the IR spectrum for the simpler system *N*-methyl carbazole. The calculations indicates that the C-H bending is coupled to aromatic C-C stretch. It is hard to see how strain should influence the aromatic C-H bending. It is much more acceptable that the aromatic C-C stretch in carbazole is sensitive to strain/stress transferred through the polymer chains. Time resolved fluorescence did not show any change. The fluorescence lifetime of the sensor unit supports this theory. The lifetime where constant around 11.8ns. The decay could be fitted by single exponential (χ_R^2 = 1.1). The reasonable fit indicates that only one species is present.

It was important to investigate the effect of the polystyrene blocks in the sensor molecules. Their function is to act as anchors that connect the sensor molecules to two PS -domains in the SIS elastomer as shown in Figure 3-6. Synthesizing a variant of probe 10 without the PS domains tested the hypothesis. This sensor was blended into the SIS elastomer at the 0.1 wt-% level and made into filmstrips. Repeating the strain experiments showed no effect on the emission spectrum. Connecting the probe to the network of the elastomer through the PS domains is therefore important for the strain sensor function.

While probe **10** is easy to synthesise and is capable of measuring strain, the problem of determining the reason of the emission change remains. In the ideal case it is related to a conformation change, where the amount of energy involved is known (or possible to determine). This knowledge could then be used to learn more of the molecular processes involved as a polymer-based material is strained. This was the original goal of the project. However, having no knowledge about which vibrations that corresponds to the individual vibronic bands observed in the emission spectrum, an energy assessment becomes difficult in the case of **10**, and we where not able to pursue this. Without knowledge of the origin of the observed emission change it is difficult to determine what the sensor molecule actually measures. As stated above, the spacing between the 0-0 and 0-1 transitions indicates that the vibration is an aromatic C-H in-plane bending. It is hard to see what mechanism is responsible for the coupling between strain and the C-H bending, and we were not able to find a likely mechanism.

3.6 Conclusion

Four different strain probes with one or two carbazole units placed in the middle of a SIS type triblock copolymer has been prepared. Fluorescence spectra of the chromophores in solution are remarkably similar and all show fluorescence expected for a simple monomeric carbazole type chromophore. This is in contrast to the very similar 2,4-(*N*-carbazolyl) pentanes studied by Vandendriessche *et al*. were evidence for partial and total overlap between the carbazole units were seen in the excimer type spectra obtained. Strain probes **10**-**13** were mixed in commercial SIS rubber at the 0.1% level and made into filmstrips. When these films were subjected to uniaxial elongation large changes from 0.7 to 1.1 in the relative fluorescence intensities at two wavelengths (around 350 and around 370 nm) was nonetheless observed. The relative change was largest for strains around 0-200% and levelled out above 300-400%. Since the results are similar for the mono- and bis-carbazole probes changes in molecular overlap giving rise to excimer type fluorescence can be excluded. The observed changes must instead be due to subtle changes in the transition probabilities of the vibronic bands of the carbazole units (probably aromatic C-H bending). This finding casts doubts on the interpretation by Ikawa *et al*. on fluorescence spectra on stretched PVCz films. It was assumed that the changes observed were related to the different ratios of overlap geometries in response to the induced strain. While this may still be the case it cannot be excluded that the variations observed was instead related to fluorescence changes in

the monomer carbazole units themselves, as in our case. The preparation of single chromophoric units imbedded in the polymer matrix proved to be crucial in separating the factors responsible for the fluorescence changes. These strain probes may also be more generally valuable since they can be used with a larger selection of polymer matrices.

3.7 Investigation of model compounds

The synthesised probes were sensitive to macroscopic strain, but the mechanism is not clear. It seems that excimer formation is not a major contribution to the emission of probes **11**-**13**. This is somewhat puzzling and we wanted to investigate this further. In addition we hoped that these studies might discover a new promising linker that favoured excimer formation. The model compounds (Figure 3-25) **20**-**23** where easily synthesized, using methodology already described.

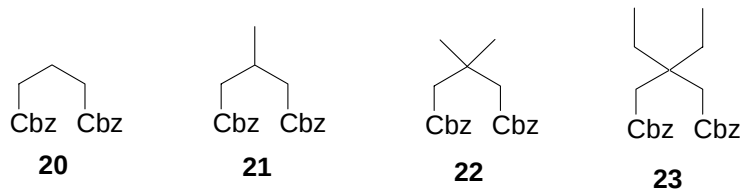

Figure 3-25. Model compounds investigated.

Below is the emission of the model compounds **20**-**23** as well as emission of *N*-propyl carbazole shown in 10^{-5}M degassed chloroform solutions (Figure 3-26). The first thing to notice is that all the spectra is very similar to *N*-propyl carbazole (monomer fluorescence). The only spectrum that is a little different is that of **20** where some partial overlap excimer is present, as evidenced by the higher peak at 367nm and a more intense shoulder around 390nm. It thus seems that methyl groups or the more bulky ethyl groups on the middle carbon atom of the linker actually hamper excimer formation, compared to the unsubstituted propane linker (!). This shows how difficult it is to design systems that favour certain conformations. According to Vandendriessche *et al.* the small amount of partial excimer in **20** is formed after excitation, thus the ground state in not excimer conducing.

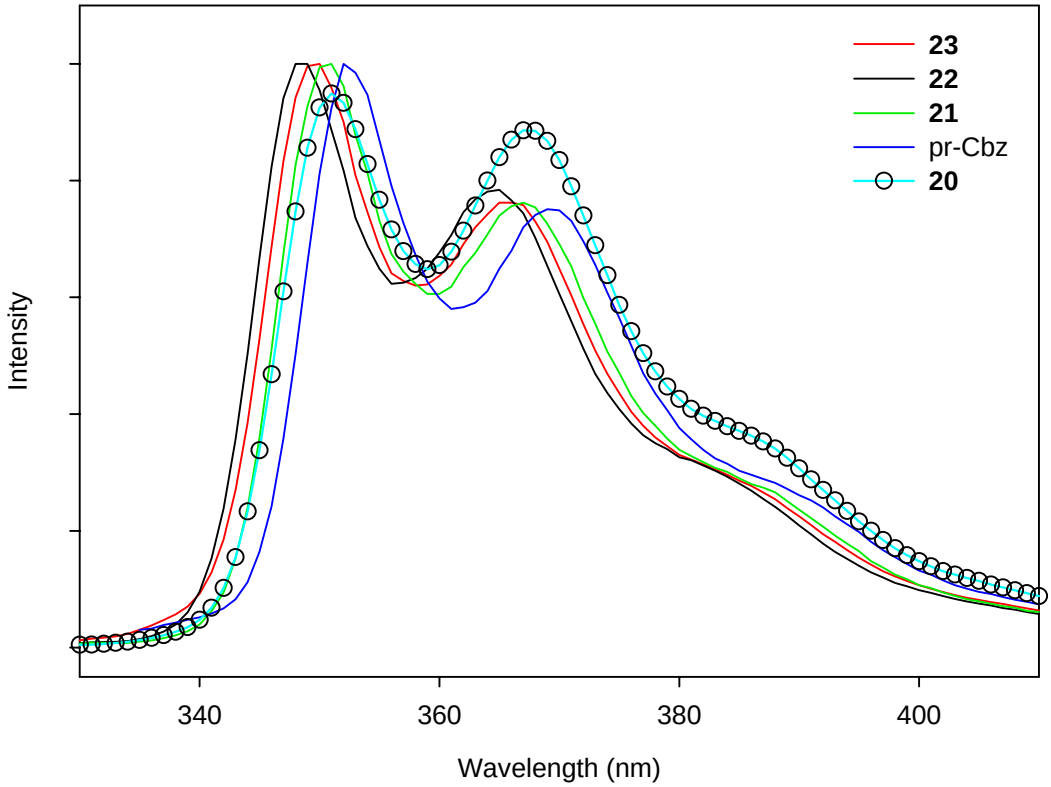

Figure 3-26. Fluorescence spectra of model compounds along with *N*-propyl carbazole. Spectra were recorded at RT in 10^{-5}M degassed chloroform solutions. Only **20** forms small amounts of partial overlap excimer.

Many studies done on excimer formation in small molecules are done at low temperatures. Vandendriessche *et al*. found that excimer formation was favoured at low temperatures (e.g. 140K has been used) in some cases. We speculated that some of the synthesised model compounds might show excimer formation at low temperaure, even though no sign of excimer formation is evident at room temperature. We thus decided to investigate the ground state conformation of the model compounds using ^{1}H NMR techniques, at temperatures below room temperature. However no changes in chemical shift values was observed, for neither the aromatic or alkyl protons, as the temperature were decreased from room temperature to 250K.

Finally, preliminary studies on the relative energy of conformations present in the model compounds, and to additional structures (**24** and **25** in Figure 3-27), were performed using Accelrys Materials Studio 2.2. Intermolecular interactions (with solvent etc.) are ignored, that is the molecule is considered to be in vacuum. As a consequence, conformations with large degrees of intramolecular interactions are favoured to some degree, e.g. the GG conformation in 1,3-bis(*N*-carbazolyl) propane

(Figure 3-28). Of course these calculations should only be used as rough indications. The results are summarized in table 1 below.

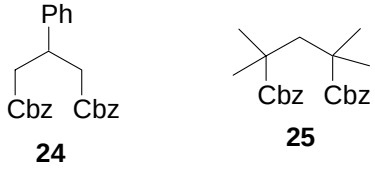

Figure 3-27. 24 and **25**.

Table 1. Calculated Relative energy (kcal/mole) of a number of bis carbazoles obtained using Accelrys Materials Studio 2.2. In cases where more than one conformation of the same type is possible (e.g. there are two TG conformations in *rac*-2,4-bis(9-cabazolyl) pentane) only the one with the lowest energy is shown.

Compound	TT (kcal/mole)	TG (kcal/mole)	GG (kcal/mole)
20	212.3	201.0	197.7
21	208.3	210.4	211.1
22	209.0	197.1	195.6
23	230.7	234.1	236.2
Meso-2,4-bis(9-cabazolyl) pentane	168.7	171.6	170.4
Rac-2,4-bis(9-cabazolyl) pentane	169.4	166.0	159.4
24	243.6	244.8	243.8
25	117.9	114.9	103.3

The TT, GT and GG conformations are defined with respect to the bonds connecting the carbazole moieties in Figure 3-28 below.

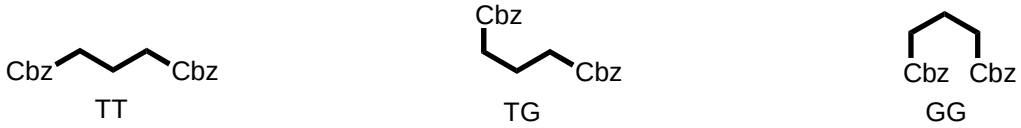

Figure 3-28. TT, TG and GG conformation of 1,3-bis(*N*-carbazolyl) propane.

The ability to form an excimer is increased with decreasing relative energy of the GG conformation. Of the synthesized compounds **20**, has the lowest relative energy of the GG conformation with 3.3 kcal/mole up to the TG conformation, which is accordance to small presence of excimer formation observed. In the case of **21** and **23** the GG conformation has the highest energy, which is in accordance with the absence of excimer formation. Even though the GG conformation of **22** has the lowest energy of

the three conformations we did not see en excimer formation. It could be related the low energy increment (1.5 kcal/mole) up to the TG conformation. *Rac*-2,4-bis(*N*-cabazolyl) pentane shows a large difference between GG and TG, which is in agreement with the large excimer emission observed for this compound (remember that the ground state conformation was identical with the partial overlap excimer conformation (Figure 3-9)). The calculations indicate that the corresponding *meso* derivative does not have ground state conformation conducive of excimer formation. This is in accordance with the findings of Vandendriessche *et al.*, that found that full overlap excimer emission take place after a conformation change. Replacing the methyl group in **21** with a phenyl group (**24**) has limited effect on the conformational distribution. **25** seems to be compound with the largest ground state excimer conformation, however this compound is probably even more difficult to make than 2,4-bis(*N*-cabazolyl) pentane. Since no of the investigated compounds seems considerably better in excimer formation than **20** no new promising spacer unit was found for a strain sensor.

References and notes

1. For more information on the basic theory of rubber elasticity see *Polymer Physics*: U.W. Gedde; Kluwer Academic Publishers, **1999**. Chapter 3.
2. *Physical Properties of Polymers*: Mark, J.E.; Am. Chem. Soc. Whasington, DC., **1984**.
3. Yang, L.; Li, H.; Wang, G.; He, B. J. *Appl. Polym. Sci*. 2001, 82, 2347.
4. Ikawa, T.; Shiga, T.; Okada, A. J. *Appl. Polym. Sci.* 1997, 66, 1569.
5. Johnson, G.E.; Good, T.A. *Macromolecules* **1982**, *15*, 409.
6. Queslel, J.P.; Jarry, J.P.; Monnerie,L. *Polymer*, 1986, 27, 1228.
7. Morton, M. *Anionic Polymerization: Principles and Practice*, Academic Press **1983**.
8. Zachariasse, K.A.; Duveneck, G.; Kühnle, W.; Reynders, P.; Striker, G. *Chem. Phys. Lett*. 1987, 133, 390.
9. Zachariasse, K.A.; Duveneck, G.; Kühnle, W. *Chem. Phys. Lett*. 1985, 113, 337.
10. Reynders, P.; Dreeskamp, H.; Kühnle, W.; Zachariasse, K.A. J. *Phys. Chem.* 1987, 91, 3982.
11. Winnik, F.M. *Chem. Rev.* **1993**, *93*, 587.
12. The 2-position of pyrene can be reached through reduction to 4,5,9,10-tetrahydropyrene (ref. 10) followed by electrophilic substitution and finally reoxidized to the pyrene derivative (ref. 11).
13. Mitchell, R.H; Chen, Y.; Zang, J. *Org. Prep. Proced. Int.* 1997, 29, 715.
14. Dyke, D.A.V.; Pryor, B.A.; Smith, P.G.; Topp, M.R. *J. Chem. Ed.* **1998**, *75*, 615.
15. Vandendriessche, J.; Palmans, P.; Toppet, S.; Boens, N.; Schryver, F.C. De; Masuhara, H. *J. Am. Chem. Soc.* **1984**, *106*, 8057.
16. Evers, F.; Kobs, K.; Memmig, R.; Terrelli, D.R. *J. Am. Chem. Soc* **1983**, 105, 5988.
17. Nelson, E.R.; Maienthal, M.; Lane, L.A.; Benderley, A.A. *J. Am. Chem. Soc.* **1957**, 79, 3467.

18. Hirao, A.; Tohoyama, M.; Nakahama, S. *Macromolecules*, **1997**, *30*, 3483.
19. Smith, K; James, D.M.; Mistry, A.G.; Bye, M.R.; Faulkner, D.J. *Tetrahedron*, **1992**, *48*, 7479.
20. Ndoni, S; Papadakis, C.M.; Bates, F.S; Almdal, K. *Rev. Sci. Instrum.* **1995**, *66*, 1090.
21. Leibowitz, M.; Weinreb, A. *Jour. Chem. Phys.* **1967**, *46*, 4652.
22. Mischenko, N.; Reynders, K.; Mortensen, K.; Overberg, N.; Reynaers, H. *J. Polym. Sci.: Part B: Polym. Phys.* **1996**, *34*, 2739.
23. Jarry, J.P.; Monnerie, L. *J. Polym. Sci. Polym. Phys. Ed.* **1980**, *18*, 1879.

CHAPTER 4

EXPERIMENTAL

4.1 Photophysical methods

UV-VIS spectra were recorded on a Cary 1E UV-VIS spectrophotometer from Varian. Emission spectra (1 sec. acquisition at each nanometer increment) and lifetimes were measured on a FLS920 combined steady-state and lifetime spectrometer from Edinburg Instruments. The instrument is fitted with a 450W Xe-lamp for steady-state measurements and a nanosecond flashlamp for lifetime measurements. The detecting system comprises a single photon counting PMT detector in a peltier cooled housing. All steady state measurements where corrected and obtained with a 1.8 nm band-pass.

4.2 Characterization

^{1}H and ^{13}C NMR were recorded on a Bruker 250 Mhz spectrometerer. Elemental analysis were performed at the University at Copenhagen, Department of Chemistry, Elemental Analysis Laboratory, Universitetsparken 5, 2100 Copenhagn (Denmark). Size Exclusion Chromatography (SEC) was carried out on a system equipped with a Viscotec Differential Refractometer/viscometer with a MIXED-D column from Polymer Laboratories, UK. THF was used as eluent and the flow rate was 1.00 mL/min. The calibration curve was established by means of commercial available polystyrene samples with low polydispersity.

4.2 Anionic polymerisation and probe synthesis

4.2.1 General

THF was distilled from sodium while the non-polar solvents (cyclohexane and methyl cyclo-hexane) were distilled from polystyryl lithium. The monomers were distilled twice from butyl magnesium. All glassware was annealed at 565°C prior to use (this also insures that trace amounts of organic matter as well as free OH groups on the glass surface is removed). BuLi was used as initiator and titrated prior to use. At all time an overpressure of argon was present inside the reaction container (a pressure gauge is used to monitor the pressure), also a magnet was used to stirrer the solution.

4.2.2 Probe synthesis

Styrene (4.9g) was dissolved in methyl-cyclohexane (300ml) under argon. BuLi (0.34mmol) was used to initiate the polymerisation. After 6h the PS-Li was allowed to react further and isoprene (20.8g) was added. After 20h at 35°C the PS-PI-Li diblock was formed (19 wt-% styrene and 81 wt-% isoprene and total a weight of 75 kg/mol). The temperature was then lowered below -50°C and the sensor unit **10**-**13** (0.34mmol) dissolved in THF (50ml) was added. A further 300ml of THF was added and the temperature was allowed to reach RT over 5h. The product was finally precipitated in MeOH.

4.2.3 Low Mw polyisoprene

Isoprene (20g) was distilled into a bottle equipped with a septum. Methyl-cyclohexane (400ml) was distilled into the same bottle and BuLi (1 mmol) was injected through the septum. After two days the product was purified as described above.

4.3 Film preparation

Commercial PS-PI-PS (*Aldrich 43,239-3*: Mw(PS) = 7.3k, Mw(PI) = 106k) was dissolved in THF (500ml) and filtered through a Millipore 0.22μm filter. The volume was reduced and the product was precipitated in methanol. About 30g of the filtered commercial triblock were dissolved in chloroform and 0.03g of the synthesized probe was added. The solution was then poured into a petri dish and the solvent allowed evaporating over 20h at 35°C.

4.4 Organic synthesis

1,3-bis(3-bromo-carbazole-9-yl)-propane (15)

3-Bromocarbazole (15.5 g; 63.3 mmol) was dissolved in dry THF (350 ml) and *t*-BuOK (70 mmol) was added. After 5 min 1,3-dibromopropane (7.65 g; 37.9 mmol) was added and the mixture was refluxed overnight. Water was added and the solution was extracted with ether (2 x 200 ml). The organic phase was dried ($MgSO_4$) and the solvent was removed *in vacuo*. Recrystallization from toluene/heptane gave the product as a white powder in 61% yield. Mp. 181°C-183°C. ^{1}H NMR (250MHz, DMSO-d_6): δ = 2.2 (m, 2H), 4.5 (t, *J* = 7.2 Hz 4H), 7.2 (t, *J* = 5.8 Hz, 2H), 7.5 (m, 8H), 8.2 (d, *J* = 8.2 Hz, 2H), 8.4 (s, 2H) ppm. ^{13}C NMR (63MHz, DMSO-d_6): δ = 27.5, 109.2, 110.9, 119.2, 120.8, 121.1, 122.8, 124.0, 126.4, 127.9, 138.5, 149.1 ppm (one aliphatic and one aromatic peak is missing). Anal. calcd. for $C_{27}H_{20}N_2Br_2$: C, 60.93; H, 3.79; N, 5.26. Found: C, 60.89; H, 3.81; N, 5.24.

1,3-Bis(3-bromo-carbazole-9-yl)-2,2-dimethyl-propane (16)

3-bromocarbazole (21.9 g; 89.0 mmol) was dissolved in dry DMF (400 ml) and treated with potassium tert-butoxide (14.4 g; 129 mmol). After 10 min. 1,3-ditosyl-2,2-dimethyl-propane (18.8 g; 45.6 mmol) was added. The dark mixture was stirred at

120°C for 20h and water was added. The precipitate, a white powder, was washed with hot ethanol yielding the product sufficiently pure for further reaction. Yield: 52% (12.9 g; 23.1 mmol). Mp. 207°C-208°C. ^{1}H NMR (250MHz, DMSO-d_6): δ = 1.0 (s, 6H), 4.6 (s, 4H), 7.2 (t, *J* = 8 Hz, 2H), 7.5 (t, *J* = 8 Hz, 2H), 7.6 (d, *J* = 9 Hz, 2H), 7.7 (d, *J* = 4 Hz, 2H), 7.8 (d, *J* = 4 Hz, 2H), 8.2 (d, *J* = 8 Hz, 2H), 8.4 (s, 2H) ppm. ^{13}C NMR (63MHz, DMSO-d_6): δ = 25.3, 43.7, 51.2, 110.8, 111.0, 112.6, 119.3, 120.6, 121.2, 122.6, 124.2, 126.3, 127.8, 140.2, 141.8 ppm. Anal. calcd. for $C_{29}H_{24}Br_2N_2$: C, 62.16; H, 4.32; N, 5.00. Found: C, 62.37; H, 4.23; N, 4.87.

1,3-bis(3-formyl-carbazole-9-yl)-propane (17)
1,3-bis(3-bromo-carbazole-9-yl)-propane (2.43 g; 4.57 mmol) was dissolved in dry THF. The solution was cooled to -78°C and treated with *n*-BuLi (16 mmol). After 5 min. dry DMF (3.3 g; 45 mmol) was added and the temperature as allowed to rise to RT. After 30 min. $HCl_{(aq)}$ was added, the volume reduced *in vacuo* and the precipitate was filtered. Recrystallization from ethanol afforded the product in 59% yield (1.16 g; 2.7 mmol). Mp: 243°C-245°C. ^{1}H NMR (250MHz, DMSO-d_6): δ = 2.3 (m, 2H), 4.6 (t, *J* = 7 Hz, 4H), 7.3 (t, *J* = 7 Hz, 2H), 7.5 (t, *J* = 8 Hz, 8H), 7.6 (d, *J* = 8 Hz, 2H), 7.7 (d, *J* = 8Hz, 2H), 7.9 (d, *J* = 8 Hz, 2H), 8.3 (d, *J* = 8 Hz, 2H), 8.7 (s, 2H), 10.0 (s, 2H) ppm. ^{13}C NMR (63MHz, DMSO-d_6): δ = 27.3, 109.5, 109.7, 120.2, 120.8, 122.3, 123.9, 126.6, 126.7, 128.4, 140.5, 143.3, 191.7 ppm (one aliphatic and one aromatic peak is missing). Anal. calcd. for $C_{29}H_{22}N_2O_2$: C, 80.91; H, 5.15; N, 6.51. Found: C, 81.13; H, 5.20; N, 6.59.

1,3-bis(3-formyl-carbazole-9-yl)-2,2-dimethyl-propane (18)
1,3-bis(3-bromo-carbazole-9-yl)-2,2-dimethyl-propane (1.97 g; 3.52 mmol) was dissolved in dry THF (150 ml) and treated with *t*-BuLi (11 ml of a 1.7 M solution in hexane, 18.7 mmol) at –78°C the temperature was allowed to rise to 0°C and then cooled to –78°C. Excess dry DMF (3 g; 41 mmol) was added and the temperature was allowed to rise to room temperature. After 30 min. $HCl_{(aq)}$ was added and the volume was reduced *in vacuo.* The precipitate was collected and recrystallised from toluene/heptane leaving the product as a yellow powder. Yield 56% (0.90 g; 2.0 mmol). Mp. 232°C-234°C. ^{1}H NMR (250MHz, DMSO-d_6): δ = 1.0 (s, 6H), 4.7 (s, 4H), 7.3 (t, *J* = 7 Hz, 2H), 7.5 (t, *J* = 7 Hz, 2H), 7.9 (d, *J* = 8 Hz, 2H), 8.0 (s, 4H), 8.3 (d, *J* = 8 Hz, 2H), 8.8 (s, 2H), 10.1 (s, 2H) ppm. ^{13}C NMR (63MHz, DMSO-d_6): δ = 25.3, 43.6, 51.2, 111.2, 111.4, 120.2, 120.6, 122.4, 122.5, 123.7, 126.3, 126.5, 128.4, 142.3, 145.0, 191.8 ppm. Anal. calcd. for $C_{31}H_{26}N_2O_2$: C, 81.20; H, 5.72; N, 6.11. Found: C, 80.91; H, 5.86; N, 5.90.

1,3-bis(3-hydroxymethyl-carbazole-9-yl)-2,2-dimethyl-propane
A mixture of 1,3-bis(3-formyl-carbazole-9-yl)-2,2-dimethyl-propane (230 mg; 0.50 mmol) and ex. $NaBH_4$ (80 mg; 2.1 mmol) was stirred in THF-ethanol (15 ml:15 ml) for 6h at RT. The volume was reduced *in vacuo* and poured into water. The white precipitate was collected and dried affording the product sufficiently pure for further reaction. Analytical pure product could be obtained by recrystallization from ethanol/toluene. Yield 86% (0.20 g; 0.43 mmol). Mp. 189°C -191°C. ^{1}H NMR

(250MHz, DMSO-d_6): δ = 1.1 (s, 6H), 4.6 (s, 4H), 4.7 (s, 4H), 5.2 (br, 2H), 7.2 (t, J = 7 Hz, 2H), 7.4 (t, J = 8 Hz, 2H), 7.4 (t, J = 8 Hz, 2H), 7.7 (d, J = 6 Hz, 4H), 7.7 (d, J = 6 Hz, 2H), 8.1 (s, 2H), 8.2 (d, J = 8 Hz, 2H). ^{13}C NMR (63MHz, DMSO-d_6): δ = 25.5, 43.8, 51.3, 63.5, 110.1, 110.5, 118.2, 118.8, 119.9, 122.0, 122.2, 124.9, 125.3, 133.2, 140.7, 141.8 ppm. Anal. calcd. for $C_{31}H_{30}N_2O_2$: C, 80.49; H, 6.54; N, 6.06. Found: C, 80.49; H, 5.76; N, 5.94.

1,3-bis(3-chloromethyl-carbazole-9-yl)-2,2-dimethyl-propane (19)

1,3-bis(3-hydroxymethyl-carbazole-9-yl)-2,2-dimethyl-propane (0.30 g; 0.65 mmol) was dissolved in chloroform (75 ml). Concentrated hydrochloric acid (25 ml) was added and the mixture was vigorously stirred at 0°C. After 30 min. the phases was separated. The organic layer was successively washed with water, $NaHCO_{3(aq)}$, water and dried ($MgSO_4$). The solvent was removed *in vacuo* leaving the product as a yellow glass in 83% yield (0.26 g; 0.54 mmol). ^{1}H NMR (250MHz, DMSO-d_6): δ = 1.0 (s, 6H), 4.6 (s, 4H), 5.0 (s, 4H), 7.2 (t, J = 7 Hz, 2H), 7.5 (t, J = 8 Hz, 2H), 7.5 (t, J = 9 Hz, 2H), 7.8 (d, J = 8 Hz, 2H), 7.8 (d, J = 8 Hz, 2H), 8.2 (d, J = 8 Hz, 2H), 8.3 (s, 2H). ^{13}C NMR (63MHz, DMSO-d_6): δ = 25.4, 43.6, 47.5, 51.3, 79.1, 110.7, 119.1, 120.0, 120.8, 122.0, 122.2, 125.7, 126,7. 128.1, 141.3, 141.9 ppm. Anal. calcd. for $C_{31}H_{28}Cl_2N_2 \bullet 0.3HCl$: C, 72.95; H, 5.59; N, 5.49. Found: C, 72.88; H, 5.58; N, 5.38.

3,6-Diformyl-*N*-propyl carbazole (24)

3,6-Dibromo-*N*-propyl carbazole (2.0 g; 5.4 mmol) was dissolved in dry THF (250 ml). The solution was cooled to –78°C and *t*-BuLi (27 mmol) was added. The temperature was allowed to rise to 0°C. The solution was recooled to –78°C and dry DMF (8 g; 100 mmol) was added. The temperature was allowed to rise to RT. After 30 min. $HCl_{(aq)}$ was added, the volume reduced *in vacuo* and the precipitate was filtered. Recrystallization from ethanol afforded the product in 43% yield (0.62 g; 2.3 mmol). Mp. 142°C-144°C. ^{1}H NMR (250MHz, DMSO-d_6): δ = 0.9 (t, J = 7.4 Hz, 3H, -CH_3), 1.8 (m, 2H), 4.5(d, J = 7.1 Hz, 2H), 7.9(d, J = 8.6 Hz, 2H), 8.1(d, J = 8.6 Hz, 2H), 8.9(s, 2H), 10.1(s, 2H) ppm. ^{13}C NMR (63MHz, DMSO-d_6): δ = 11.1, 21.7, 44.3, 110.6, 122.3, 124.3, 127.2, 129.2, 144.4, 191.8 ppm. Anal. calcd. for $C_{17}H_{15}NO_2$: C, 76.96; H, 5.70; N, 5.28. Found: C, 76.76; H, 5.74; N, 5.18.

CHAPTER 5

AN EXCEPTIONAL RED SHIFT OF THE EMISSION MAXIMA UPON FLUORINE SUBSTITUTION

This chapter is based on the article: *An exceptional red shift of the emission maxima upon fluorine substitution* (appendix 2). My contribution to the paper has been the characterization of compounds, synthesised by Frederik Krebs, using fluorescence. All work performed by me is described in the paper. In this chapter I will only elaborate on some of the key aspects, especially the fluorescence emission dependency on solvent polarity.

5.1 Introduction

The effect of perfluorination on the photophysical properties was investigated through synthesis and photophysical characterisation of two isostructural donor-acceptor-donor dye molecules 1,4''-bis(1*H*-phenanthro[9,10-*d*]imidazol-2-yl)-2',5'-difluoro-3',6'-diperfluorooctyl-*p*-terphenylene (**1**) and 1,4''-bis(1*H*-phenanthro[9,10-*d*]imidazol-2-yl)-2',5'-dioctyl-*p*-terphenylene (**2**) shown in Figure 5-1.

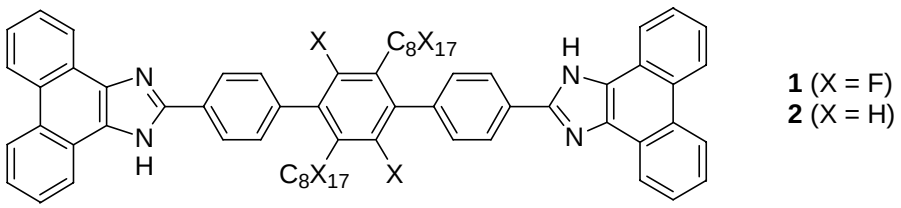

Figure 5-1. **1** and **2**

The dye molecules **1** and **2** have very similar absorption spectra in both apolar (toluene) and polar (THF) solvents as shown in Figure 5-2. The main differences between **1** and **2** in the absorption spectra are a slightly lower extinction coefficient, a small blue shift of

the entire spectrum by 2nm and a small shoulder at the absorption edge for the fluorinated compound **2**.

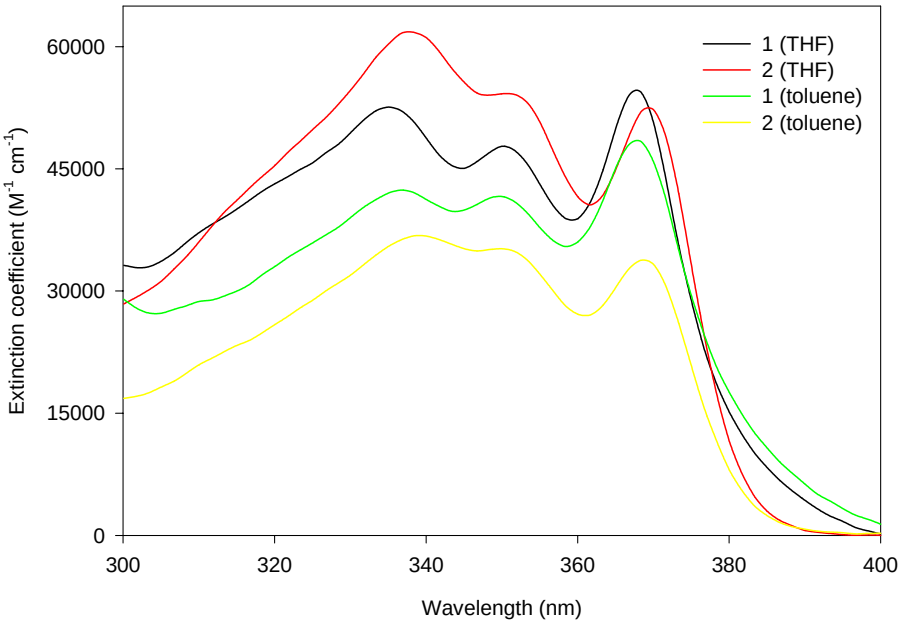

Figure 5-2. Absorption spectra of compounds **1** and **2** in THF and toluene.

Though the absorption of the **1** and **2** is very similar there is large difference in the fluorescence emission shown in Figure 5-3, where the emission spectrum of **1** and **2** in THF and hexane is showed. In all cases the spectra were broad and there was no sign of fine-structure. The emission maximum of **1** showed a large redshift going from non-polar to polar solvents. This is in marked contrast to the emission spectrum of **2** that show virtually no solvent dependence.

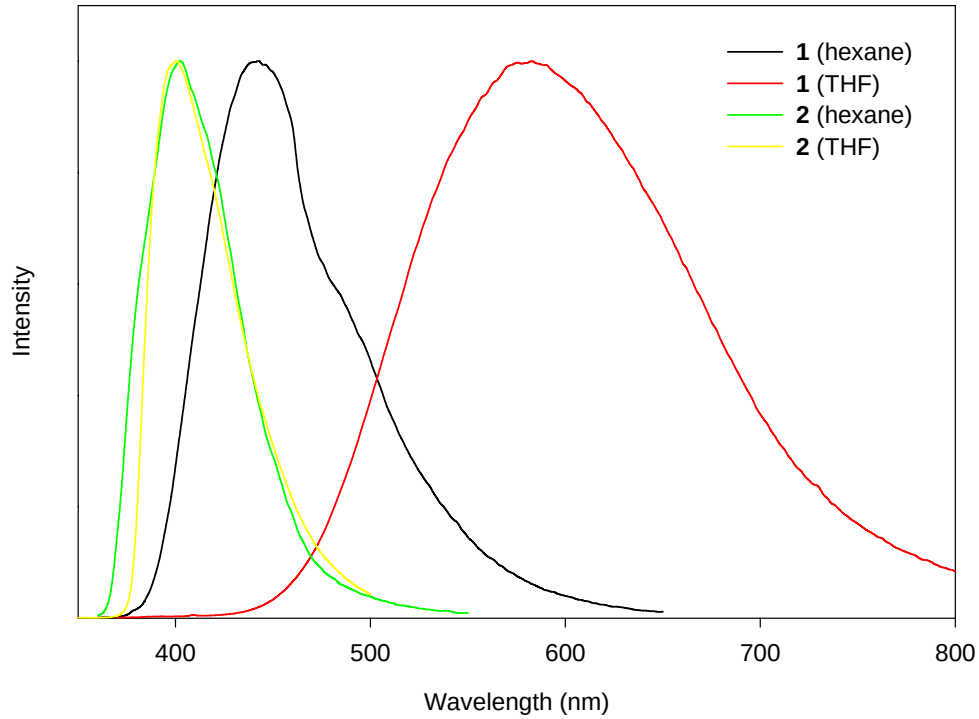

Figure 5-3. The emission spectra obtained for **1** and **2** in polar (THF) and non-polar (hexane) solvents under magic angle conditions. All spectra are normalised for easy comparison. Notice the extreme polarity dependence of the emission maximum in the case of **1**.

5.2 Solvent effect on emission spectra[1]

As described in chapter one fluorescence emission occurs at a longer wavelength than absorption due to a number of processes leading to energy loss. Solvent effects can shift the wavelength even more. Generally the molecular dipole moment (μ_E) of an excited molecule is larger than the dipole in the ground state (μ_G). Immediately after excitation the molecule reach the Franck-Condon state (the Franck-Condon principle is described in chapter 1). In this state the solvent molecules (as well as the molecule it self) has not yet equilibrated. The larger molecular dipole moment in the excited state leads to a reorientation of the solvent molecules in order to stabilize the excited molecule. The effect is naturally stronger in more polar solvents (this is illustrated in Figure 5-4). After 10^{-10}s the process of reorientation of the solvent molecules is completed and the system has reached equilibrium.

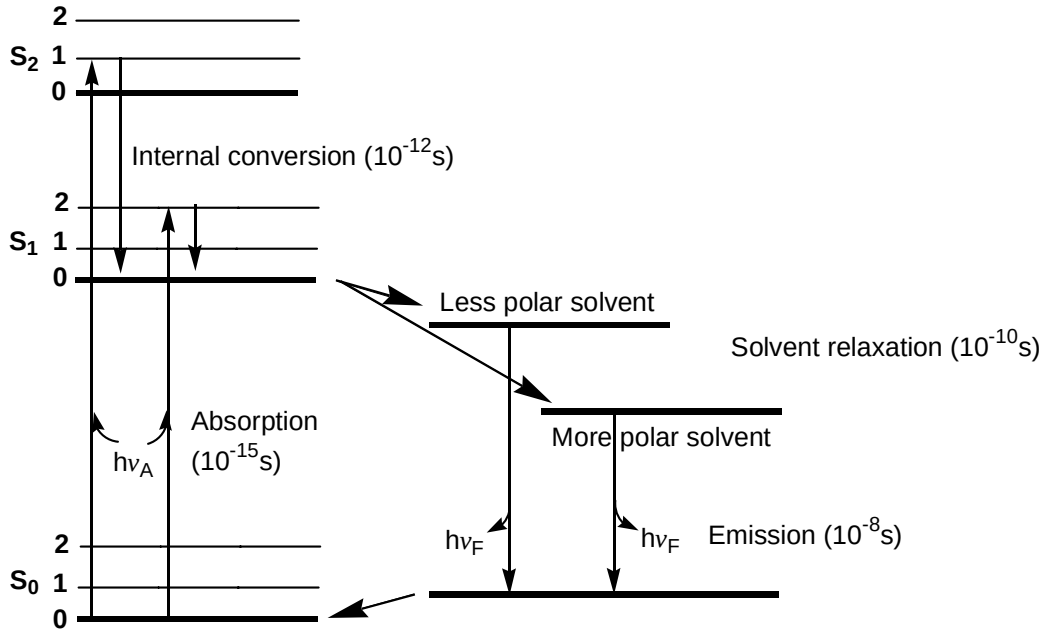

Figure 5-4. Jabłoński diagram emphasising solvent effects.

The time constants show why the absorption spectra, in general, are not as solvent dependent as the emission spectra. Absorption occurs within 10^{-15}s, which is too short for solvent relaxation that occurs within 10^{-11}s - 10^{-10}s. Fluorescence lifetimes on the other hand are of the order of 10^{-9}s - 10^{-8}s, which leaves plenty of time for solvent relaxation and stabilizing of the S_1 state before emission. To be stabilised in polar solvents a molecule must posses a molecular dipole, and the larger the dipole the greater the stabilisation. This explains the relative low red shift normally observed of nonpolar compounds such as hydrocarbons.

5.3 The Lippert-Mataga equation

Excluding specific solvent effects (hydrogen bonding etc.) the emission wavelength can be described by the Lippert-Mataga equation,[2] as a first approximation:

$$\nu_F = C_1 - C_2 \mu_E (\mu_E - \mu_G) \Delta f \qquad (1)$$

where C_1 and C_2 are constants, μ_E and μ_G are the molecular dipole moments in the excited and ground state respectively. The absorption wavenumber is included in C_1. Δf is the solvent polarity and is given by equation 2 where ε is the dielectric constant and n is the optical refractive index.

$$\Delta f = \frac{\varepsilon - 1}{2\varepsilon + 1} - \frac{(n^2 - 1)}{(2n^2 + 1)} \qquad (2)$$

According to equation 1 and 2 the emission will be more redshifted as the term $\mu_E(\mu_E-\mu_G)$ is increasing, with increasing dielectric constant (ε) and decreasing refractive index (n). The effect of ε is expected. However, the influence of n is not so clear. The refractive index is related to the motion of electrons within the solvent molecules, which is very fast. Due to this, the electrons can reorient while light is absorbed, and stabilising S_1 prior to solvent reorientation. The effect is that the distance between S_1 and S_0 is reduced. Thus while ε is a static property n is dynamic. The effect of n is the explanation that most chromophores display a redshifted absorption in solvents compared to the gasphase absorption.

5.4 The Lippert-Mataga equation used on compound 1

Equation 1 assumes the presence of a molecular dipole. However **1** does not have a dipole moment, since it contains a centre of symmetry, but a quadropole moment with a -2δ on the central terphenylene unit and $+\delta$ situated on each of the two 1*H*-phenanthro[9,10-*d*]imidazol-2-yl groups. We speculate that because **1** is a rather large molecule its quadrupole moment can be approximated by two isolated dipole moments. This approximation is most valid around the 1*H*-phenanthro[9,10-*d*]imidazol-2-yl unit and the least valid around the centre of the molecule (the terphenylene unit) where the two dipoles will cancel each other somewhat. This means that the observed redshift is less than should be expected if the dipoles were truly isolated. Strehmel *et al.* have also applied the Lippert-Mataga equation to molecules without a net molecular dipole moment, but as in our case, with a quadrupole.[3]

Despite the lack of a dipole moment, the redshift of **1** in dichloromethane-hexane mixtures can be described by the Lippert-Mataga equation (see Figure 5-5). ν_f is linear function of Δf with a slope of -21300 cm^{-1}. Individual points obtained for solutions in pure solvents were also obtained and a linear fit to this data gave a slope of -19000 cm^{-1}. The slope is relatively steep indicating that the quadrupole moment in the excited state is substantially larger than the ground state quadrupole. Further, the slope is substantially steeper than that obtained for donor-π-acceptor molecules such as dialkylaminonaphthalenesulfonamides (-10600 cm^{-1}) and coumarins (-11300 cm^{-1}), but similar to the slope obtained for a series of donor-π-acceptor molecules forming twisted intramolecular charge transfer states upon excitation (the TICT mechanism described in chapter two) such as dimethylaminobenzonitriles (from -15000 cm^{-1} to -24200 cm^{-1}) and dimethylaminobenzoic esters (-27200 cm^{-1}). This suggests that there is a substantial charge transfer upon excitation.

It is interesting to notice that for **1** in ethanol-hexane mixtures ν_f is a non-linear function of Δf suggesting a specific interaction between ethanol and **1**, possibly H-bonding

between ethanol and the amine or imine functionality on the 1*H*-phenanthro[9,10-*d*]imidazol-2-yl group.

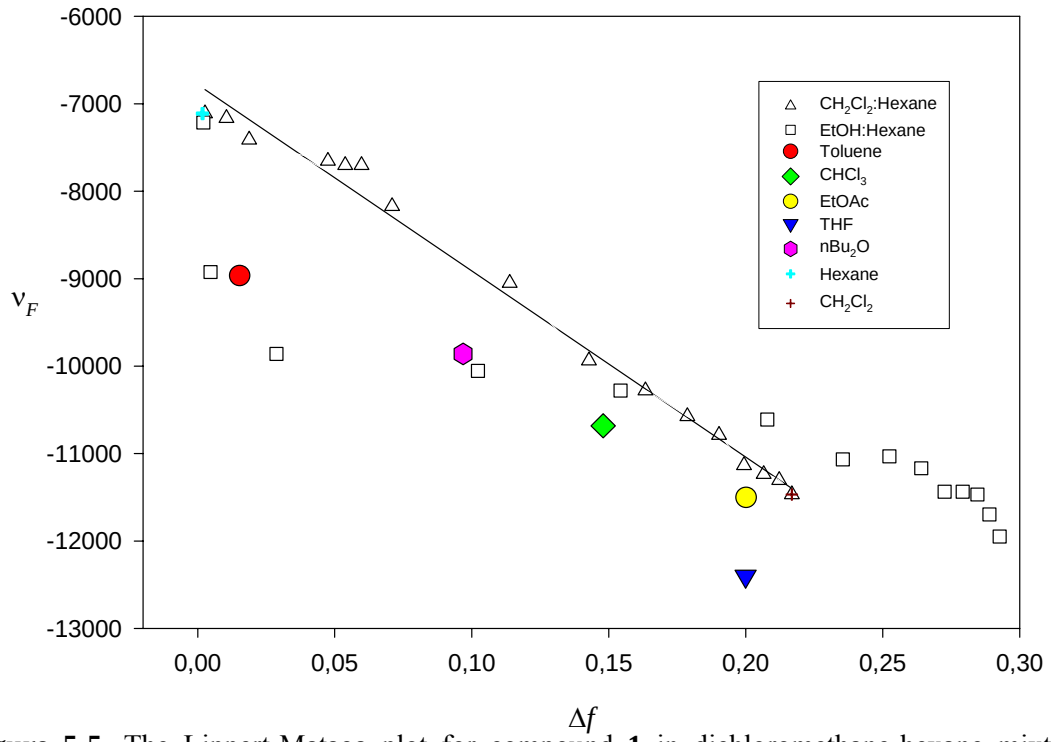

Figure 5-5. The Lippert-Mataga plot for compound **1** in dichloromethane-hexane mixtures (triangles with linear fit) and for ethanol-hexane mixtures (squares) showing a non-linear relationship. Additionally the single points are obtained from solutions in pure solvents with different dielectric constants.

References and notes

1. See chapter 6 in Principles of Fluorescence Spectroscopy, sec. Ed, J.R. Lakowicz, Kluwer Academic / Plenum Publishers, New York: 1999.
2. Baumann, W.; Bischof, H; Fröhling, J.C.; Brittinger, C, Rettig, W.; Rotkiewicz, K. J. Photochem. Photobiol. A: Chem. **1992**, *64*, 49.
3. Strehmel, B.; Sarker, A. M.; Malpert, J. H.; Strehmel, V.; Seifert, H.; Neckers, D. C. J. Am. Chem. Soc. **1999**, *121*, 1226-1236.

CHAPTER 6

ENERGY TRANSFER IN POLYMERS

This chapter summarizes my contribution to the articles: *Synthesis, Properties and Langmuir-Blodgett Film Studies of an Ionic Dye Terminated Rigid Conducting Polymer* (appendix 3) and *Directional synthesis of a dye linked conducting homopolymer* (appendix 4). The molecules investigated are spin-offs from a larger project aiming at polymer based solar cells. This work was carried out during the last 6 months of my Ph.D. study. More general information about the field can be found in the references provided.

6.1 Introduction

Conducting polymers and in particular the application of conducting polymers for diverse functions such as light emitting diodes,[1] all polymer displays,[2] all polymer electronic circuits[3] and all polymer solar cells[4] have received recent attention. Two systems will be described in this chapter: A-J (Figure 6-1) and J-P-J (Figure 6-2). Both structures consist of a conjugated polymer (termed the J-domain) and a chromophore. In the case of A-J the chromophore is an azadioxatriangulene dye (A-domain) while J-P-J has the chromophore, a porphyrin (P-domain) dye, in the middle. The possibility of having porphyrin dyes incorporated into the backbone of a conducting polymer has been explored by Jones Jr. *et al.*[5] Further multi-porphyrin arrays[6] and their light harvesting properties have also been examined in great detail by Lindsey *et al*.[7] with particular emphasis on the influence of the molecular design upon the energy transfer properties.

A polymer-based solar cell must be able to absorb light (energy), which can be transported to a unit capable of utilising the energy in charge separation that can run an external circuit. Thus efficient energy transport is only one requirement out of many in a successful polymer based solar cell. In a solar cell, fluorescence is wasted energy; rather the energy should drive an external circuit. Both A and J fluoresce strongly, and neither is capable of charge separation. However, the fluorescence measurements allow us to monitor some aspects of the energy transport properties of the J-domain.

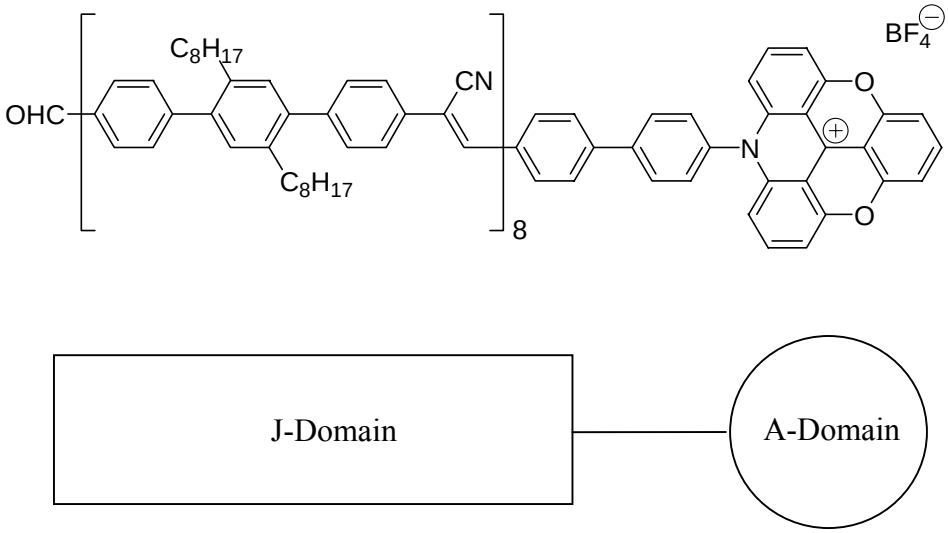

Figure 6-1. A-J structure (top) and a schematic representation (bottom). The A-domain is an ADOTA dye, and the J-domain is an oligomer of an average of 8 monomer units.

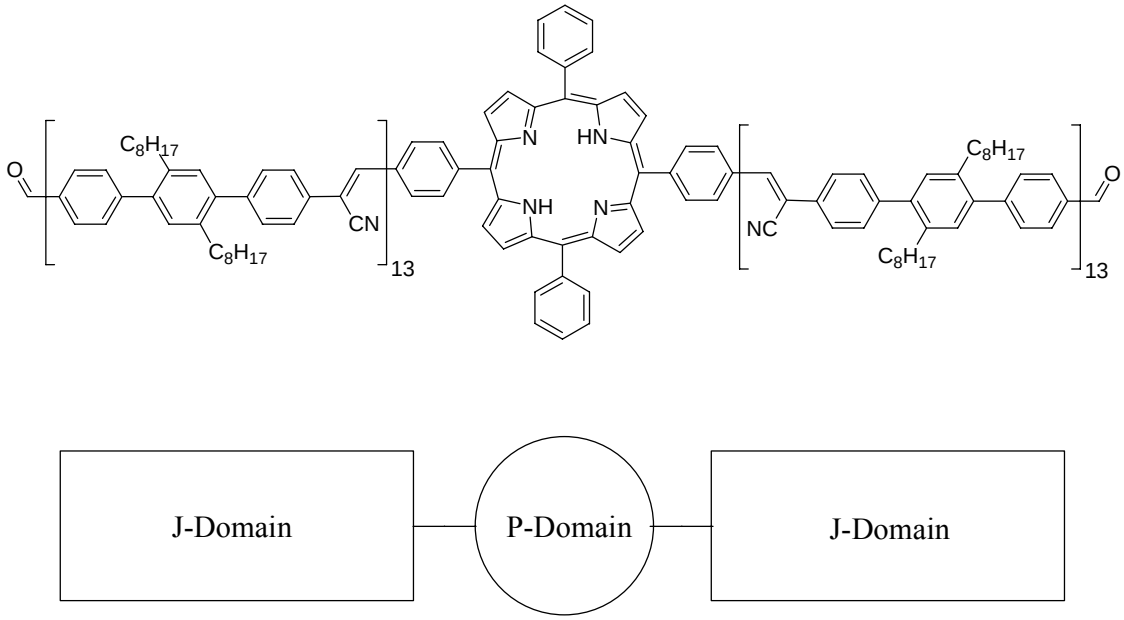

Figure 6-2. J-P-J structure (top) and a schematic representation (bottom). The P-domain is porphyrin, and the J-domain is an oligomer of an average of 13 monomer units.

6.2 Photophysical characterisation of A-J

The absorption spectra of the J-domain, A-domain and A-J in chloroform are shown below (Figure 6-3). Notice that the absorption spectrum of A-J is a sum of the individual domains A and J. The J-domain efficiently absorbs light with a maximum at 350nm where there is a window in the absorption spectrum of the A-domain. Thus the J-domain of A-J can selectively be exited by using wavelengths in the 350nm range.

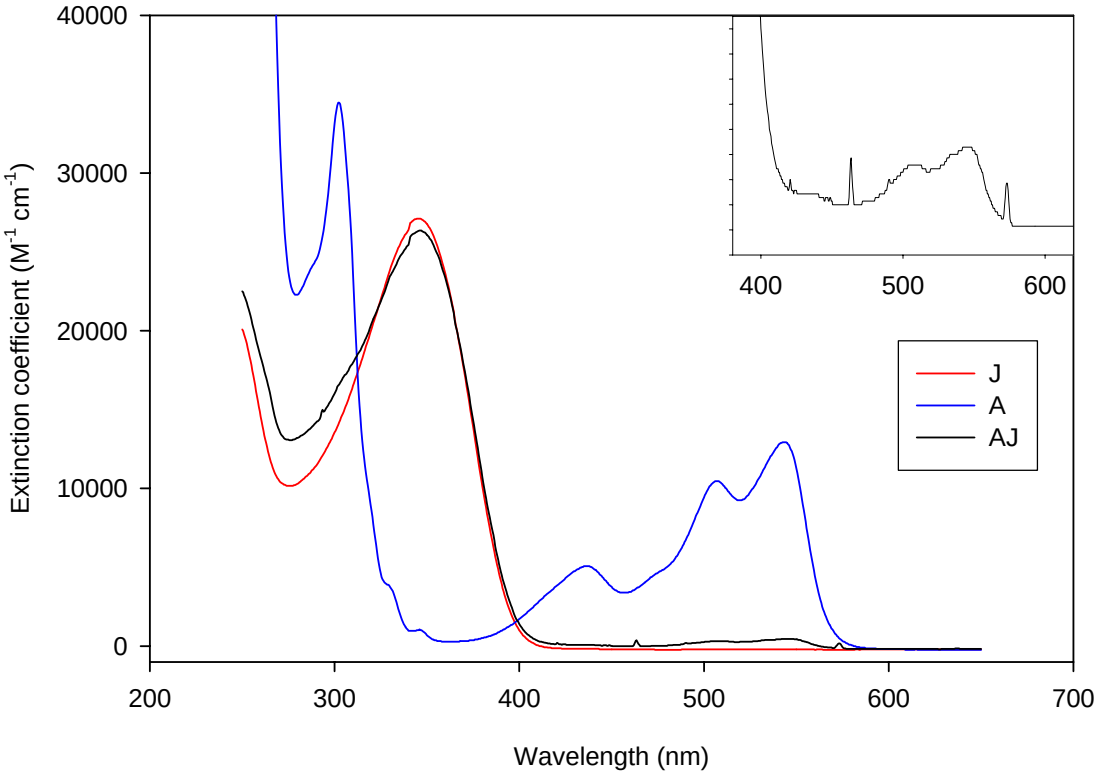

Figure 6-3. Absorption of the A- and J-domain along with A-J in chloroform. The 400-600nm portion of the spectrum of A-J has been enlarged (8 times) to show the similarity with the pure A-domain. The spectra of the J-domain and the AJ-assembly has been normalized. The low absorbance of A-J in the 400-600nm region is due to the relative low concentration of the A-domain. The small sharp peaks in the inset are noise from the spectrometer.

Using 350nm as the excitation wavelength, the fluorescence emission spectra of A and J in solution and of an AJ-film are shown in Figure 6-4. The emission from the J-domain in solution is a broad peak centred around 450 nm and the emission from the A-domain in solution has a broad maximum centred around 570nm with a broad shoulder centred around 610 nm. The emission from the A-domain is very weak due to the low absorbance at 350 nm. When the A- and J-domain are connected in the AJ-assembly (in

a LB-film or in solution), the emissions from the two domains retain their shape and wavelength. However, the relative intensity of emission from the A-domain in the AJ-assembly is much larger (55 times larger) than expected from a simple mixture of the A- and J- domain. This is due to energy transfer from the J-domain that effectively absorbs at 350 nm. No energy transfer was observed by simply mixing J and A in chloroform.

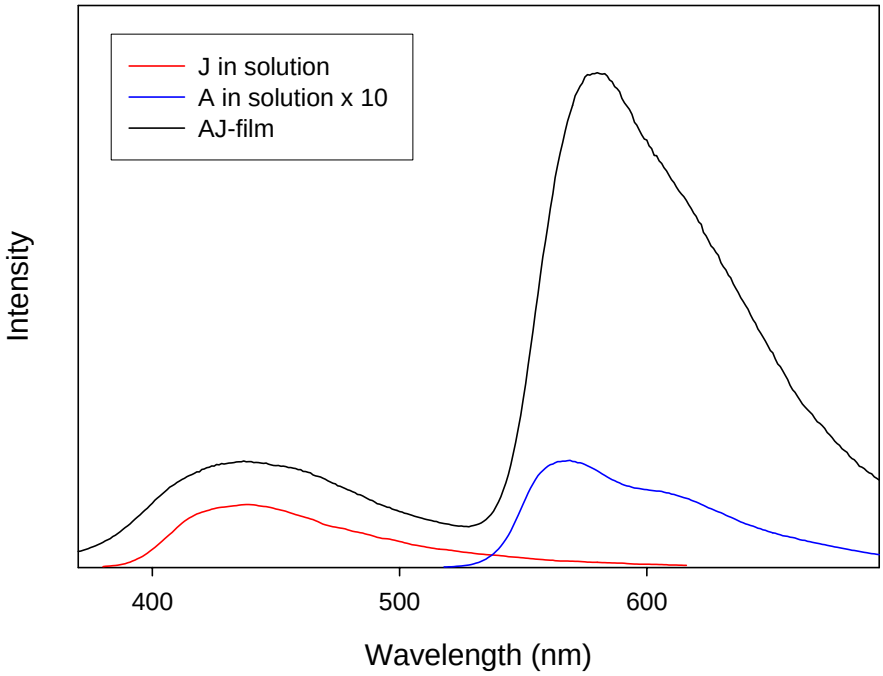

Figure 6-4. Fluorescence emission spectra of the A-domain and J-domain in degassed chloroform and of an AJ-film, all excited at 350nm (the intensity of the A-domain spectrum is multiplied by 10 for clarity). The large emission from A in A-J is due to energy transfer from J. The larger intensity around 450 nm from the film is due to the higher quantum yield of the J-domain fluorescence in the LB-film compared to the J-domain in solution. The optical density of the A- and J-domain in solution was equal and in this case the lower emission from the A-domain compared to the J-domain in solution is due to the lower absorbance of the A-domain at 350 nm.

By selectively exciting the A domain the quantum yield of the A-domain fluorescence was determined using DPA (di-phenyl anthracene) as quantum yield reference.[8] From the quantum yield of A and the absorption and emission spectra of A-J, a photon balance of the AJ-assembly can be derived (Figure 6-5) where the absorption, emission, and energy transfer are accounted for. Absorption and fluorescence can be measured, but not the non-radiative processes. The non-radiative processes have been calculated under the assumption that the fluorescence quantum yield of the isolated domains is retained in the AJ-assembly.

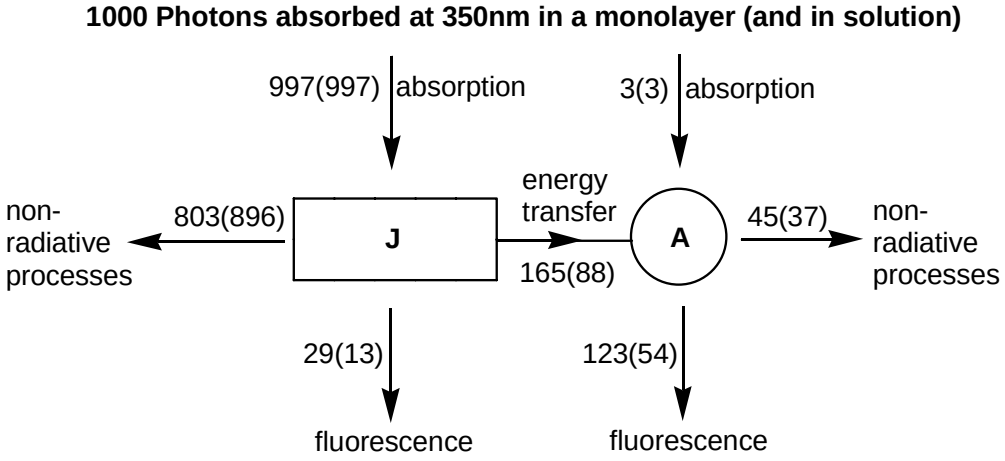

Figure 6-5. A schematic representation of the light harvesting and energy transfer processes and efficiencies obtained for the AJ-assembly in a LB-film. The values in parenthesis are obtained from measurements in solution.

The fluorescence quantum yield of A is very similar in film and solution, in contrast to this; the quantum yield of J is reduced by a factor 2 in solution, probably due to the decreased motional freedom in the solid state. We believe that this is the origin of the lower emission from A in solution compared to the film. Finally it is important to notice that the A- and J-domain retain their emission properties (shape and wavelength) when connected in the AJ-assembly. The energy transport from J to A was investigated further using TRES (time resolved emission spectroscopy) where it was possible to investigate the dynamics of the energy transfer. By excitation at 350nm the time decay profile was obtained for both the J-domain and A-domain in chloroform AJ-film (Figure 6-6). The apparent delay in the emission from the A-domain is caused by the relatively long lifetime compared to the lifetime of the J-domain, which has a short lifetime similar to the lamp profile. Also, it was found that the decay profile from A depends on whether A is excited directly or it gets excited indirectly from J. In the former case the decay profile is single exponential, whereas it is double exponentials in the later. It seems reasonable that indirect excitation from J makes the decay a more complex event.

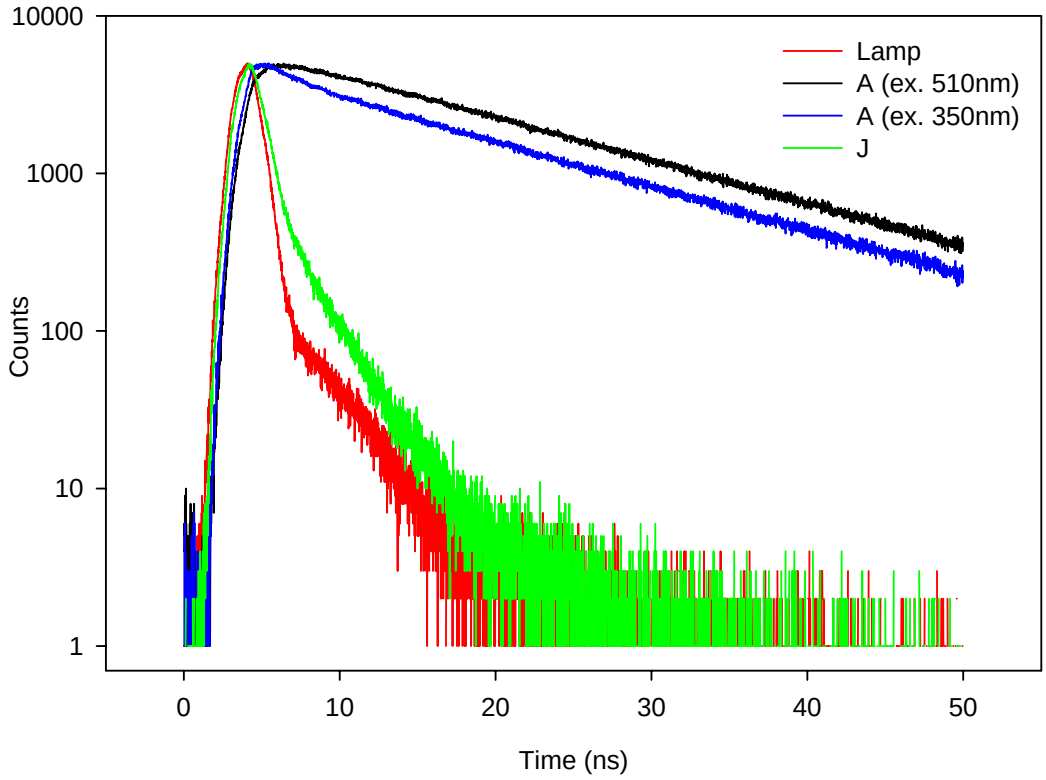

Figure 6-6. Time decay profile of AJ in chloroform, and the lamp profile (FWHM 1.8ns) on a semilogarithmic plot. Peak counts are 5000. When exciting AJ at 350nm, the fluorescence lifetime of J could be fitted by a double exponential decay: 0.13ns (79%) and 2.0ns (21%). And the decay profile of A could also be fitted by a double exponential decay: 1.4ns (6.4%) and 14.8ns (93.6%) However, when the A-domain was directly at 510nm the decay profile could be fitted by a single exponential decay: 16.7ns.

6.2 Photophysical characterisation of J-P-J

The characterisation of J-P-J was performed in similar manner as the characterisation of A-J. One difference between A and P is that the absorption of P is dependent on pH. At low pH the two imine functionalities becomes protonated[9] (Figure 6-7). This has also has an effect on the absorption spectrum. In Figure 6-10 the absorption spectra of J-P-J under acidic and basic conditions are shown. Acidification with H_2SO_4 leads only to a slight hyperchromic shift for J-domain absorption (at 350nm) whereas the signals from the P-domain change dramatically upon acidification where a large red-shift (23nm) is observed for the strong absorption known for porphyrins. In this case the shift of the maximum is from 421nm to 444nm. Further the normally very weak band in porphyrins at 645nm is upon acidification red-shifted by 14nm and becomes very intense.

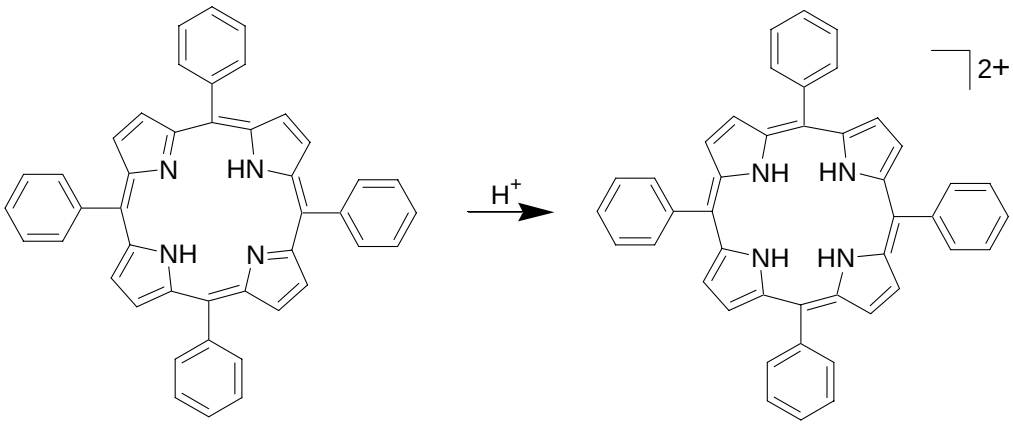

Figure 6-7. The imine functionalities of tetraphenyl porphyrin can be protonated.

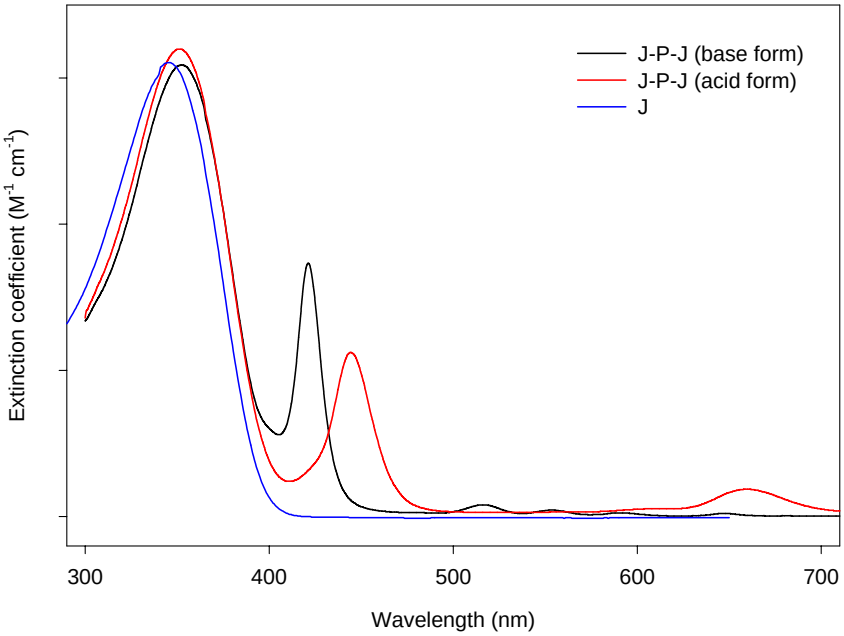

Figure 6-8. Absorption spectra of J and J-P-J in chloroform. The acid form was obtained be adding a drop of sulphuric acid to the solution.

As in the A-J case, the J-domain can be selectively exited at 350nm. The emission spectra of spincoated films of J-P-J are shown Figure 6-9. In both the base and acid form, the J-domain emission is a broad featureless peak in the 400-550nm region (maxima at 430nm). The corresponding solution spectra are very similar to the solid-state spectra. Sulfuric acid was used to obtain the acid form. Beside the dramatic change in the UV-VIS spectrum of the P-domain upon acidification an effect is also seen in the

emission spectrum in both solution (degassed chloroform) and spincoated film; in the base form the porphyrin gives two peaks at 655nm and 721nm, but in acid form only one broad peak at 709nm.

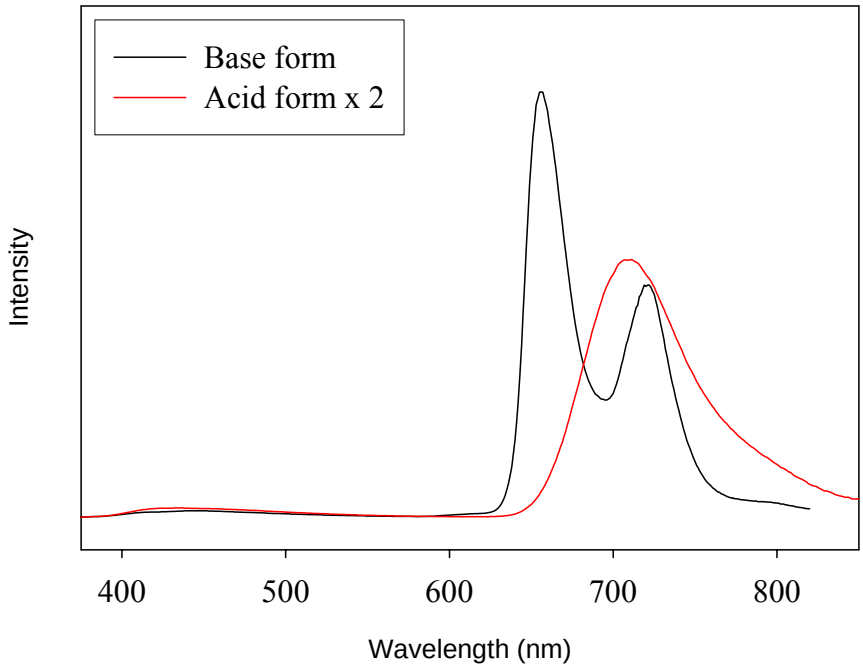

Figure 6-9. Emission spectra of spincoated J-P-J films. The spectra have been scaled to reflect the relative fluorescence quantum yields of the acid and base form. The acid form has been multiplied by 2.

The energy balance can be summarised as absorption, emission, transfer and non-radiative processes as shown in Figure 6-10. Using the same procedure as in the A-J case, the P-domain was selectively excited and the fluorescence quantum yield of P-domain determined. From the quantum yield of P, the emission and the absorption spectrum of J-P-J, the shown photon balance was derived. From this it is clear that the J-domains acts as a very efficient antenna for light harvesting for the P-domain, especially in the solid phase. From TRES measurements we found that in general the exciton transfer happened instantaneous.

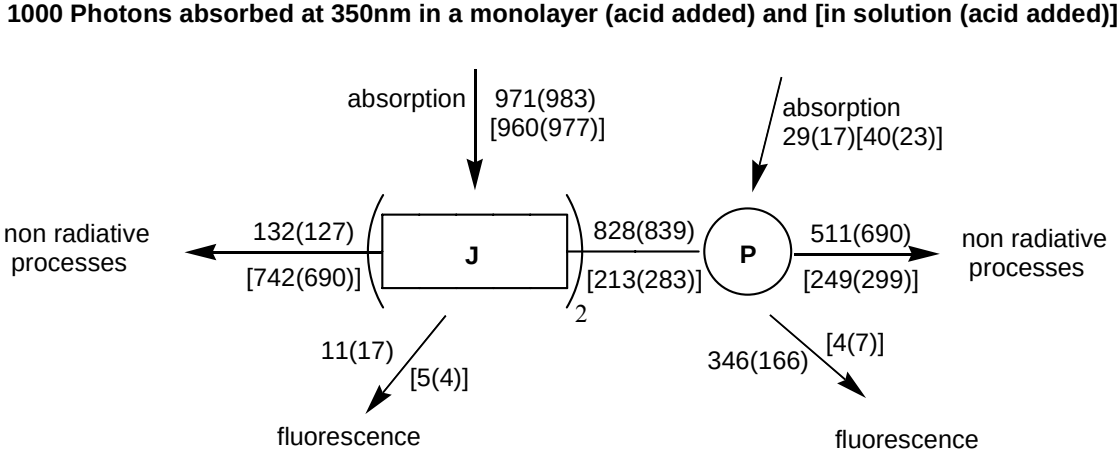

Figure 6-10. Photon balance for JPJ in four situations: JPJ in spincasted film (in base and acid form) and JPJ in chloroform solution (in base and acid form). Solution values are within brackets. Values for the acid form are in parentheses. The excitation wavelength is set at maximum absorption of the J-domain 350 nm.

References and notes

1. a) Ho, P. K. H.; Kim, J.-S.; Burroughes, H.; Becker, S. F. Y.; Brown, T. M.; Caclalli, F.; Friend, R. H. *Nature* **2000**, *404*, 408. b) Yang, Y. *Mater. Res. Soc. Bull.* **1997**, *22*, 16-24.
2. Huitema, H. E. A.; Gelinck, G. H.; van der Putten, J. B. P. H.; Kuijk, K. E.; Hart, C.M.; Cantatore, E.; Herwig, P. T.; van Breemen, A. J. J. M.; de Leeuw, D. M. *Nature* **2001**, *414*, 599.
3. a) Katz, H. E.; Lovinger, A. J.; Johnson, J.; Kloc, C.; Siegrist, T.; Li, W.; Lin, Y.-Y.; Dodabalapur, A. *Nature* **2000**, *404*, 478-480. b) Drury, C. J.; Mutsaers, C. M. J.; Hart, C. M.; Matters, M.; de Leeuw, D. M. *Appl. Phys. Lett.* **1998**, *73*, 108-110. c) Sirringhaus, H.; Tessler, N.; Friend, R.H. *Science* **1998**, *393*, 619-620.
4. Granström, M.; Petritsch, K.; Arias, A. C.; Lux, A.; Andersson, M. R.; Friend, R. H. *Nature* **1998**, *395*, 257-260.
5. A) Jiang, B.; Yang, S. –W.; Jones Jr., W. E. *Chem. Mater.* **1997**, *9*, 2031-2034. B) Jiang, B.; Jones Jr., W. E. *Macromolecules* **1997**, *30*, 5575-5581. C) Jiang, B.; Yang, S. –W.; Niver, R.; Jones Jr., W. E. *Syn. Met.* **1998**, *94*, 205-210.
6. Burrell, A. K.; Officer, D. L.; Plieger, P. G.; Reid, D. C. W. *Chem. Rev.* **2001**, *101*, 2751-2796.
7. A) Wagner, R. W.; Lindsey, J. S.; Seth, J.; Palaniappan, V.; Bocian, D. F. *J. Am. Chem. Soc.* **1996**, *118*, 3996-3997. B) Wagner, R. W.; Johnson, T. E.; Lindsey, J. S. *J. Am. Chem. Soc.* **1996**, *118*, 11166-11180. C) Hsiao, J.-S.; Krueger, B. P.; Wagner, R. W.; Johnson, T. E.; Delaney, J. K.; Mauzerakk, D. C.; Fleming, G. R.; Lindsey, J. S.; Bocian, D. F.; Donohoe, R. J. *J. Am. Chem. Soc.* **1996**, *118*, 11181-

11193. D) Seth, J.; Palaniappan, P.; Wagner, R. W.; Johnson, T. E.; Lindsey, J. S.; Bocian, D. F. *J. Am. Chem. Soc.* **1996,** *118*, 11194-11207.
8. Ware, R. W.; Rothman, W. *Chem. Phys. Lett.* **1976**, *39*, 449.
9. A) Silvers, S. J.; Tulinski, A. *J. Am. Chem. Soc.* **1967**, *89*, 3331-3337. B) Kano, K.; Fukuda, K.; Wakami, H.; Nishiyabu, R.; Pasternack, R. F. *J. Am. Chem. Soc.* **2000**, *122*, 7494-7502. C) Arnoff, S. *Chem. Rev* **1950**, *47*, 175.

Appendices – List of publications

Appendix 1:
Spanggaard, H.; Jørgensen, M.; Almdal, K. "Mechanical strain sensing in a SIS type elastomer with single site strain probes based on carbazole". *Macromolecule*s, **2003,** *36,* 1701-1705.

Appendix 2:
Krebs, F.C.; **Spanggaard, H** "An exceptional red shift of the emission maxima upon fluorine substitution", *J. Org. Chem.* **2002**, *67*, 7185.

Appendix 3:
Krebs, F.C.; **Spanggaard, H**; Rozlosnik, N; Larsen, N.B.; Jørgensen, M "Synthesis, Properties and Langmuir-Blodgett Film Studies of an Ionic Dye Terminated Rigid Conducting Polymer", *Langmuir*, submitted.

Appendix 4:
Krebs, F.C.; Hagemann, O.; **Spanggaard, H.** "Directional synthesis of a dye linked conducting homopolymer", *J. Org. Chem.* **2003**, *68*, 2463.